ELSEVIER

Marine and Petroleum Geology 21 (2004) 225–276

Marine and Petroleum Geology

www.elsevier.com/locate/marpetgeo

Quantitative Meso-/Cenozoic development of the eastern Central Atlantic continental shelf, western High Atlas, Morocco

Rainer Zühlke[a,*,1], Mohammed-Said Bouaouda[b], Brahim Ouajhain[b], Thilo Bechstädt[a,2], Reinhold Leinfelder[c,3]

[a]*Institute of Geology and Paleontology, Ruprecht Karl University, Im Neuenheimer Feld 234, D-69120 Heidelberg, Germany*
[b]*Department of Geology, Faculty of Sciences, Chouaib Doukkali University, B.P. 20, 24000 El Jadida, Morocco*
[c]*Geosciences and Environmental Sciences—Paleontology, Ludwig Maximilian University, Richard-Wagner-Str. 10, D-80333 München, Germany*

Received 12 August 2002; received in revised form 12 August 2003; accepted 14 November 2003

Abstract

The well exposed Late Paleozoic to Cenozoic succession in the western High Atlas (Morocco) documents the early rift to mature drift development of the eastern Central Atlantic continental shelf basin. Vertical sections, depositional geometries and unconformities have been used to reconstruct the basin architecture prior to Atlasian inversion. Two-dimensional reverse basin modeling has been performed to quantitatively analyze the development of the continental shelf between the latest Paleozoic to Early Cenozoic. Basin evolution stages include (i) early rift, Late Permian to Anisian; (ii) rift climax, Ladinian to Carnian; (iii) sag, Norian to Early Pliensbachian; (iv) early drift, Late Pliensbachian to Tithonian; (v) mature drift, Berriasian to Cenomanian; (vi) mature drift with initial Atlasian deformation, Turonian to Late Eocene; (vii) Atlasian deformation; Late Eocene to Early Miocene; (viii) Atlasian uplift and basin inversion, Early Miocene to Recent. The Late Permian to Late Cretaceous basin development comprises eight subsidence trends of 10–35 Myr duration. Trends were initiated by changes in thermo-tectonic subsidence, which in turn triggered positive and negative feedback processes between sediment flux, flexural and compaction-induced subsidence. Plate-tectonic reconfigurations in the Atlantic domain controlled the thermo-tectonic subsidence history and the basin development of the Agadir segment of the northwest African passive continental margin: (1) major shifts in the sea-floor spreading axis; (2) significant decreases in sea-floor spreading rates; (3) the stepwise migration of crustal separation and sea-floor spreading in and beyond the Central Atlantic; (4) African–Eurasian relative plate motions and convergence rates. During the Early Pliensbachian/Toarcian to Cenomanian the first three plate-tectonic reconfigurations triggered changes in ridge-push forces and modulated the extensional stress field of Central Atlantic plate drifting. Since the Turonian, African–Eurasian relative plate motions and convergence rates represented the dominant control on the thermo-tectonic subsidence history in the Agadir Basin. Major variations in sediment flux and total subsidence characterize the development of the northwest African passive continental margin. The explanation of typical stratigraphic sequences as caused predominantly by sea-level fluctuations, and rough assumptions on sediment input/production and subsidence, is not necessarily applicable to passive continental margins. The methodology applied in this study, including the newly developed tool of 'Compositional Accommodation Analysis', allows to develop more rigorous genetic models for the development of continental shelf basins.

Keywords: Continental margin; Basin modeling; Central Atlantic; Morocco; Agadir Basin; Ridge push; Intra-plate compression; Subsidence trends; Compositional accommodation analysis; Mesozoic; Cenozoic

1. Introduction

The Meso- to Cenozoic Central Atlantic represents an almost symmetrical oceanic basin with the two conjugate margins of North America and northwest Africa to western Europe. Meso- to Cenozoic shelf basins on the North American continental margin are almost exclusively situated in onshore subsurface and offshore positions.

* Corresponding author. Tel.: +49-6221-54-6055; fax: +49-6221-54-5503.

E-mail addresses: zuehlke@uni-hd.de (R. Zühlke); bouaoudamsaid@hotmail.com (M.S. Bouaouda); brahimouajhain@hotmail.com (B. Ouajhain); bechstaedt@uni-hd.de (T. Bechstädt); r.leinfelder@lrz.uni-muenchen.de (R. Leinfelder).

[1] http://www.rainer-zuehlke.de.

[2] http://geopal.uni-hd.de/sediment/staff/bechstaedt.html.

[3] http://www.palaeo.de/inst_home.htm.

0264-8172/$ - see front matter © 2004 Elsevier Ltd. All rights reserved.
doi:10.1016/j.marpetgeo.2003.11.014

Structural and sedimentological data were derived from seismic lines as well as from few scientific and published commercial wells (Speed, 1994). A number of DSDP legs (Sites 370, 415, 416) reached the early continental shelf successions of Late Jurassic age. Except for the Triassic Newark halfgraben, information for the Triassic to earliest Jurassic rift and post-rift basin stages is restricted to very few deep wells (e.g. COST G1, G2; Schlee & Klitgord, 1988).

By comparison the Mesozoic Central Atlantic continental margins of northwest Africa have been studied in less detail. They cover extensive parts of the recent coastal plains and continental shelves of Morocco, Mauritania and Senegal. In Morocco (Fig. 1), available information is focused on the Essaouira Basin, which was until currently the most important oil and gas producing basin. More recently, additional focus has been placed on the Tarfaya Basin, which yields local, but significant heavy oil accumulations (Jabour, Morabet, & Bouchta, 2000; Morabet, Bouchta, & Jabour, 1998). Further Atlantic Basins of Morocco include the Doukkala Basin to the North and the Souss, Tarfaya, Layoune and Dakhla Basins to the South. Except for the Late Cretaceous succession, these southern basins are in onshore subsurface and offshore position. The northern Doukkala and Essaouira Basins are mainly onshore subsurface and offshore. Surface outcrops of the Late Triassic to Jurassic succession are very limited. The Cretaceous succession is better exposed.

The western High Atlas (WHA) mountain range of Morocco, situated between the Essaouira and Souss Basins

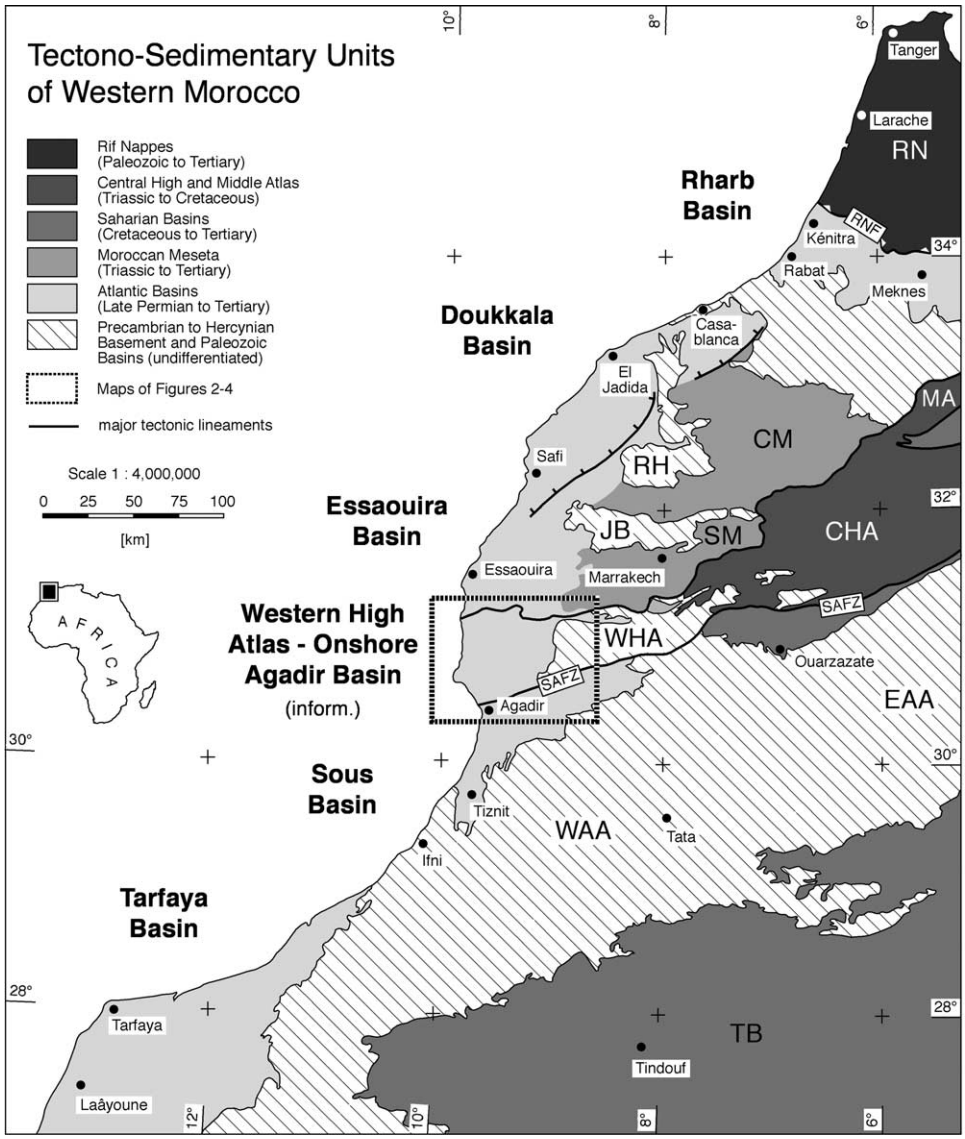

Fig. 1. Major tectono-sedimentary units of western Morocco with Atlantic Basins (light grey, bold letters; based on Saadi (1982)). The box (thick broken line) indicates the onshore Agadir Basin as shown in Figs. 2–4. Legend: CHA—Central High Atlas; CM—Central Meseta; EAA—Eastern Anti-Atlas; JB—Jebilet; MA—Middle High Atlas; RH—Rehamna; RN—Rif Nappes; RNF—Rif Nappe Front; SAFZ—South Atlas Fault Zone; SM—southern Meseta; TB—Tindouf Basin; WAA—western Anti-Atlas; WHA—western High Atlas.

(Fig. 1), offers excellent exposures of the Late Paleozoic to Early Cenozoic succession. Peak compression, uplift and basin inversion started in the latest Eocene (Gomez, Beauchamp, & Barazangi, 2000). The WHA includes the continental rift, proto-oceanic rift (sensu Leeder, 1995) and continental terrace (sensu Bond, Kominz, & Sheridan, 1995) or the rift and continental margin basin (sensu Einsele, 2000) of the eastern Central Atlantic. The basin has been referred to as (1) the South Atlas (Agadir) Basin (von Rad, Hinz, Sarnthein, & Seibold, 1982), (2) the Essaouira–Agadir Basin (Einsele, 2000), (3) the Souss–Agadir Basin (Heyman, 1989) or (4) the Haha Basin (Amrhar, 1995) in its westernmost part. This paper attributes the informal designation 'Agadir Basin' for the Permian to Eocene continental shelf succession between Im-n-Tanout, Agadir and Cap Tafelney (Fig. 2).

In contrast to all other circum-Central Atlantic Basins, the rift to continental margin basin preserved in the WHA of Morocco stands out for several reasons: (1) the Late Permian to Early Tertiary succession is well preserved over a lateral distance of almost 120 km; (2) the rift and passive margin successions are in autochthonous contact with the Hercynian basement; (3) deposition prevailed for much of the Late Permian to Early Tertiary time interval. Long-term and basinwide depositional and erosional gaps are restricted to the Early Jurassic and the easternmost basin margin; (4) because of large-scale outcrops in the WHA, facies, large-scale depositional geometries and biostratigraphy can be studied in detail. Spatial and time resolution significantly exceed the resolution of most subsurface data in other Atlantic Basins of northwest Africa; (5) during rift and early passive continental margin times, the deposition of evaporites was largely absent. The rift and continental margin basin architecture has not been significantly complicated by subsequent salt halokinesis.

Because of the combination of these features, the WHA offers a unique opportunity to study the long-term development of the eastern Central Atlantic continental shelf in detail. This paper includes a number of both qualitative and quantitative datasets: (1) the first litho- and biostratigraphic scheme for a northwest African rift to continental margin basin considering large-scale facies variations between the inner and outer shelf as well as the time diachronicity of lithostratigraphic units; (2) synthetic sections which have been measured and compiled between the Meso-/Cenozoic paleo-coastlines and shelf edge positions; (3) geometries of continental shelf-interior ramp/basin transitions; (4) biostratigraphy; (5) all lithofacies, thickness, paleobathymetry and biostratigraphy data have been processed for 2D numerical basin modeling.

The main objectives include: (1) a 2D architectural model along a 116 km long transect which covers the early rift basin and subsequent continental shelf until the Late Eocene; (2) a qualitative model of the rift to continental margin basin development based on facies, biostratigraphy, regional and basin-scale unconformities; (3) 2D numerical basin modeling of the Agadir Basin between the Late Permian to Late Eocene providing rates of total, thermotectonic, flexural and compaction-induced subsidence as well as sediment flux; (4) a genetic, process-oriented model of the basin development tied to the plate-tectonic history of the Atlantic and adjacent domains; (5) quantitative passive margin sequence stratigraphy and correlation to eustatic sea-level charts.

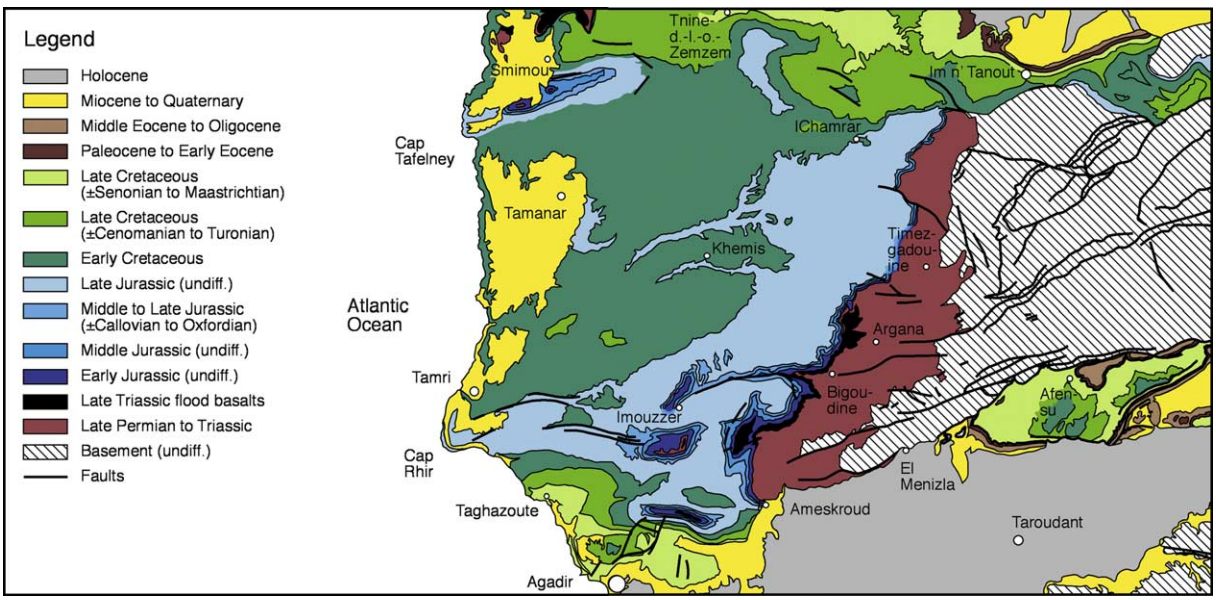

Fig. 2. Geological map of the western High Atlas (inverted Agadir continental margin basin), the southern part of the Essaouira Basin and the northern part of the Souss Basin (cf. Fig. 1; simplified after Jaïdi, Bencheqroun, and Diouri (1970a,b), Ouzzani, Eyssautier, Marçais, Choubert, and Fallot (1956), and Saadi (1982)).

2. Geological setting

The inverted rift and continental margin basin preserved in the WHA (Fig. 1) is limited (1) to the east by the Hercynian basement of the WHA; (2) to the south by the South Atlas Fault System (syn. Tiz-n-Test Fault System) and the Tertiary Souss Basin; (3) to the west by the recent continental shelf margin and slope; (4) to the north by the Essaouira Basin and the southern part of the Moroccan Meseta. Latest Eocene to Recent N–S to NNW–SSE directed compression (Gomez et al., 2000) formed three ENE–WSW trending structural zones (Ambroggi, 1963; Amrhar, 1995). They are separated by regional flexures or faults and characterized by different rates of orogenic uplift (Fig. 3).

The northern Sub-Atlasian Zone covers the area between Cap Tafelney, Cap Rhir, Argana and Im-n-Tanout. It is little deformed and largely in sub-horizontal position. Regional anticlines and flexures characterize the northern margin. The Axial Zone covers the area between Cap Rhir, Argana and the South Atlas Fault (Ida-ou-Tanane region) and is characterized by a set of ENE–SSW trending anticlines and synclines. Anticlines have been deeply cut and eroded and provide insight to the deeper basin levels. The southern Sub-Atlasian Zone covers the area between the South Atlas Fault and the southern Sub-Atlas Fault, immediately north of Agadir. The two faults represent separate branches of the Tiz-n-Test Fault System (Mustaphi, Medina, Jabour, & Hoepffner, 1997) further to the east. It has a polyphase origin with normal faulting in the Triassic to Jurassic (Medina & Errami, 1996) and inverse to subordinately left-lateral strike-slip faulting in the Tertiary. Weijemars (1987) proposed that the Tiz-n-Test Fault System was the location of the boundary between the Eurasian and African plates and represented the lateral equivalent of the Hayes Fracture Zone in the Central Atlantic Ocean. Subsequent studies (Jacobshagen, 1992) have shown that the Eurasian–African plate boundary is buried below the Rif nappes (see Fig. 1) of northern Morocco and that the Tiz-n-Test Fault System and the Hayes Fracture Zone are not connected. The Hayes Fracture Zone represents a flow line (Pitman & Talwani, 1972), which can be traced from the East Coast Magnetic Anomaly (Vogt, 1973) offshore Nova Scotia on the North American continental margin throughout the Central Atlantic to the S1 magnetic anomaly 1–3°W of the onshore termination of the Tiz-n-Test Fault System (Gradstein et al., 1990; Klitgord & Schouten, 1986). Depending on the degree of left-lateral strike-slip shear in the Triassic Central to North Atlantic rift zone, the southern Nova Scotian shelf (e.g. LaHave Basin; Keen et al., 1990; Wade & MacLean, 1990) to Connecticut shelf (Long Island Platform; Klitgord, Hutchinson, & Schouten, 1988) identify as the North American conjugate continental margin of the northwest African Agadir margin.

Existing balanced cross-sections focus on the Central High Atlas (Beauchamp et al., 1999; Gomez et al., 2000) and indicate shortening rates of 25%. According to Gomez et al. (2000) crustal shortening decreases from the Central High Atlas to the WHA and was directed NNW–SSE (Miocene 355°, Pliocene 340°). Mustaphi et al. (1997) calculated shortening rates of 11–12% for a transect from the Souss Basin (El Klèa Anticline, Fig. 3) to the Ida-ou-Tanane area (Axial Zone, Anklout-Tazenakht Anticline, Fig. 3). The northern Sub-Atlasian Zone remained largely unaffected by crustal shortening.

The trace of the Agadir Basin transect (Fig. 4) presented in this paper runs NE–SW (235°), at an angle of 105–120° to the direction of Mio-/Pliocene shortening. It crosses

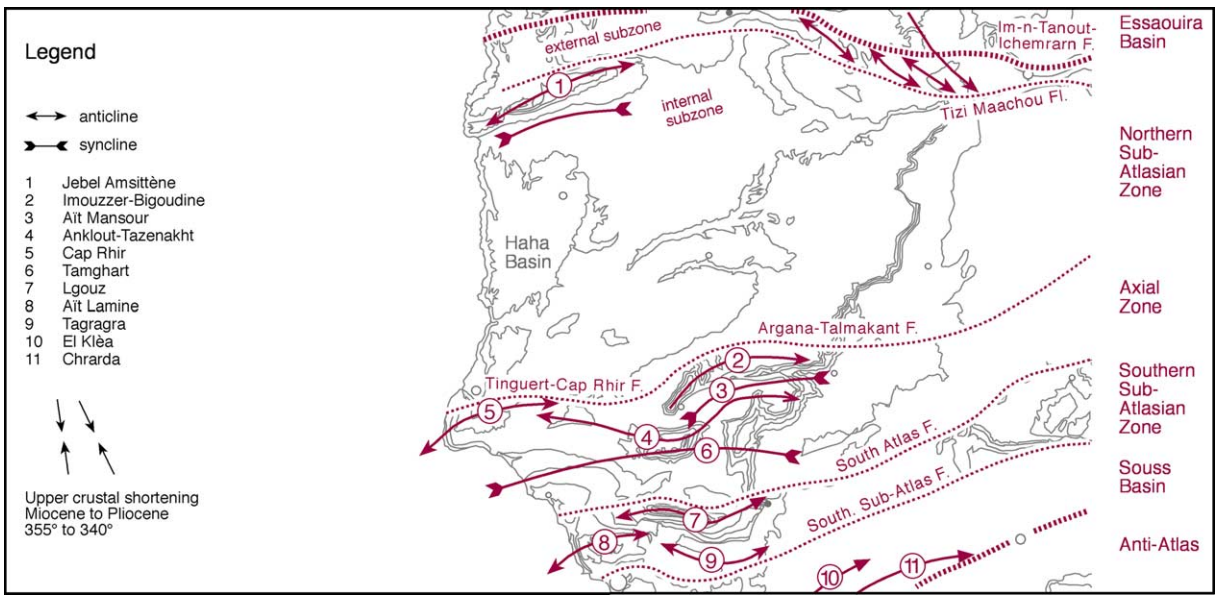

Fig. 3. Structural map of western High Atlas (inverted Agadir continental margin basin), the southern part of the Essaouira Basin and the northern part of the Souss Basin (cf. Fig. 1; after Ambroggi (1963), Amrhar (1995), Duffaud (1960), and Gomez et al. (2000)).

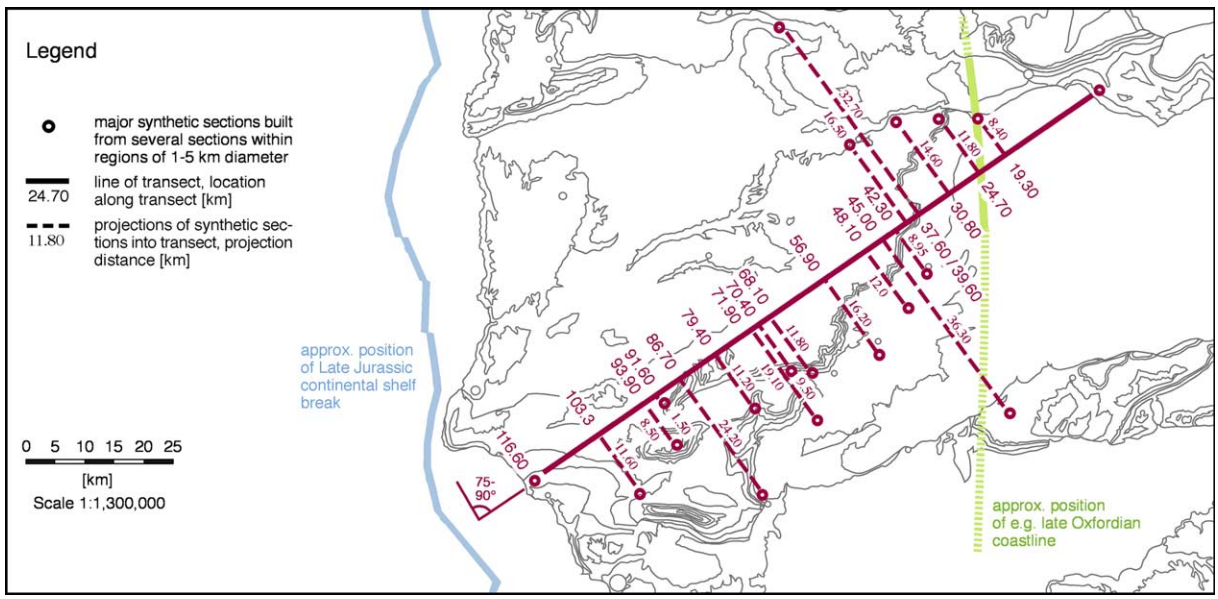

Fig. 4. Geological transect through the inverted Agadir continental margin basin including the locations of major synthetic sections projected into the transect. The transect runs NE–SW between east of the cities of Im-n-Tanout and north of Agadir. Approximate position of the Late Jurassic continental shelf break according to Hafid (2000).

the northern Sub-Atlasian Zone to Axial Zone. Two synthetic sections with data for the Triassic and the Tertiary succession were projected from the southern Sub-Atlasian Zone. Gradual lateral changes of depositional environments in the WHA (this study) and fault kinematic results by Fraissinet et al. (1988) and Morel, Zouine, Andrieux, and Faure-Muret (2000) in the Central High Atlas exclude significant wrench tectonics. Therefore, the original width and internal architecture of the Meso-/Cenozoic shelf margin basin is adequately represented in the transect. Geometric reconstructions show that crustal shortening in NNW–SSE direction resulted in less than 10–15% length reduction of the 116 km transect.

The onshore Agadir Basin transect covers the Mesozoic inner and outer continental shelf of the eastern Central Atlantic. Between the Early Jurassic and the Eocene, coastlines ran NNW–SSE to NNE–SSW (Fig. 4) along the western margin of the Hercynian basement and shifted back and forth for several tens of kilometers. The Mesozoic continental shelf margin ran N–S to NNW–SSE. Its approximate position in time is seismically constrained in the offshore extension of the Agadir Basin. During the Mid- and Late Jurassic it was located about 5–15 km seaward of the present coastline north of Agadir (Hafid, 2000).

3. Previous studies

A considerable number of regional and stratigraphic studies exist for the Agadir Basin and adjacent Moroccan Atlantic Basins. Few studies focused on basin-scale stratigraphy and Meso-/Cenozoic basin development of the Agadir Basin.

Duffaud, Brun, and Plauchut (1966) presented the first synthetic lithostratigraphy of the Agadir Basin (see Fig. 5(B)). Their scheme introduced a large number of local, lithology-based names, which were adapted by subsequent studies.

Medina (1994) studied the structural evolution of the WHA. Medina applied a 1D backstripping approach (isostatic modeling) to three sections at Agadir, Essaouira and Im-n-Tanout. The Jurassic to Eocene vertical succession in the three sections was subdivided into 18–21 time units. Backstripping did not consider the pre-Jurassic basin fill. Medina distinguished two tectono-stratigraphic sequences, which were related to the opening of the Central Atlantic: (1) a syn-rift sequence of probably Anisian to earliest Jurassic age; (2) a post-rift sequence of Jurassic to Cretaceous age affected by mild tectonism. Subsidence analysis revealed four stages of tectonic subsidence at 198–175 Myr (Early Liassic to Early Aalenian), 144–128 Myr (Early Kimmeridgian to Albian), 113–110 Myr (around the Barremian/Albian boundary) and 96–84 Myr (Cenomanian to Santonian), the first three of which were related to normal faulting.

Amrhar (1995) investigated the structural geology and basin inversion of the WHA. His study included lithostratigraphic information of limited temporal and spatial resolution. With the beginning of sea-floor spreading in the Central Atlantic, NNE–SSW to NE–SW trending normal faults developed and remained active until the Early Late Jurassic. The emplacement of doleritic dikes during this period was related to increased spreading rates in the Central Atlantic. In the earliest Cretaceous, fault movement was reduced owing to decreased sea-floor spreading rates.

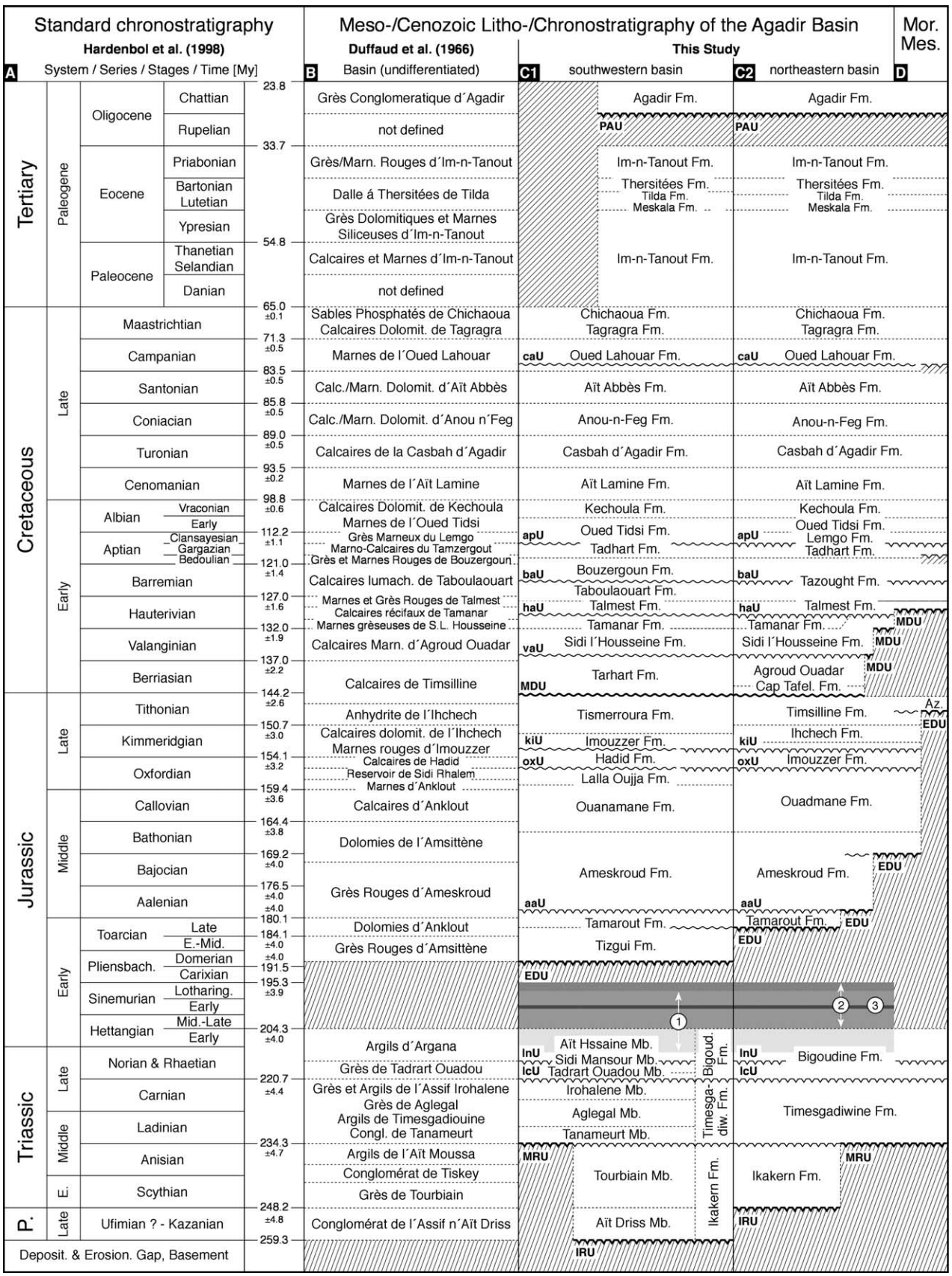
Standard chronostratigraphy
Hardenbol et al. (1998)
A
System / Series / Stages / Time [My]
Meso-/Cenozoic Litho-/Chronostratigraphy of the Agadir Basin
Duffaud et al. (1966)
B
Basin (undifferentiated)
This Study
C1
southwestern basin
C2
northeastern basin
D
Mor. Mes.
Tertiary
Paleogene
Oligocene
Chattian
Rupelian
Eocene
Priabonian
Bartonian
Lutetian
Ypresian
Paleocene
Thanetian
Selandian
Danian
Cretaceous
Late
Maastrichtian
Campanian
Santonian
Coniacian
Turonian
Cenomanian
Early
Albian
Vraconian
Early
Aptian
Clansayesian
Gargazian
Bedoulian
Barremian
Hauterivian
Valanginian
Berriasian
Jurassic
Late
Tithonian
Kimmeridgian
Oxfordian
Middle
Callovian
Bathonian
Bajocian
Aalenian
Early
Toarcian
Late
E.-Mid.
Pliensbach.
Domerian
Carixian
Sinemurian
Lotharing.
Early
Hettangian
Mid.-Late
Early
Triassic
Late
Norian & Rhaetian
Carnian
Middle
Ladinian
Anisian
E.
Scythian
P.
Late
Ufimian ? - Kazanian
Deposit. & Erosion. Gap, Basement
23.8
33.7
54.8
65.0 ±0.1
71.3 ±0.5
83.5 ±0.5
85.8 ±0.5
89.0 ±0.5
93.5 ±0.2
98.8 ±0.6
112.2 ±1.1
121.0 ±1.4
127.0 ±1.6
132.0 ±1.9
137.0 ±2.2
144.2 ±2.6
150.7 ±3.0
154.1 ±3.2
159.4 ±3.6
164.4 ±3.8
169.2 ±4.0
176.5 ±4.0 ±4.0
180.1
184.1 ±4.0
191.5
195.3 ±3.9
204.3 ±4.0
220.7 ±4.4
234.3 ±4.7
248.2 ±4.8
259.3
Grès Conglomeratique d´Agadir
not defined
Grès/Marn. Rouges d´Im-n-Tanout
Dalle á Thersitées de Tilda
Grès Dolomitiques et Marnes Siliceuses d´Im-n-Tanout
Calcaires et Marnes d´Im-n-Tanout
not defined
Sables Phosphatés de Chichaoua
Calcaires Dolomit. de Tagragra
Marnes de l´Oued Lahouar
Calc./Marn. Dolomit. d´Aït Abbès
Calc./Marn. Dolomit. d´Anou n´Feg
Calcaires de la Casbah d´Agadir
Marnes de l´Aït Lamine
Calcaires Dolomit. de Kechoula
Marnes de l´Oued Tidsi
Grès Marneux du Lemgo
Marno-Calcaires du Tamzergout
Grès et Marnes Rouges de Bouzergoun
Calcaires lumach. de Taboulaouart
Marnes et Grès Rouges de Talmest
Calcaires récifaux de Tamanar
Marnes grèseuses de S.L. Housseine
Calcaires Marn. d´Agroud Ouadar
Calcaires de Timsilline
Anhydrite de l´Ihchech
Calcaires dolomit. de l´Ihchech
Marnes rouges d´Imouzzer
Calcaires de Hadid
Reservoir de Sidi Rhalem
Marnes d´Anklout
Calcaires d´Anklout
Dolomies de l´Amsittène
Grès Rouges d´Ameskroud
Dolomies d´Anklout
Grès Rouges d´Amsittène
Argils d´Argana
Grès de Tadrart Ouadou
Grès et Argils de l´Assif Irohalene
Grès de Aglegal
Argils de Timesgadiouine
Congl. de Tanameurt
Argils de l´Aït Moussa
Conglomérat de Tiskey
Grès de Tourbiain
Conglomérat de l´Assif n´Aït Driss
Agadir Fm.
PAU
Im-n-Tanout Fm.
Thersitées Fm.
Tilda Fm.
Meskala Fm.
Im-n-Tanout Fm.
Chichaoua Fm.
Tagragra Fm.
caU
Oued Lahouar Fm.
Aït Abbès Fm.
Anou-n-Feg Fm.
Casbah d´Agadir Fm.
Aït Lamine Fm.
Kechoula Fm.
Oued Tidsi Fm.
apU
Tadhart Fm.
Lemgo Fm.
Bouzergoun Fm.
baU
Tazought Fm.
Taboulaouart Fm.
Talmest Fm.
haU
Tamanar Fm.
MDU
Sidi l´Housseine Fm.
vaU
Agroud Ouadar
Cap Tafel. Fm.
Tarhart Fm.
Tismerroura Fm.
Timsilline Fm.
Az.
EDU
Ihchech Fm.
kiU
Imouzzer Fm.
oxU
Hadid Fm.
Lalla Oujja Fm.
Ouanamane Fm.
Ouadmane Fm.
Ameskroud Fm.
aaU
Tamarout Fm.
Tizgui Fm.
1
2
3
Aït Hssaine Mb.
lnU
Sidi Mansour Mb.
lcU
Tadrart Ouadou Mb.
Bigoud. Fm.
Bigoudine Fm.
Irohalene Mb.
Aglegal Mb.
Tanameurt Mb.
Timesga-diw. Fm.
Timesgadiwine Fm.
MRU
Tourbiain Mb.
Ikakern Fm.
Aït Driss Mb.
IRU

Labbassi (1997) and Labbassi, Medina, Rimi, Mustaphi, and Bouatmani (2000) applied a 1D backstripping approach to the Essaouira Basin. The Middle Triassic to Tertiary vertical succession in six wells was subdivided into 15 time units. Several basin evolution periods were recognized: (1) a syn-rift phase during the Late Triassic to earliest Liassic (240–201 Myr), associated with extensional tectonism; (2) post-rift phases during the Late Liassic (187–167 Myr), the Late Jurassic to Early Cretaceous (141–130 Myr) and the Hauterivian to Aptian (120–108 Myr). The amount of crustal stretching in the onshore area amounts to $\beta = 1.19–1.56$ or $\beta = 1.17$, when Triassic sediments are distributed in a uniform basin.

Le Roy (1997) presented a seismostratigraphic study of the Atlantic margin of Morocco including the Doukkala, Essaouira and Tarfaya/Agadir Basins (sic, Tarfaya Basin and northern adjacent areas up to the city of Agadir). The continental margin basin preserved in the WHA (Agadir Basin of this study) was not included. Based on seismic unconformities, five seismostratigraphic units within the Permian to Eocene basin fill were distinguished in the Essaouira Basin. Unconformities occur (1) at the top Early Liassic; (2) in the Berriasian; (3) in the Barremian to Aptian; (4) in the Albian to Cenomanian; (5) in the Turonian. Le Roy followed a qualitative allostratigraphic approach to define long-term transgressive and regressive trends. For 1D backstripping analyses, the Jurassic to Cretaceous vertical succession was subdivided into 12 time units. Backstripping did not consider the pre-Jurassic basin fill. Le Roy distinguished four basin evolution stages: (1) Late Triassic to Early Liassic rifting; (2) largely stable continental shelf (plateforme) development in the Liassic to Berriasian; (3) large-scale gentle flexure and transpression between the Berriasian and the Albian; (4) progradation of the continental shelf from the Cenomanian to the Cenozoic.

Hafid (1999, 2000) and Hafid, Salem, and Bally (2000) studied the Meso-/Cenozoic development of the Essaouira Basin, situated to the north of the Agadir Basin, by a qualitative approach based on seismic lines and wells. Their model considered ten seismostratigraphic units in the Mid-Triassic to Paleogene sedimentary succession. Hafid (2000) focused on the structural development of Late Triassic to Early Liassic halfgrabens and their inversion in the Tertiary. Hafid et al. (2000) dealt with the extension of the onshore Jebilet–High Atlas system and its intersection with the Atlantic passive margin.

So far, the following information and models are lacking for the Agadir Basin: (1) synthetic basin stratigraphy along 2D transects and at the time resolution of geological stages; (2) basin architecture in time; (3) flexural reverse basin modeling; (4) a genetic, process-oriented model of the basin development based on the quantitative analysis of subsidence/uplift components, sea-level changes and sediment flux; (5) detailed correlation of the Agadir Basin development with the evolution of the Central/North Atlantic at the time resolution of stages and magnetic polarity chronozones. Information and models listed under (1) and (2) are partly existent for other Moroccan Atlantic Basins, however at a considerably lower resolution of time. Information and models listed under (3)–(5) do not exist for northwest African Atlantic Basins.

4. Meso- to Cenozoic stratigraphy and depositional setting of the Agadir Basin

Initial deposition in the Agadir Basin occurred in the Stephanian to Autunian. However, the main basin development associated to the initial breakup of Pangea started in the Early/Late Permian to Early Triassic and continued throughout the Mesozoic until the Tertiary. The Mesozoic to Cenozoic basin fill was considerably influenced by the Late Permian to Triassic paleotopography and the location of depocenters. The following description of the stratigraphy and the depositional settings of the Agadir Basin fill includes long-term, basin-scale developments of second order (3–10 Myr; Duval, Cramez, & Vail, 1992). Special focus is on the Jurassic, where high-resolution biostratigraphic data are available and where detailed spatial and geometric data have been measured in the field as part of this project. Data for the Triassic have limited time but reasonable spatial resolution and were derived from the literature. Data for the Cretaceous to Tertiary succession also come from the literature and have good biostratigraphic and moderate spatial resolution. So far, seismic sections or

Fig. 5. Meso- to Cenozoic litho- and chronostratigraphic schemes for the Agadir Basin. Time axis is not to scale. (A) Standard chronostratigraphy according to Hardenbol et al. (1998). Absolute ages in Million years according to Gradstein et al. (1994) (Mesozoic) and Berggren et al. (1995) (Cenozoic). Time horizons indicated have been included in reverse numerical basin modeling of the Agadir Basin. (B) Lithostratigraphic scheme for the Agadir Basin according to Duffaud et al. (1966). (C) Litho- and chronostratigraphic scheme for the northeastern and southwestern part of the Agadir Basin developed and compiled for this study. Cross-hatched areas indicate long-term depositional and/or erosional gaps. Bold capitals (e.g. **IRU**) and thick lines indicate erosive and/or angular unconformities and correlative conformities at the resolution of time layers. Bold normal letters (e.g. **aaU**) and thin lines indicate erosive and/or angular unconformities and correlative conformities below the resolution of time layers. Short-term depositional and/or erosional gaps (below stage resolution) are not indicated. Zig-Zag lines represent erosive and/or angular unconformities, wavy lines correlative conformities and thin broken lines formation boundaries. For unconformities see text and Figs. 6–8. (D) Litho- and chronostratigraphic scheme for the southern part of the Moroccan Meseta (Mor. Mes.), 35 km east of 0 km AT (transect see Fig. 4), near Amizmiz. Legend: 1—absolute ages of tholeiites in the High/Middle Atlas (Fiechtner, Friedrichsen, & Hammerschmidt, 1992; Table 4); 2—absolute ages of tholeiites on the Guyana and Guinea margins (Deckart et al., 1997; Table 4); 3—average age of tholeiites on the Guyana and Guinea margins.

well data for the onshore Agadir Basin have not been published.

4.1. Late Permian to Early Jurassic

The Late Permian to Liassic succession is mainly comprised of terrigenous clastics ranging from conglomerates to red silt- and sandstones. It rests unconformably on the Hercynian (Cambrian to Silurian?) basement. The Triassic series has been studied by Brown (1980), Brown and Fischer (1974), Duffaud et al. (1966), Medina (1994, 1995), Tixeront (1973, 1974), and Tourani, Lund, Benaouiss, and Gaupp (2000).

Late Permian to Early Mid-Triassic—The Ikakern Fm. (0–2500 m) is divided into two members. The basal Aït Driss Mb. shows alluvial fan conglomerates and sandstone channels, which reach total thicknesses of up to 1500 m in the type area. The middle and upper part of the formation is represented by the Tourbiain (syn. Tourbihine) Mb. with fluvial conglomerates, sandstones, intercalated siltstones and shales and maximum thicknesses of 1000 m. The Ikakern Fm. occurs only in the Argana Valley between Argana and Assif N'Aït Dris. Deposition was confined to large graben valleys, triggered by initial rifting of the basement. Maximum total thicknesses of the Ikakern Fm. in the central graben valley reach 900–1700 m (Brown, 1980; Tourani et al., 2000). The formation pinches out completely against the Hercynian high in the NE. The age of the Ikakern Fm. was disputed. It ranged between post-Early Permian to Mid-Triassic (Medina, 1994) and Late Triassic (Hafid, 1999). Based on vertebrate remains, Jalil (1999) and Jalil and Dutuit (1996) showed that the Ikakern Fm. is partly or completely of Late Permian age (Ufimian to Kazanian).

Late Middle Triassic to Late Triassic—The Timesgadiwine Fm. lies unconformably on the Ikakern Fm. The basal Tanameurt Mb. extends over wide parts of the Argana Valley with thicknesses of 0–30 m. The boundary to the Aglegal Mb. (800–1500 m) is defined by a thin (25 m) calcareous interval. Characean algae and ostracods indicate intermittent lacustrine depositional environments. Shales and intercalated channel sandstones dominate the Aglegal Mb. The Irohalene Mb. (200–500 m) with thick channelized sandstones and red shales occurs mainly in the southern part of the basin (Medina, 1994). According to the majority of studies (Brown, 1980; Dutuit & Heyler, 1983) depositional environments changed from coastal plains to estuaries (indicated by phyllopods) and delta tops. Vertebrate remains indicate a Late Triassic age (Dutuit, 1966).

Late Triassic to Early Jurassic (Sinemurian)—The Bigoudine Fm. unconformably overlies the Timesgadiwine Fm. Basal alluvial quartzite conglomerates were transported from SE/E to NW/W. Subsequently, eolian to deltaic depositional environments prevailed as indicated in the Tadrart Ouadou Mb. (0–150 m) exposed in the Amzri-Bigoudine area. Delta plain sand- and siltstones comprise the Sidi Mansour Mb. (0–200 m). It contains the phyllopods *Estheria minuta* and *Estheria destombesi* (Defrentin & Fauvelet, 1951). The upper part of the Bigoudine Fm. shows mainly shales (Aït Hssaine Mb., 300–1100 m) deposited in a wide mud flat which was locally cut by anastomosing channels. Basalts with thicknesses of up to 150 m conclude the Late Triassic to Early Liassic Agadir Basin development.

Basalt flows occur on the North American (Olsen, 1997), South American and African continental margins (Deckart, Feraud, & Bertrand, 1997) of the Central Atlantic (see Table 4). Along the 4500 km stretch of the future eastern Central Atlantic margin between Liberia and Iberia intense magmatic activity occurred between 204 and 195 Myr (Middle Hettangian to latest Sinemurian, probably less for the bulk of the magmatism) and marks the initial breakup of the Pangean supercontinent. Breakup of the continental lithosphere centered in the south of the region (Guyana, Guinea) but seems to have affected the whole Central Atlantic within a time span of 9 Myr. The data of Deckart et al. (1997) and Olsen (1997) indicate, that the distal parts of the northwest African and North American margin have actually represented a volcanic continental margin and not a non-volcanic margin as otherwise assumed (Minshull & Charvis, 2001).

The Late Permian to Early Liassic basin stage marks continental rifting with regional graben valleys, which were quickly filled by terrigenous to marginal marine sediments. Rift basins were limited by NNE–SSW to NE–SE trending master faults against the Hercynian basement. Internal structural highs and lows are separated by ENE–WSW to E–W trending transfer faults (Le Roy & Piqué, 2001; Schaer, 1987; Tixeront, 1974). The basin transect of this paper (Fig. 4) runs obliquely to the overall trend of the Permo-Triassic rift basin. It is focused on the high-resolution architecture and development of the Jurassic to Early Tertiary continental margin basin with ENE–WSW to ESE–WNW dipping depositional gradients.

4.2. Early to Late Jurassic

In the Late Early to Early Middle Jurassic, open marine deposition established on the Moroccan continental margin. Depositional environments range from carbonate ramps to deltas. Biostratigraphic and lithofacies data for the Jurassic basin fill come from Bouaouda (1987, 2002) and, to a large extent, from sections measured in detail during this project.

Early Jurassic (Pliensbachian to Toarcian)—The Middle Hettangian to Early Pliensbachian (Carixian) of the Agadir Basin is represented by a major subaerial hiatus. In the northern Essaouira Basin, carbonate ramps were deposited at the same time. The regressive trend in the Agadir Basin continues with fluvial deposits of the Tizgui Fm. (Figs. 5 and 7; Bouaouda, 1987) with thicknesses between 0 and 200 m. They are confined to the western part of the basin. Excellent outcrops exist in the Anklout Anticline, at Immouzzer and Lgouz. Towards the east (Ameskroud)

the age of the Tizgui Fm. changes gradually to Domerian to Middle Toarcian, based on correlations with equivalent series at the Jebel Amsittène Anticline in the southern Essaouira Basin (Bouaouda, 1987; Du Dresnay, 1988; Duffaud et al., 1966).

Late Toarcian to Early Aalenian—In the Late Toarcian the first major transgression reached the Agadir Basin from the west. Thicknesses of the Tamarout Fm. (Adams, Ager, & Harding, 1980) diminish from 300 m in the west to approximately 5 m in the east. Deposition took place on a wide carbonate-evaporite ramp. Brachiopod faunas indicate the Late Toarcian to Early Aalenian (?) age of the Tamarout Fm. In the eastern part of the basin, the Tamarout Fm. outsteps considerably the underlying Tizgui Fm. In this part of the basin, the Late Toarcian series overlies directly the Early Hettangian red shales of the upper Bigoudine Fm (Aït Hssaine Mb., syn. Hasseine Mb.). However, transgressions did not reach the eastern border of the Late Jurassic Agadir Basin until the Bajocian.

Early Aalenian to Middle Bathonian—Regression resulted in the deposition of thick conglomerates, sand- and siltstones of the Ameskroud Fm. Thicknesses reach 200–400 m in the western part of the basin, but diminish to 10–70 m in the E, where fluvial deposition took place. Short-term marine incursions in the Ameskroud Fm. are restricted to the western Agadir Basin.

Late Bathonian to Callovian—In the Late Bathonian a renewed transgression started, which became more pronounced than the Late Toarcian transgression. Time-equivalent transgressions are known from the eastern North American continental margin. The Late Bathonian to Early Callovian transgression steps considerably over the previous eastern basin margins. Marine deposition shifts as far as east of Im-n-Tanout. Near Seksaoua, Late Bathonian lagoonal to coastal depositional environments exist. Biostratigraphic ages are based on a rich fauna of ammonites, brachiopods, benthic foraminifera and dasycladacean algae (Ambroggi, 1963; Bouaouda, 1987; Duffaud, 1960). During the Callovian, open marine depositional environments developed over wide parts of the continental margin. In the western part of the Agadir Basin (Anklout, Immouzzer) distal carbonate ramps of the Ouanamane Fm. were initiated with total thicknesses of 80–120 m. They are mainly oolitic and bioclastic carbonates with abundant brachiopods and intercalated marls. Towards the NE of the Agadir Basin, near Im-n-Tanout, thicknesses become strongly reduced to 5–30 m and depositional settings change to marginal marine and terrestrial in the Late Callovian.

Mid-Oxfordian—Deposition shifted to rimmed carbonate shelves. Homoclinal ramps, distally steepened ramps and thin intra-shelf platforms with abundant marginal reefs and local sand bars developed in the western Agadir Basin (Lalla Oujja Fm.; Adams et al., 1980; Bouaouda, 1987). Other lithofacies include boundstones and massive, porous dolomites with thicknesses of 15–80 m. The geometry of intra-shelf ramp/platform-to-basin transitions is strongly influenced by the pre-existing bathymetric relief and by local variations in sediment production and input. Ramp/platforms and basins were irregularly distributed over the continental shelf. No continuous linear reef trend existed. In the eastern part of the basin time-equivalent inner lagoonal to coastal deposits are strongly condensed (2–10 m).

Late Oxfordian to Early Kimmeridgian—The Hadid Fm. (syn. Iggui El Behar Fm.; Adams et al., 1980; Bouaouda, 1987) thickens from NE to SW to a maximum of 80–120 m and comprises mud-/wackestones, bioturbated bioclastic carbonates and dolomites. Only in the westernmost part of the basin (Cap Rhir), local reefs persisted from the Middle Oxfordian to the Early Kimmeridgian. The western to central basin shows low-energy deposition in inner shelf (lagoonal) environments. Near Im-n-Tanout this succession is reduced to thicknesses of 10–15 m and changes laterally into deltaic environments. The Middle Oxfordian to Early Kimmeridgian series did not overstep the Callovian extension of the Agadir Basin (cf. Medina, 1994, p. 102).

Early Kimmeridgian—During the Early Kimmeridgian terrigenous input into the Agadir Basin strongly increased (sandstones, marls, evaporites, dolomites). In the western part of the basin, the Immouzzer Fm. (80–150 m) shows red marls with intercalated carbonates and alternating lagoonal to sabkha carbonates and marginal marine shales. Deposition took place in low-energy inner shelf settings. Marine intercalations vanish towards the NE. Fluvial, deltaic and marginal marine siltstones, marls and evaporitic dolomites with total thicknesses of 15–251 m dominate in the eastern basin. In the Early Kimmeridgian deposition extended further to the NE, although truly open marine environments were restricted to the western basin. The Immouzzer Fm. may reach into the Late Kimmeridgian.

Late Kimmeridgian to Tithonian—Carbonate-evaporite deposition replaced the terrigenous-detrital deposition of the Early Kimmeridgian. Persistent shallow marine to supratidal environments in the western basin resulted in the 300–400 m thick Tismerroura Fm. (Adams et al., 1980). The base shows bioclastic open lagoonal carbonates (20–55 m). Inner lagoonal, intertidal carbonates and evaporites (dolomites, marls, anhydrite) represent the middle part (200–300 m thickness). The top of the Tismerroura Fm. (Late Tithonian) indicates a shift to open marine, outer shelf environments. In the eastern part of the basin, deposition was more restricted. Inner lagoonal sandstones, dolomites and anhydrites with thicknesses of 40–60 m developed (Ihchech, Timsilline Fms.). The Late Kimmeridgian to Tithonian series is considerably thinner than the 200–250 m indicated by Medina (1989). In the Late Tithonian, continental deposition in the Agadir Basin reached its largest Jurassic extension towards the NE. It reached as far as Amizmiz, 60 km east of Im-n-Tanout (Canerot et al., 1986; Choubert, 1957; Duffaud, 1981; Rey, Canerot, Peybernes, Taj-Eddine, & Thieuloy, 1988) (see Fig. 5(D)).

4.3. Cretaceous

Data for the Cretaceous basin succession come from Adams et al. (1980), Algouti (1991), Algouti, Chbani, and Azzaoui (1993), Ambroggi (1963), Behrens et al. (1978), Behrens and Siehl (1982), Duffaud (1960), Duffaud et al. (1966), Ettachfini (1992, 1993), Ettachfini, El Kamali, and Bilotte (1989), Medina (1989, 1994), von Rad et al. (1982), Rey et al. (1988), Stamm and Thein (1982), Taj-Eddine (1991), and Wiedmann, Butt, and Einsele (1978, 1982).

Berriasian—The Tarhart Fm. (Adams et al., 1980) comprises 100–130 m of bioclastic carbonates, deposited in open marine outer shelf environments of the western Agadir Basin. The top of the formation is Early Valanginian. In the central and eastern basin carbonates of the Cap Tafelney Fm. and the Agroud Ouadar Fm. developed in increasingly more inner shelf to marginal marine settings. At the eastern basin margin, in the area near Im-n-Tanout, the Early Cretaceous period is characterized by a subaerial hiatus (see below).

Valanginian—Green marls and sandy/silty carbonates build the lower part of the Sidi Houssseine Fm. Towards the top silt- and sandstones prevail. The total thickness of the formation is 30–50 m. Deposition took place in upper to lower prodelta environments.

Hauterivian—The Hauterivian comprises the Tamanar and Talmest Fms. as well as the lower part of the Taboulaouart Fm. Total thicknesses range between 150 and 180 m. Bioclastic, mainly lamellibranch-rich carbonates (Tamanar Fm., 40–50 m), deposited in inner to middle shelf settings prevail (Anklout region). Towards the E, sandstones become more frequently intercalated. Near Im-n-Tanout, the Tamanar Fm. pinches out. In the same area, the overlying Talmest Fm. includes sandstones, conglomerates and red shales. Intercalations of carbonates rich in lamellibranchs indicate progressively open marine conditions which become more abundant towards the W (70–100 m). At the present-day shoreline, north of Agadir, green shales and pelagic marls with total thicknesses of 250–300 m prevail. From NE to SW, depositional environments in the Talmest Fm. changed laterally from fluvio-deltaic conditions (eastern part of the basin) to inner shelf (central basin) and outer shelf settings (western part of the basin). Latest Hauterivian carbonates belong to the basal Taboulaouart Fm.

Barremian—In the Agadir area, lamellibranchian carbonates and marls of the Taboulaouart Fm. (40–70 m) continue into the Early Barremian. Deposition took place in inner to middle shelf environments. In the Late Barremian (Bouzergoun Fm.), intercalations of sandstones and reddish marls become more frequent. Finally, subaerial conditions were established which lasted until the Early Aptian (Bedoulian) over wide parts of the basin. In the eastern basin, near Im-n-Tanout, fluvial sand- and siltstones of the Tazought Fm. (30–40 m) were deposited throughout the Barremian.

Aptian—The Mid-Aptian (Gargazian) is represented by the Tadhart Fm. The Gargazian includes a 5–30 m thick succession of carbonates and marls with ammonites (*Aconoceras nisus*). In the western basin, the Late Aptian (Clansayesian) corresponds to 7–16 m thick green and yellow marls with ammonites and intercalated sandy dolomites and red sandstones (lower Oued Tidsi Fm.). Deposition took place in an outer shelf environment. Open marine water circulation is indicated by a high-diversity benthonic fauna. In the eastern basin, near Im-n-Tanout, the Tadhart Fm. of the Mid-Aptian shows carbonates and marls with open marine faunas (thickness 50–70 m) followed by the Lemgo Fm., 15–20 m thick, with subordinate detritic input and dolomites. In general, the Aptian shows strongly transgressive conditions. In the Late Aptian (Clansayesian), the maximum Early Cretaceous transgression occurred and shifted the eastern coastline of the Agadir Basin to the Amizmiz area, situated 60 km east of Im-n-Tanout. As a result a large marine gulf came into existence, which reached its largest extent in the Late Aptian to Early Albian.

Albian—Between the Late Aptian and the Early Albian deposition continued without major breaks in lithofacies or depositional environments. In the western basin, the Albian succession is exceptionally thick and reaches 500–600 m. It is subdivided into the Oued Tidsi and Kechouala Fms. Shales and marls with cephalopods of the Oued Tidsi Fm. (250–480 m) document open marine conditions and outer shelf to basin margin settings. Carbonates and some intercalated marls build the Kechouala Fm. (60–150 m). On regional submarine highs, intra-formational breccias and arenites resulting from ravinement by strong submarine currents mark the boundary between both formations. In the Late Albian, regressive calcareous dolomites of the middle and upper Kechouala Fm. developed. In the eastern basin 50–150 m thick marls and carbonates with ammonites were deposited.

Cenomanian—In the western basin marls and carbonates of the Aït Lamine Fm. (300–500 m) represent the Cenomanian. Between the Early to Late Cenomanian, shallow marine environments changed to relatively deep, open marine outer shelf environments. In the eastern basin, Cenomanian deposits reach thicknesses of 150–200 m and comprise marls, calcareous dolomites and sandstones with intercalations of anhydrite. Deposition took place in an inner shelf, peritidal setting. On a basinwide scale, the Late Albian to Cenomanian contains the most significant transgression during the Cretaceous. This transgressive peak is well recorded in the western basin succession where the maximum water depths of the Meso-/Cenozoic continental shelf interior of the Agadir Basin are encountered. At the eastern basin margin, however, the Cenomanian transgressive peak is less evident.

Turonian—The Turonian deposits form a conspicuous succession within the Late Cretaceous basin fill (Casbah d'Agadir Fm.). In the western basin the 85 m thick succession includes organic-rich deep-water carbonates

and phosphorites with dominantly planktonic faunas. In the northeastern part of the basin, near Im-n-Tanout, bioclastic carbonates and dolomites with total thicknesses of 50–70 m prevail. The Turonian initially shows a transgressive trend, followed by a marked regression. The paleogeography is characterized by a single marine gulf which extends also over the Essaouira Basin.

Senonian (Coniacian to Santonian)—Two contradicting paleogeographic models exist for the Senonian. According to older studies (Duffaud et al., 1966) the large-scale paleogeography of the Agadir and the adjacent Essaouira Basins was completely changed in the Senonian. Two large marine gulfs, trending E–W and separated by a central high in the Haha area (Fig. 2) developed. The northern gulf extended between Essaouira and Im-n-Tanout. The southern gulf extended between Agadir and Taroudant. According to Wurster and Stets (1982) the Senonian paleogeography shows a single marine gulf, covering both the Essaouira and Agadir Basins.

Coniacian—The Coniacian is represented by the Anoun-Feg Fm. with a thickness of 140 m in the western and approximately 50 m in the eastern part of the basin. In the westernmost basin, the formation includes marls, siltstones and some carbonate intercalations deposited in an inner shelf to peritidal setting. In the western to central part of the basin, carbonates and marls with lamellibranchs at the base change upsection to sandy dolomites, red silty mudstones and, towards the top, evaporites. In the eastern part of the Agadir Basin, a peritidal to marginal marine succession of (calcareous) dolomites prevails.

Santonian—The Santonian shows mainly inner shelf to peritidal environments. Marly carbonates and marls build the Aït Labbes Fm. with thicknesses of 80–120 m in the western part of the basin. Thicknesses increase to 475 m towards the east, in the region of Erguita, where sandstones and red marls with evaporites prevail.

Campanian—In the westernmost basin, marls and dolomites of the Oued Lahouar Fm. were deposited in outer to inner shelf environments. Towards the central basin sandy dolomites become more frequent. Thicknesses range between 100 and 200 m. In the eastern part of the basin, marginal marine conditions resulted in the deposition of silicified marls and marly dolomites (40–75 m).

Maastrichtian—Different paleogeographic models exist for the Maastrichtian. According to Ambroggi (1963) two separate basins existed—a western basin in the region of Agadir and an eastern basin in the region of Erguita and Im-n-Tanout trending N–S. According to Medina (1994) both subbasins were connected. The Tagrara and Chichaoua Fms. represent a 160–240 m thick succession in the western part of the basin and comprises silicified bioclastic carbonates and marls deposited in a marginal marine setting. In the eastern basin, thicknesses reach 300 m. Sandstones and phosphate-rich clastics with plant remains prevail.

4.4. Tertiary

Data for the Tertiary stratigraphy and lithofacies come from Duffaud et al. (1966) and Trappe (1992). They refer mainly to the Paleocene to Eocene in the eastern part of the Agadir Basin.

Paleocene—The Paleocene series in the eastern part of the basin is represented by the Im-n-Tanout Fm. with carbonates deposited in inner shelf to lagoonal settings. Thickness is approximately 50–60 m. Phosphorites increase towards the W.

Eocene—The uppermost 15–20 m of the Im-n-Tanout Fm. reach into the Early Eocene. No significant shift in facies or depositional/erosional hiatus exists between the Thanetian (Late Paleocene) and the Early Eocene. The Lutetian (Middle Eocene) is subdivided into the Meskala (porcelanites, 25 m), Tilda (marls, 30–35 m) and Thersitées Fms. (inner shelf bioclastic carbonates with bryozoans, 50–60 m). West of Im-n-Tanout phosphoritic carbonates and molluscan carbonates become more frequent. East of Im-n-Tanout, estuarine to inner lagoonal environments existed. The Late Eocene is again represented by the Im-n-Tanout Fm. with sandstones and red marls. Marine deposits of Eocene age only exist between Im-n-Tanout and Essaouira in the N and Taroudant in the S. According to Trappe (1992), a single marine gulf covered the basin in the Eocene.

Oligocene—In the western Agadir Basin, sandstones and conglomerates of the Agadir Fm. overlie unconformably the Maastrichtian succession. They pinch out towards the west. The thickness near Agadir is approximately 1 m. In the eastern Agadir Basin, near Im-n-Tanout, the Agadir Fm. is up to 20 m thick and rests unconformably on the Late Eocene succession.

5. Basin architecture and development

The synthetic sections located on the NE–SW trending transect through the Agadir Basin (Fig. 4) and the lithostratigraphic framework (Fig. 5), which includes bio- and allostratigraphic information, provide the database for the reconstruction of the pre-Atlasian basin architecture (Fig. 8). The datum is the top Eocene (33.7 Myr), which was the approximate time of maximum burial depths. Subsequent time layers were subject to Atlasian compression, uplift and basin inversion (Fig. 3). Starting from the paleobathymetric/topographic model for the top Eocene, the thicknesses of time layers were incrementally added to the top basement surface. Lateral thickness variations between synthetic sections indicated in Fig. 8 are based on large-scale depositional geometries in the field, additional lithofacies information and/or linear interpolation between adjacent synthetic sections.

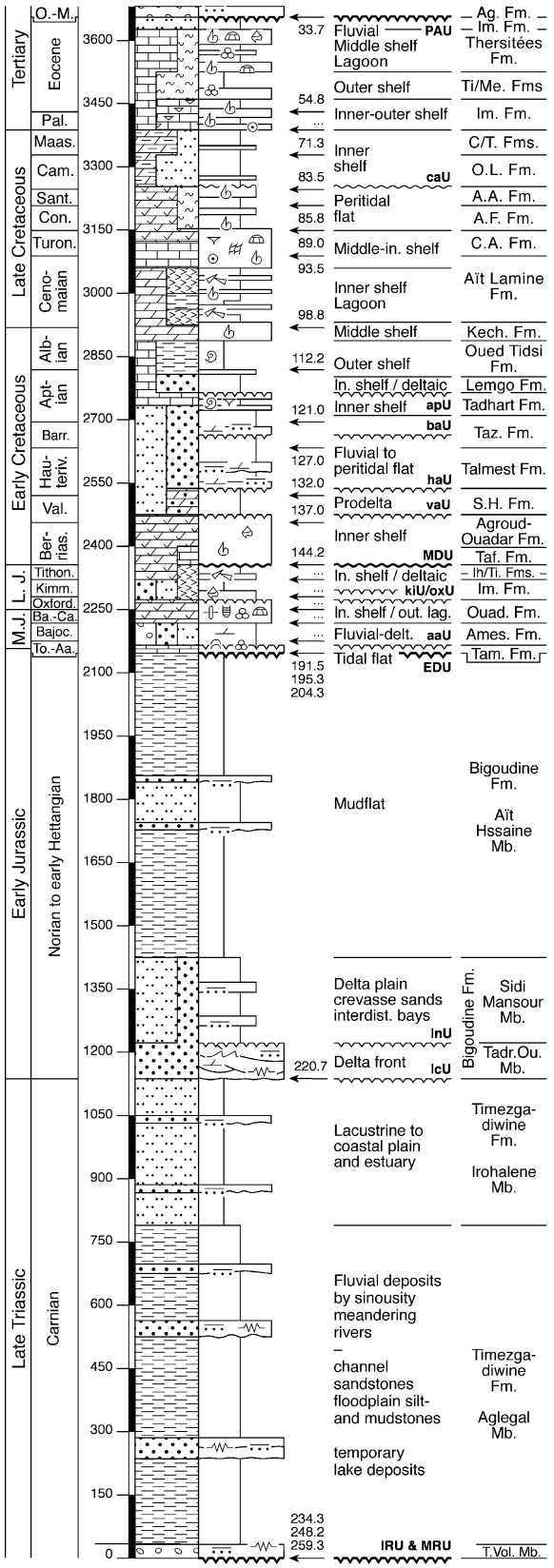

Fig. 6. Synthetic basin section for the northeastern, proximal part of the Agadir Basin at 24.7 km AT (cf. Fig. 4, Oumsissène-NE in Fig. 8). Late Triassic to Early Jurassic volcanites are not shown. Legend (sorted by columns): (1) Formations and Members (sorted by time, Oligocene to Permian): Ag. Fm.—Agadir Fm.; T/T/M. Fm.—Thersitées, Tilda and Meskala Fms.; Ti/Me. Fms.—Tilda and Meskala Fms.; Im. Fm.—Im-n-Tanout Fm.; C/T. Fms.—Chichaoua and Tagragra Fm.; O.L. Fm.—Oued Lahouar Fm.; A.A. Fm.—Aït Abbès Fm.; A.F. Fm.—Anou-n-Feg Fm.; C.A. Fm.—Casbah d'Agadir Fm.; Kech. Fm.—Kechoula Fm.; Tadh. Fm.—Tadhart Fm.; Bouzer. Fm.—Bouzergoun Fm.; Taboul. Fm.—Taboulaouart Fm.; Taz. Fm.—Tazought Fm.; S.H. Fm.—Sidi l'Housseine Fm.; Taf. Fm.—Cap Tafelney Fm.; Ih/Ti. Fm.—Ihchech and Timsilline Fms.; Im. Fm.—Imouzzer Fm.; L. Oujja Fm.—Lalla Oujja Fm.; Ouad. Fm.—Ouadmane Fm.; Ames. Fm.—Ameskroud Fm.; Tam. Fm.—Tamarout Fm.; Tadr. Ou. Mb.—Tadrart Ouadou Mb.; T. Vol. Mb.—Tanameurt Volcaniclastic Mb; (2) Systems, series and stages (sorted by time, Oligocene to Permian): O.-M.—Oligo- to Miocene; Pal.—Paleocene; Maas.—Maastrichtian; Cam.—Campanian; Sant.—Santonian; Con.—Coniacian; Barr.—Barremian; Val.—Valanginian; L.J.—Late Jurassic; Kimm.—Kimmeridgian; Ba.-Ca.—Bathonian to Callovian; M.J.—Middle Jurassic; To.-Aa.—Toarcian to Aalenian; (3) Other: I., In.—Inner; M., Mid.—Middle; O., Out.—Outer; (4) Unconformities at the resolution of time layers (see Figs. 5 and 8): IRU—Initial Rift Unconformity; MRU—Main Rift Unconformity; EDU—Early Drift Unconformity; MDU—Mature Drift Unconformity; PAU—Peak Atlasian Unconformity; (5) Unconformities below the resolution of time layers (see text, Fig. 5): lcU—Late Carnian unconformity; lnU—Late Norian to Rhaetian unconformity; aaU—Early Aalenian unconformity; oxU—Late Oxfordian unconformity; kiU—Early Kimmeridgian unconformity; vaU—Early Valanginian unconformity; haU—Early Hauterivian unconformity; baU—Early Barremian unconformity; apU—Late Aptian unconformity; caU—Early (?) Campanian unconformity; (6) Lines: thick zigzag—basin-scale unconformities; thick wavy—basin-scale correlative conformities; thin zigzag—unconformities of substage duration and without onlap of younger time layers; thin wavy—conformities correlative with unconformities of substage duration and without onlap of younger time layers.

5.1. Unconformities at the resolution of time layers

Basin-scale erosional and/or angular unconformities have been defined by stratal terminations of time layers. Terminations represent major onlaps against older unconformities and migrated laterally for kilometer- to tens of kilometer-distances in time. The reconstructed basin architecture of the onshore Agadir Basin strongly resembles the architecture of other continental shelf basins on the northwest African margin and the conjugate North American margin (e.g. USGS seismic lines 19/20, Wade & MacLean, 1990). Five large-scale unconformities subdivide the basin fill, whose thickness ranges between 1 km in the NE and 8 km in the SW (Figs. 5–8).

The Initial Rift Unconformity (IRU, angular unconformity; cf. basal t1 unconformity of Tixeront (1973)) has an age of pre-259.3 Myr (Late Permian) between 40 and 80 km AT (AT-along transect). It marks the onset of continental deposition in an initial rift halfgraben of the central onshore Agadir Basin. Alluvial deposits of the Ikakern Fm. (Aït Driss, Tourbiain Mbs.) onlap against the eastern master fault and the western flank of the rift halfgraben. Thickness distributions in time, the eastward shift of the western onlap and the westward shift of the eastern onlap document the gradual filling and leveling of the initial rift topography between 259.3 and 234.4 Myr.

The Main Rift Unconformity (MRU, angular unconformity; cf. t1–t2 boundary of Tixeront (1973); cf. H unconformity of

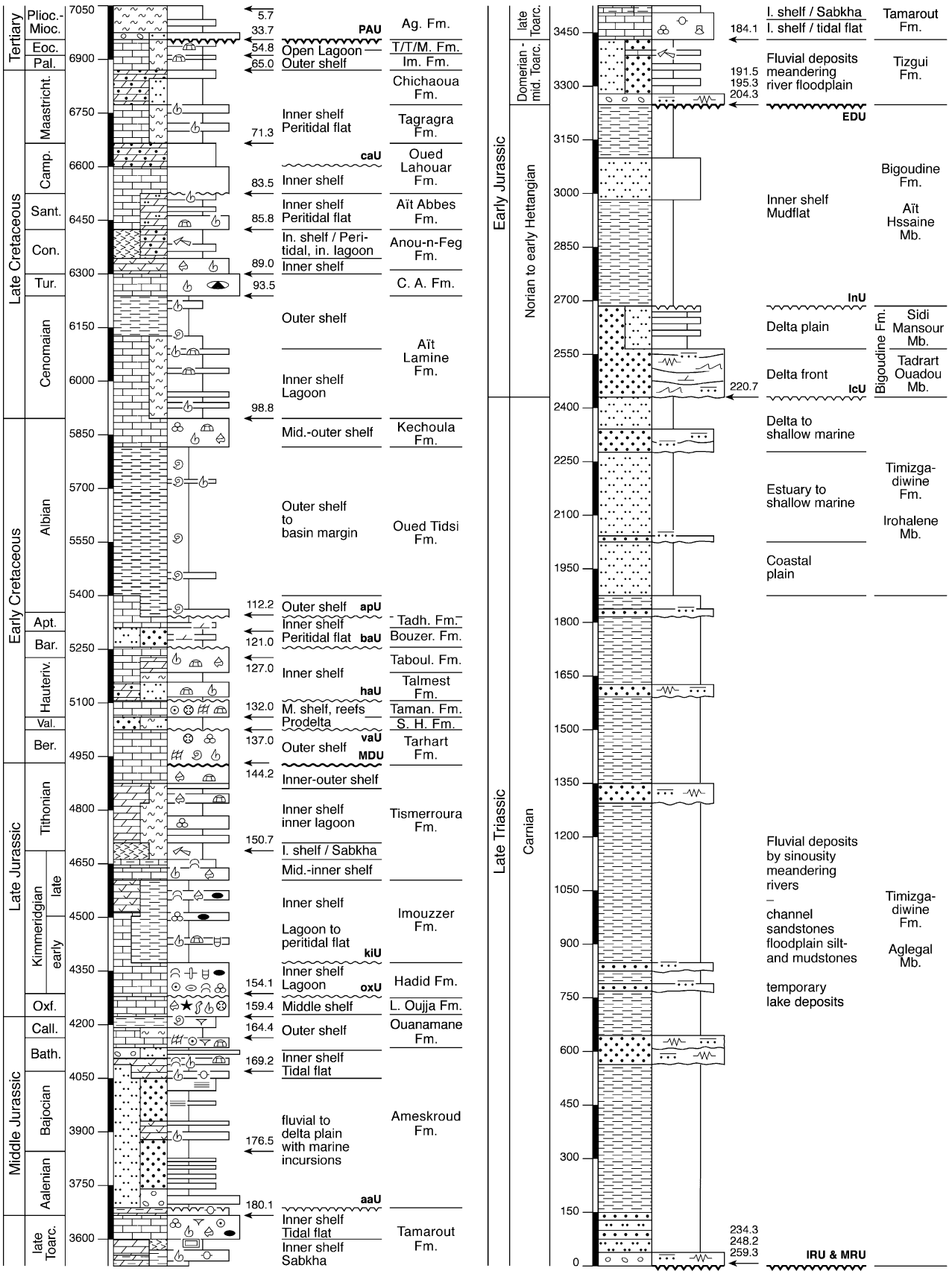

Fig. 7. Synthetic basin section for the southwestern, distal part of the Agadir Basin at 103.3 km AT (cf. Fig. 4, Aït Chehrid Tizgui in Fig. 8). For legend see Fig. 6.

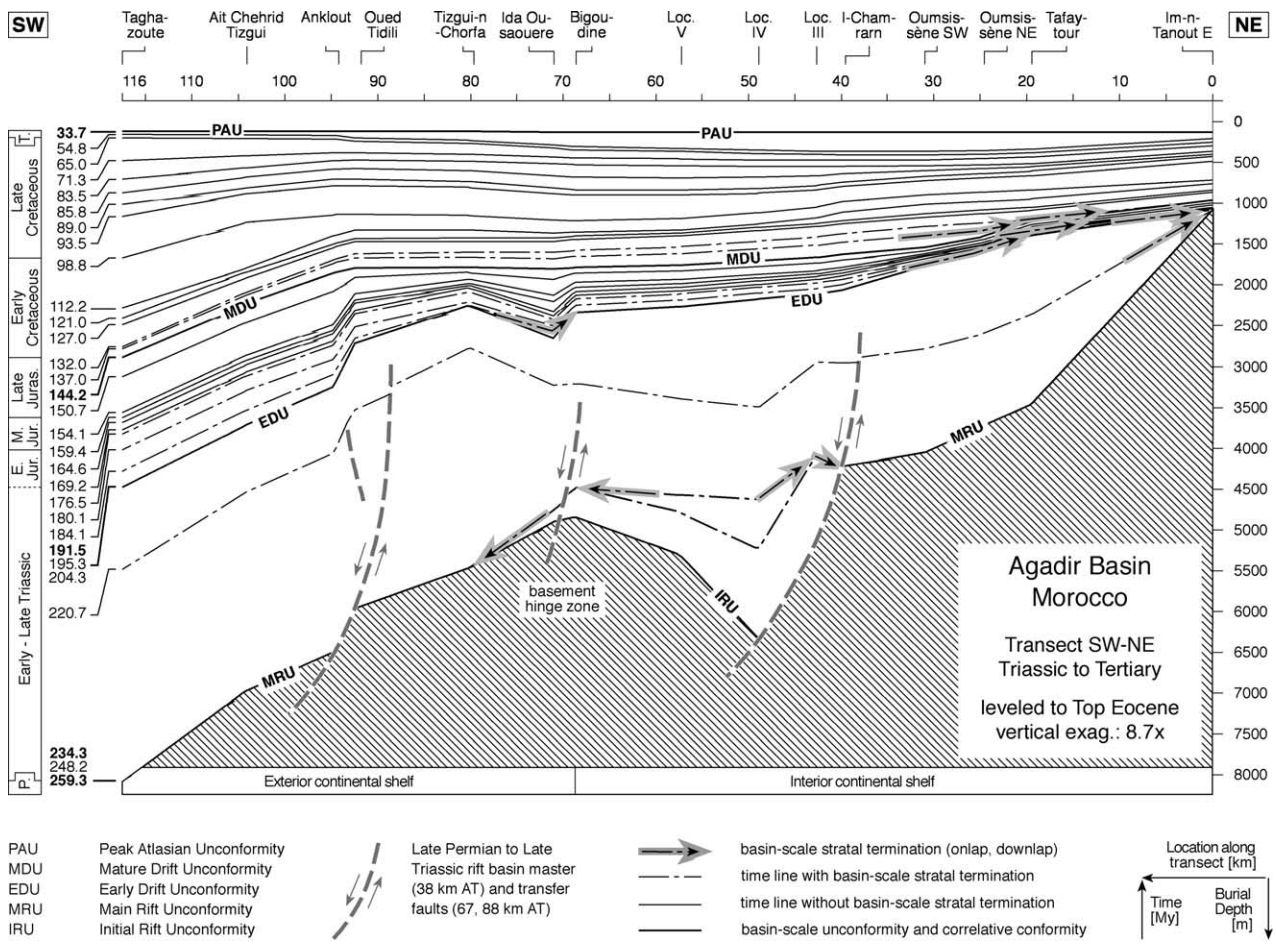

Fig. 8. Reconstructed basin architecture along the transect indicated in Fig. 4 with the time layers used in 2D numerical reverse basin modeling (cf. Fig. 5, column A). The left column indicates systems, stages and absolute ages according to Hardenbol et al. (1998). Basin scale unconformities have been defined based on large-scale onlaps of time layers and depositional/erosional gaps of stage resolution. For substage unconformities and correlative conformities see Figs. 5–7. Late Permian to Triassic rift basin master and transfer faults have been assumed based on structural data (Le Roy & Piqué, 2001; Tixeront, 1973) and seismic data in the Essaouira Basin (Hafid et al., 2000). Faulted sections are largely restricted to the Ikakern to Timesgadiwine Fms. (Olsen, 1997) or the Triassic to Liassic (Le Roy & Piqué, 2001). They occur below the EDU of this study (pre-204.3 to 191.5 Myr).

Le Roy and Piqué (2001)) has an age of pre-234.4 Myr (top Anisian). It marks the onset of basinwide continental deposition, i.e. for the first time outside the initial rift halfgrabens. Alluvial to deltaic sandstones to shales of the Timesgadiwine and Bigoudine Fms. overlie both the Hercynian basement and previous rift deposits. The time layer of 234.4–220.7 Myr (top Anisian to top Carnian) shows thickness increasing gradually from 0 m in the east to more than 2500 m in the west. Between 220.7 and 204.3 Myr (top Carnian to top Early Hettangian) the depocenter shifted towards the east to the area of the Late Permian to Early Mid-Triassic halfgraben (at 50 km AT). This shift was probably related to the reactivation of rift master faults and to a backtilting of the western Agadir Basin towards the SE. The current database indicates that the rift master faults were never significantly reactivated after the Early Hettangian. During the rift to sag basin stages (259.3–191.5 Myr) the basement hinge zone was located immediately west of the halfgraben at 70 km AT.

The Early Drift Unconformity (EDU, angular unconformity; cf. t8-i1 unconformity of Tixeront (1973); cf. J unconformity of Le Roy and Piqué (2001)) has an age of 204.3 Myr (top Early Hettangian) to at least 191.5 Myr (top Early Pliensbachian, Carixian). The depositional and/or erosional gap extended until 169.2 Myr (top Bajocian) in the easternmost part of the Agadir Basin. Initial deposition following 191.5 Myr was restricted to the westernmost basin, where alluvial deposits of the Tizgui Fm. overlie the EDU. At 184.1 Myr (top Mid-Toarcian) continental onlap was located at 70 km AT in the central to eastern Agadir Basin. Condensed fluvio-deltaic to tidal flat deposits of the Tamarout Fm. unconformably overly the Aït Hssaine Mb. of the Bigoudine Fm. Continental onlap shifted rapidly to 20 km AT until 180.1 Myr (top Toarcian) and finally until 169.2 Myr, to the east of Im-n-Tanout, outside the transect. Michard (1976) described the so-called 'Dorsale du Massif Hercynien Central' (DMHC; Schaer, 1987), an Early/Middle Jurassic arch with an E–W extension of approximately 50 km. It was regarded as the limit of the Atlantic and Tethyan domains. The pattern of onlap terminations during the Early Pliensbachian to Bajocian in the eastern Agadir Basin confirms

the existence of this structural high. Numerical basin modeling will show that the DMHC was caused by minimum to zero subsidence in the proximal part of the continental margin basin, while subsidence prevailed in the distal part. The DMHC represents a feature of differential subsidence. The time layers 164.4 Myr (top Bathonian) to 144.2 Myr (top Tithonian) show an increase in thickness from east to west with a minor depocenter at 70–75 km AT. Between 191.5 and 144.2 Myr the basement hinge zone migrated 10–15 km to the west and formed a subsurface high located between 75 and 95 km AT. Late Pliensbachian (Domerian) to Tithonian time layers show considerable offlap from the west and east against this subsurface high. However, large-scale onlap did not develop. In contrast to the time layers 184.1–176.5 Myr, the layers 169.2–144.2 Myr do not significantly onlap against the EDU within the Agadir Basin. They do include low-angle offlap against the topographically elevated eastern basin margin located between 25 and 0 km AT. The EDU is comparable to the 'post-rift unconformity' described for the western Central Atlantic continental margin basins (e.g. Georges Bank Basin; Klitgord et al., 1988).

The Mature Drift Unconformity (MDU) has an age of 144.2 Myr (top Tithonian) to 132.0 Myr (top Valanginian). It is restricted to the easternmost basin margin and grades into several correlative conformities towards the west. The time layers 137.0 Myr (top Berriasian) and 132.0 Myr show large-scale onlap against the MDU. Successive time layers until approximately 98.9 Myr (top Albian) include significant low-angle offlap of continental to marine successions against the eastern basin margin. Between 112.2 Myr (top Aptian) and 65 Myr (top Maastrichtian) all time layers show a gradual increase in thickness from east to west. The Tithonian to Berriasian inner to outer shelf successions in the western and central to eastern basin are conformable. In the western basin the succession includes the Tismerroura and Tarhart Fms., in the central to eastern basin the Timsilline to Agroud Ouadar Fms. Until 98.9 Myr, the basement hinge zone migrated further westward to 100–105 km AT as indicated by significant increases in the thickness of time layers. Subsequent time layers and their lateral thickness distributions indicate, that the basement hinge zone became inactive after the Albian or was located offshore outside the transect.

Between 54.8 Myr (top Paleocene) and 33.7 Myr (top Eocene) the basin architecture began to change. A new depocenter in the central and eastern Agadir Basin (55–15 km AT) came into existence. This was probably related to increased Atlasian compression and tectonic uplift. The Peak Atlasian Unconformity (PAU) developed since the Late Eocene to Early Oligocene over the whole onshore Agadir Basin.

5.2. Unconformities below the resolution of time layers

Significant depositional/erosional gaps, erosional/angular unconformities and associated stratal terminations exist below the resolution of geologic stages. They do not show up in the large-scale reconstruction of the basin architecture (Fig. 8), which is based on time layers at the resolution of geologic stages, but are indicated in the synthetic basin sections and the litho-/chronostratigraphic scheme (Figs. 5–7). Unconformities below the resolution of geological stages indicate important reconfigurations of the basin architecture and partly correlate with time equivalent unconformities in basins of the northwest African and North American continental margins:

(1) Late Carnian angular and erosional unconformity (lcU, pre-220.7 Myr; cf. t2–t3 of Tixeront (1973); cf. TSII–TSIII of Olsen (1997); cf. Tr1-a/Tr1-b of Hafid et al. (2000));
(2) Late Norian to Rhaetian angular and erosional unconformity (lnU, cf. t5–t6 of Tixeront (1973));
(3) Early Aalenian erosional unconformity (aaU; approx. 179 Myr);
(4) Late Oxfordian erosional unconformity (oxU, approx. 156 Myr);
(5) Early Kimmeridgian erosional unconformity (kiU, approx. 153 Myr);
(6) Early Valanginian erosional unconformity (vaU, approx. 135 Myr);
(7) Early Hauterivian erosional unconformity (haU, approx. 130 Myr);
(8) Early Barremian erosional unconformity (baU, approx. 124 Myr);
(9) Late Aptian erosional/angular unconformity (apU, Gargazian, approx. 117 Myr);
(10) Early (?) Campanian angular (8–10°) unconformity (caU, approx. 83–80 Myr?).

Approximately 35 km east of 0 km AT, at the southern margin of the Moroccan Meseta near Amizmiz, the Early Drift (EDU), the Early Aalenian (aaU), the Late Oxfordian (oxU) and the Early Kimmeridgian (kiU) unconformities converge to a single erosional and angular unconformity (approx. 204–146 Myr, Fig. 5). It is overlain by the Amizmiz Fm. with alluvial conglomerates and sandstones of Late Tithonian age. In the area of Im-n-Tanout, immediately east of 0 km AT, the Main Drift Unconformity (MDU), the Early Valanginian (vaU) and the Early Hauterivian (haU) unconformities and their correlative conformities of the western to eastern Agadir Basin also converge to a single erosional and angular unconformity. It represents a depositional and erosional gap between the latest Tithonian/Early Berriasian to Early Hauterivian (approx. 144–130 Myr).

5.3. Basin stages

Nine basin development stages (Table 1) have been identified in the onshore Agadir Basin, based on unconformities, stratal terminations of time layers, basin architecture in time, the results of 2D numerical modeling and the biostratigraphic correlation to magnetic polarity

Table 1
Basin development stages in the Agadir and Essaouira Basins

Onshore Agadir Basin						Onshore Essaouira Basin			
Basin development	Bound. Unconf.	Absolute ages, stages, polarity chronozones	Key features	Subsid. trends	Ages (Myr)	Basin development	Absolute ages, stages	Seismic seq.	Ages (Myr)
Atlasian uplift and basin inversion		19.0–0.0 E. Miocene to Recent C6–C1	Major N–S to NW–SE convergence Uplift and basin inversion See Gomez et al. (2000)						
Atlasian deformation		34.7–19.0 L. Eocene to E. Miocene C13–C6	Major N–S convergence Major erosional unconformity (PAU) Continental deposition			Compression	95.8–23.8 ? Cenom. to Paleogene	Ce Cr2b Cr2a	65.0–23.8 93.5–65.0 106.2–93.5
	PAU	approx. 33.7	See Gomez et al. (2000)						
Mature drift with initial Atlasian deformation		93.5–34.7 Turonian to L. Eocene C14–C13	Marine deposition over whole basin Unconformities: caU Initial N–S convergence between African-Eurasian plates	ST8 ST7	83.5–65.0/54.8 93.5–83.5				
Mature drift		144.2–93.5 Berriasian to Cenoman M19–C34	Marine deposition spreads over the whole Agadir basin Unconformities: vaU, haU, baU, apU Depositional/erosional hiatus in the eastern basin (Berrias.–Hauteriv.)	ST6 ST5	121.0–93.5 144.0–121.0	Drift and salt tectonics	195.3–95.8 Pliensb. to ? Cenom.	Cr1b Cr1a J2–3 J1–2 ?	137.0–106.2 144.2–137.0 164.4–144.2 189.6–164.4 195.3–189.6
	MDU	144.2–132.0	Increased oceanward tilting						
Early drift		191.5–144.2 L. Pliensb. to Tithonian S1–M19	Predominantly marine deposition Continental margin basin develops Unconformities: aaU, oxU, kiU	ST4 ST3 ST2	159.4–144.2 169.2–159.4 204.3–169.2				
	EDU	204.3–191.5	Initial sea-floor spreading						
Sag		220.7–191.5 Norian to E. Pliensb.	Basaltic volcanism Continental deposition and basinwide depositional/erosional hiatus Unconformities: lnU	ST1	259.3–204.3	Upper Sag	? 204.3–195.3 ? Early Liassic	Tr2	204.3–195.3 (? approx.)
			Correlates with lower sag basin in Essaouira Basin			Lower Sag	? 220.7–204.3	Tr1-b	220.7–204.3
	lcU	pre-220.7	No sedimentary record equivalent to upper sag basin in Essaouira Basin				? L. Trias. to E. Liassic		(? approx.)
Rift climax		234.4–220.7 Ladinian to Carnian	Rift halfgrabens filled Basinwide continental deposition			Synrift	? 241.7–220.7 ? Mid. to Late Triassic	Tr1-a	241.7–220.7 (? approx.)
	MRU	pre-234.3	Block faulting largely sealed						
Early rift		259.3–234.3 L. Permian to Anisian	Initial rift grabens Continental deposition in grabens Unconformities						
	IRU	pre-259.3–234.4	Block faulting						
Basement		pre-259.3	Lower Carboniferous deformation			Basement	? pre-241.7		

Agadir Basin stages (this study) are based on surface data. Essaouira Basin stages (Hafid, 2000; Hafid et al., 2000) were based on seismic data.

chronozones in the Central Atlantic sea-floor (Cande & Kent, 1995; Gradstein et al., 1994). The basin classification follows the schemes of Kingston, Dishroon, and Williams (1983), Leeder (1992), and Prosser (1993).

6. Numerical reverse basin modeling

6.1. Database

Chrono- and biostratigraphy—Numerical modeling of the Agadir Basin includes a total of 29 time layers for the Early Jurassic to Late Cretaceous. Chronostratigraphic information from radiometric age dating is not available from the Atlantic Basins of northwest Africa except for Late Triassic to Early Jurassic basalts. Absolute ages of biostratigraphically defined time lines have been taken from the biostratigraphic chart of Hardenbol et al. (1998), which is based on the time scales of Gradstein et al. (1994, 1995; Mesozoic) and Berggren, Kent, Swisher, and Aubry (1995; Cenozoic). All absolute ages cited from existing studies have been recalibrated to these two time scales. The time resolution of the basin model is on the stage level for the Jurassic to Cretaceous. Given the reverse basin modeling approach, the currently available bio- and chronostratigraphic information is insufficient to increase time resolution to the substage or zonal level. Substage information is partly available based on assemblage biozones. However, assemblage zones may be influenced by facies and, given the current stage of biostratigraphic research, are not available on a basinwide scale. Age error intervals of stage boundaries range between ± 4.0 and ± 4.8 Myr in the Triassic, ± 2.6 and ± 4.0 Myr in the Jurassic and ± 0.1 and ± 2.1 Myr in the Cretaceous.

Burial depth—Burial depths have been measured, compiled and reconstructed as described for the reconstruction of the basin architecture. All information from synthetic sections has been orthogonally projected into the modeling transect (see Fig. 4).

Paleobathymetry—The spectrograms of Fig. 9 show estimates on paleowater depths (column A) and the rates of paleobathymetric change (column D) between the top Domerian and top Eocene. Estimates are based on facies, associations of reef-building organisms (Leinfelder, Schmid, Nose, & Werner, 2002) and large-scale depositional geometries of intra-shelf ramp-to-basin transitions. Because the Agadir Basin transect covers the inner to outer part of the Meso-/Cenozoic continental shelf, paleowater depths never exceeded 250 m.

(De-)compaction parameters—The numerical modeling of the Agadir Basin includes a total of 21 lithologies. Average values of initial porosities, bulk rock densities and maximum depths of compaction have been taken from among others Welte, Horsfield, and Baker (1997). Modeling in this study uses strictly textural initial porosities for standard lithologies. Initial porosities, compaction coefficients and exponential compaction paths are based on particle size, mud/shale content and matrix-/grain-support.

Crustal flexural parameters—Hartley, Watts, and Fairhead (1996) presented estimates for the elastic lithospheric thickness of present-day African margins. It denotes the elastic upper interval of the lithosphere, which is sufficiently rigid to retain elastic stresses over geological time scales (Allen & Allen, 1990). Its lower boundary is defined by the 475/675 °C isotherm (wet/dry olivine rheology; Turcotte & Schubert, 2002). The elastic thickness is one of the key parameters determining the flexural behavior of the lithosphere. In contrast, the thermal thickness of the lithosphere is limited by the ~1330 °C isotherm, where mantle rocks reach their solidus temperature. Gravimetric data for the Essaouira Basin to the north indicate (thermal) lithospheric thicknesses of ~25–30 km (Bernardin, 1988; Tadili, Ramdani, Ben Sari, Chapochnikov, & Bellot, 1986). In the Agadir Basin, the effective elastic thickness of the lithosphere is approximately 10 km (Hartley et al., 1996), the normal lithospheric (thermal) thickness 30 km (Makris, Demnati, & Klussman, 1985). Reverse modeling in this study is based on a elastic lithospheric thickness of 11 km in the drift basin stage, which corresponds to a total thickness of 35 km (Burov & Diament, 1995). Projection taper widths of the sediment load amount to 100–500 km.

Sea-level history—Haq, Hardenbol, and Vail (1987) and Hardenbol et al. (1998) present eustatic sea-level and coastal onlap data for Mesozoic to Recent times. Reverse basin modeling in this project considers exclusively second order changes in eustatic sea-level. Third order sea-level changes have not been included, because the exact timing and amplitude of individual fluctuations are a matter of debate especially in the Mesozoic. Long-term, second order sea-level changes are better constrained. Their time intervals are comparable to the durations of Mesozoic stages, which range between 2.3 Myr at minimum and 13.4 Myr at maximum.

6.2. Methodology

Based on Turcotte and Schubert (1982), Allen and Allen (1990) and Leeder (1999) partitioned total subsidence into different genetic components: (1) tectonic driving forces; (2) sediment loading and flexural support; (3) heat flow. Sequence stratigraphic studies commonly embrace these different genetic components as subsidence (undifferentiated) or ‘tectonic subsidence’.

Reverse basin modeling in this study follows the sequence stratigraphic concept, which considers the creation/destruction of accommodation space and its infill as the two principal controls on sedimentary systems and basins (Fig. 10). Accommodation represents the space available for potential sediment including (1) leftover space not filled during an earlier time interval; (2) plus new space being made available during a contemporaneous time interval (Posamentier, Jervey, & Vail, 1989). The accommodation

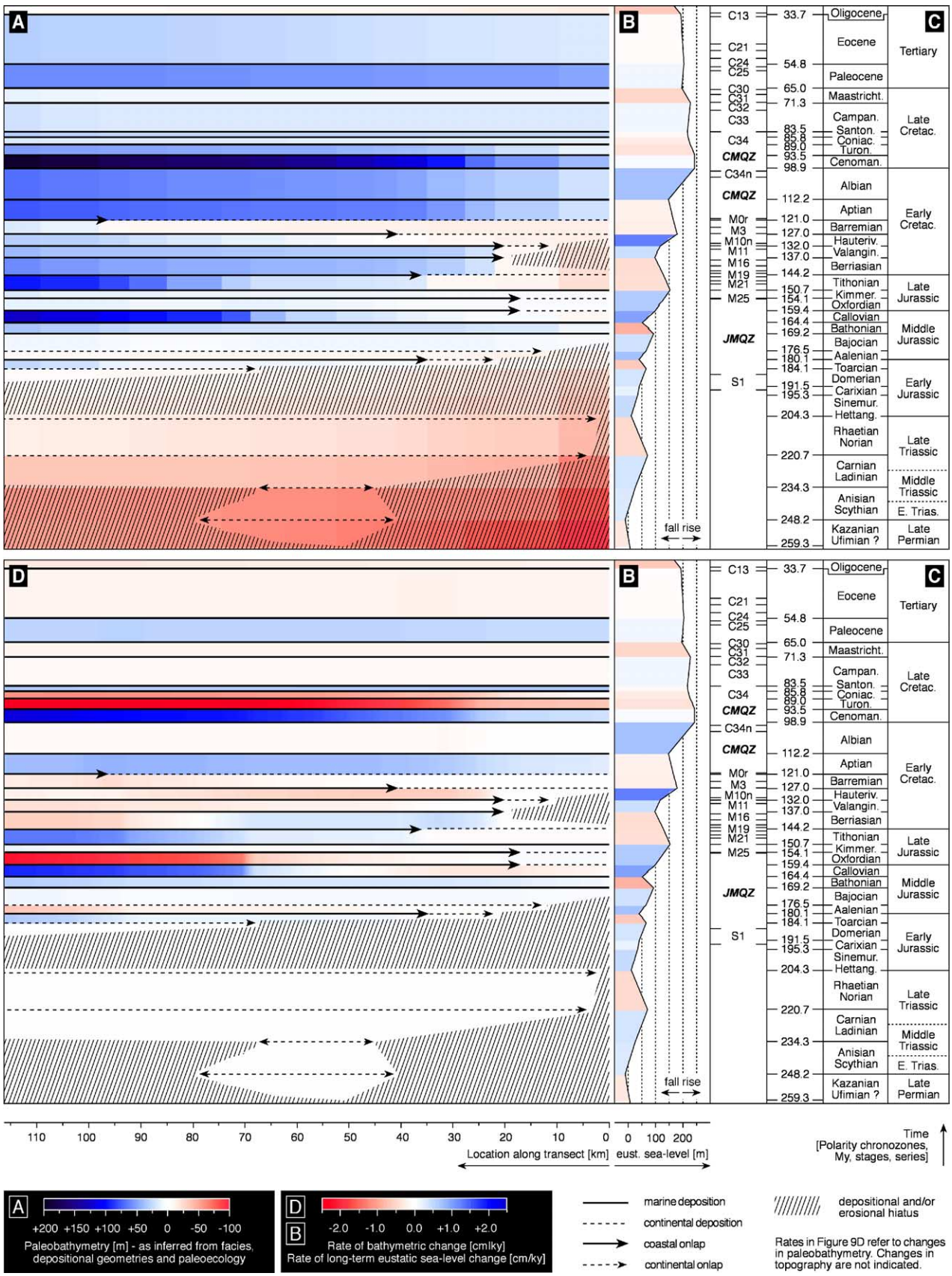
A
B
C
D
C13
C21
C24
C25
C30
C31
C32
C33
C34
CMQZ
C34n
CMQZ
M0r
M3
M10n
M11
M16
M19
M21
M25
JMQZ
S1
33.7
54.8
65.0
71.3
83.5
85.8
89.0
93.5
98.9
112.2
121.0
127.0
132.0
137.0
144.2
150.7
154.1
159.4
164.4
169.2
176.5
180.1
184.1
191.5
195.3
204.3
220.7
234.3
248.2
259.3
Oligocene
Eocene
Paleocene
Maastricht.
Campan.
Santon.
Coniac.
Turon.
Cenoman.
Albian
Aptian
Barremian
Hauteriv.
Valangin.
Berriasian
Tithonian
Kimmer.
Oxfordian
Callovian
Bathonian
Bajocian
Aalenian
Toarcian
Domerian
Carixian
Sinemur.
Hettang.
Rhaetian
Norian
Carnian
Ladinian
Anisian
Scythian
Kazanian
Ufimian ?
Tertiary
Late Cretac.
Early Cretac.
Late Jurassic
Middle Jurassic
Early Jurassic
Late Triassic
Middle Triassic
E. Trias.
Late Permian
fall rise
110 100 90 80 70 60 50 40 30 20 10 0
Location along transect [km]
0 100 200
eust. sea-level [m]
Time
[Polarity chronozones, My, stages, series]
+200 +150 +100 +50 0 -50 -100
Paleobathymetry [m] - as inferred from facies, depositional geometries and paleoecology
-2.0 -1.0 0.0 +1.0 +2.0
Rate of bathymetric change [cm/ky]
Rate of long-term eustatic sea-level change [cm/ky]
marine deposition
continental deposition
coastal onlap
continental onlap
depositional and/or erosional hiatus
Rates in Figure 9D refer to changes in paleobathymetry. Changes in topography are not indicated.

space or envelope varies with its upper and lower reference boundaries moving up or down: (1) base level; (2) a datum (surface) at or near the sea floor (Emery & Myrers, 1996).

Base level is placed at the sea-level, which is a valid simplification at the sedimentary basin scale. The datum is placed at the lower boundary of the accommodation space for each specific time interval in the basin development. In the sequence stratigraphic concept of Posamentier et al. (1989) the position of this datum is controlled exclusively by changes in subsidence/uplift. However, compaction in the buried sedimentary basin fill, i.e. between the sea floor/datum and the top of the rheological basement significantly influences the position of the datum. Rheological basement denotes any pre-Late Permian magmatic, metamorphic and sedimentary succession, which had reached its late to final state of compaction in the Late Permian. Although compaction is not a genetic component of basement-related subsidence, it represents a major control on changes in accommodation space. Therefore it has been incorporated as compaction-induced subsidence in the numerical modeling of the Agadir Basin.

Reverse basin modeling in this study partitions total subsidence to three components (Fig. 10): (1) thermo-tectonic subsidence; (2) flexural subsidence; (3) compaction-induced subsidence. Accommodation space is partitioned to eustatic sea-level changes and total subsidence including all three genetic components.

Subsidence component, accommodation and sediment flux histories are calculated for each of the 29 time layers identified in the Late Permian to Eocene basin fill. Rates are calculated for each time layer with the effects of flexural loading, changes in paleobathymetry, changes in sea-level and compaction removed. The modeling starts from the time of maximum burial depths in the basin history, the top Eocene (33.7 Myr). Reconstructed time layers (Figs. 8 and 11) are incrementally removed until the oldest layer, representing the top of the rheological basement, is reached. After a specific layer has been removed, the next older layer is adjusted according to the paleobathymetric information provided. The underlying layers are decompacted according to the petrophysical parameters defined. The flexural backstripping procedure applied in the reverse basin modeling of this study is based on the equations introduced by Dickinson et al. (1987) and Turcotte and Schubert (1982, 2002). It has been described by Bowman and Vail (1999) for forward stratigraphic modeling.

6.3. Results

Fig. 11 shows a graphic representation of the results of numerical reverse basin modeling for 10 out of 29 time layers. Most subsidence modeling studies of basins bordering the Central and northern Atlantic were restricted to 1D backstripping (isostatic modeling) and presented time/burial depth paths of the top basement ('geohistory plots'; Labbassi, 1997; Labbassi et al., 2000; Le Roy, Guillocheau, Piqué, & Morabet, 1998; Medina, 1995). In order to more easily compare the results of these studies to the 2D flexural basin model of this study, time depth paths for the top basement in the Agadir Basin have been calculated for five localities along the transect (Fig. 12). Color-coded spectrograms are a common type of plot to present rates of subsidence in time along 2D transects (Bellingham & White, 2000). Fig. 13 presents spectrograms for total subsidence (A), thermo-tectonic subsidence (B), flexural subsidence, (C) and compaction-induced subsidence (D).

6.4. Subsidence trends

The Late Permian to Early Tertiary development of the Agadir Basin includes 8 subsidence trends (ST1–8, Fig. 14). Differential subsidence in ST1, which covers the early rift to sag basin stages, is considerable. Changes in subsidence/uplift in time depend strongly on the position within the rift system. The modeling transect runs obliquely to the large-scale topographic gradient of the Late Permian to Early Hettangian basin. A uniform basinwide subsidence signature does not exist within ST1. The subsidence trends ST2–8 cover the late sag to mature drift basin with initial Atlasian compression stages. Between the Middle Hettangian to Early Tertiary, the large-scale topographic/bathymetric gradient ran subparallel to the line of the transect (Fig. 4). ST2–8 show specific, basinwide variations of subsidence in time. Each subsidence trend includes (1) initially low to zero subsidence or uplift; (2) a gradual increase in

Fig. 9. Spectrogram indicating paleobathymetry/topography, long-term (second order, 3–10 Myr; Duval et al., 1992) rates of eustatic sea-level changes and rates of bathymetric changes in the Agadir Basin between the Late Permian and Tertiary. Rates are interpolated for the time layers shown in column C. Coastal and continental onlaps refer exclusively to the top of stages. As time resolution is on the stage level for the Jurassic to Late Tertiary, the plot does not indicate short-term, intra-stage bathymetric changes, eustatic changes (third order, 0.5–3 Myr; Duval et al., 1992) and onlap shifts. The *X*-axis indicates kilometers along transect (0–117 km AT, see Figs. 4 and 8). The *Y*-axis indicates time in (Myr) full-scale. (A) Paleobathymetry and topography as well as coastal and continental onlap in time (Wheeler Diagram) along the transect of Fig. 4. Positive values and white to blue colors indicate water depth, negative values and white to red colors topographic elevation (estimates). Water depth has been estimated based on facies, large-scale (≥km) depositional geometries in the field and paleoecology. (B) Rates of long-term eustatic sea-level change calculated from the sea-level charts of Haq et al. (1987) and Hardenbol et al. (1998). Blue colors indicate rates of global sea-level rise, white color stationary global sea-level and red colors rates of global sea-level fall. Rates have been interpolated for the time layers shown in column C. The *X*-axis indicates eustatic sea-levels in meters compared to today (0 m). (C) Late Permian to Eocene time scheme. Absolute ages according to Berggren et al. (1995) and Gradstein et al. (1994); magnetic polarity chronozones according to Hardenbol et al. (1998). Absolute ages represent time steps in the reverse basin modeling. (D) Rates of bathymetric change as well as coastal and continental onlap in time (Wheeler Diagram). The color code represents rates of bathymetric change. Increases in bathymetry (transgressions) are shown in blue, decreases in bathymetry (regressions) in red. Rates of changes in paleotopography have not been calculated because paleotopography values are little constrained.

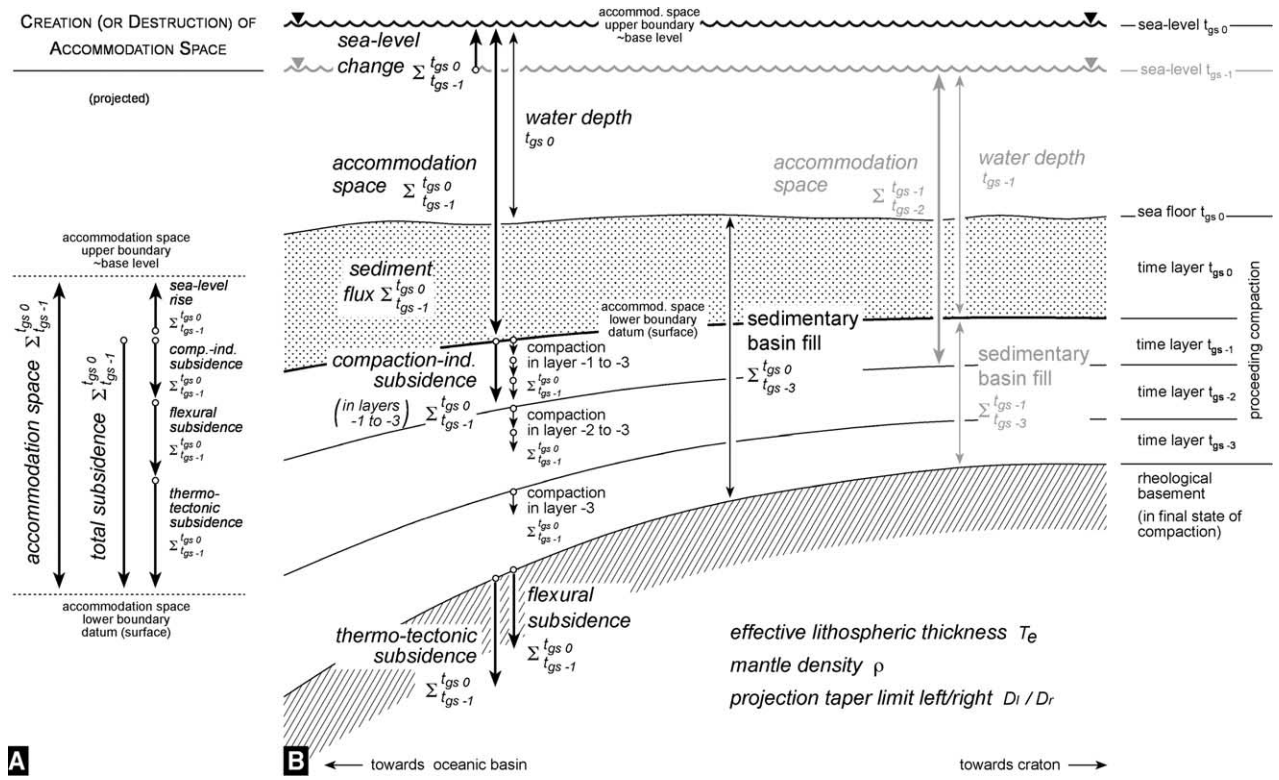

Fig. 10. Genetic components and principal parameters of basin development in the accommodation-oriented 2D reverse basin modeling. (A, right) The current time layer/interval 0 is indicated as $t_{gs\ 0}$ (gs—geological stage; dotted signature). Abbreviations $t_{gs\ -1}$ to $t_{gs\ -3}$ indicate consecutively older time layers. Major components (accommodation, sea-level changes, subsidence components, sediment flux) are printed in italics. (B, left) In the accommodation-oriented basin analysis approach of this study, total subsidence is leveled to the datum (lower boundary) of accommodation space/envelope and includes thermo-tectonic, flexural and compaction-induced subsidence. Basement-related subsidence refers exclusively to thermo-tectonic and flexural subsidence. The norm-vectors to the left show resulting total subsidence and accommodation. The scheme depicts a configuration, where all rates are positive, i.e. subsidence and an eustatic sea-level rise occur. Sediment flux during time layer 0 is significantly increased compared to during time layers $t_{gs\ -3}$ to $t_{gs\ -1}$. Although eustatic sea-level has risen and thermo-tectonic subsidence has remained constant from time layer $t_{gs\ -1}$ to $t_{gs\ 0}$, water depth has decreased. Flexural and compaction-induced subsidence have increased from time layer $t_{gs\ -1}$ to $t_{gs\ 0}$.

subsidence to maximum rates; (3) in some trends (ST2 and ST4), a final moderate decrease in rates occurs.

Total durations of the subsidence trends range between 9.8 and 35.1 Myr each (Fig. 14). All subsidence trends equally apply to total and thermo-tectonic subsidence rates, accommodation rates and are corroborated by compositional accommodation analysis (CA-analysis). The subsidence trends ST2–8 can be recognized primarily in the western to central basin, where significant temporal variations in the subsidence components existed. The same shifts occur at the eastern basin margin but with reduced amplitudes.

6.5. Compositional accommodation analysis (CA-analysis)

CA-analysis is a new tool for quantitative basin analysis It has been developed as part of this study and applied to the Agadir Basin (Fig. 15). CA-analysis supports the development of genetic accommodation models. It determines whether accommodation space was created or destroyed and whether total subsidence or uplift, eustatic sea-level rise or fall exerted the dominant control on changes in accommodation. Requirements for CA-analysis include:

(1) quantified rates of total subsidence including its three components thermo-tectonic, flexural and compaction-induced subsidence, derived from numerical reverse basin and/or forward stratigraphic modeling.
(2) quantified rates of second or third order eustatic sea-level change.

CA-analysis considers:

(1) the relative quantities of total subsidence and eustatic sea-level change.
(2) positive/negative domains of rates of total subsidence/uplift and eustatic sea-level rise/fall.
(3) the resulting change in accommodation space.

The respective positive values denote rates of total subsidence, sea-level rise and accommodation space added. The respective negative values denote rates of total uplift, sea-level fall, and accommodation space destroyed. For reasons of simplification and clarity, eight indicative parameter configurations have been defined and selected from all theoretically possible configurations (Fig. 15(C)). The components of total subsidence/uplift have been

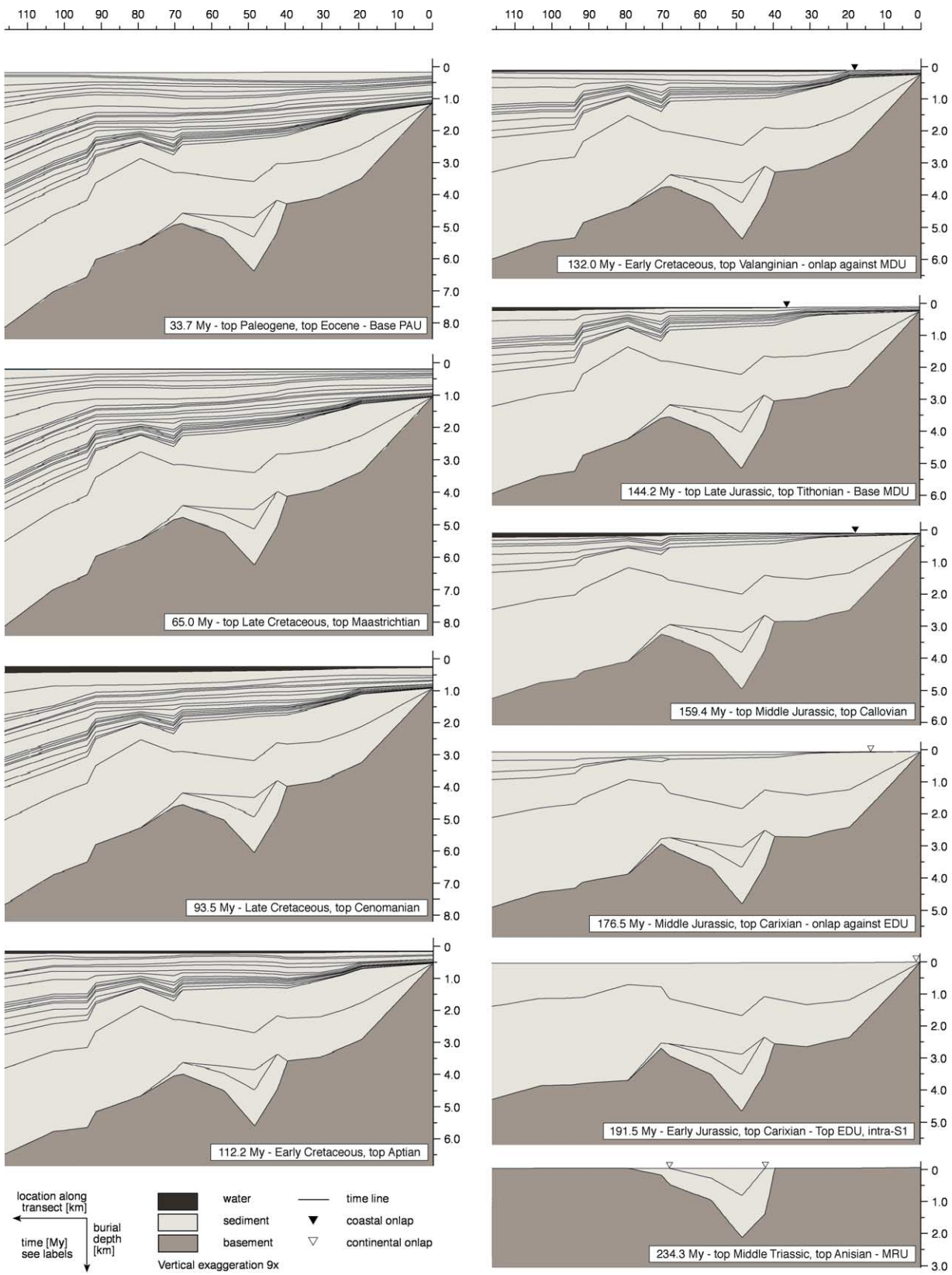

Fig. 11. Meso- to Cenozoic development of the Agadir Basin based on 2D reverse numerical basin modeling. The figure shows the basin architecture for 10 selected times (indicated in the box in the lower right corner of each plot). Paleobathymetry of <50 m is not visible because of the small-scale. Vertical exaggeration is $8.9\times$. Compare Fig. 8 for the Late Eocene basin architecture and labeled time lines. See Fig. 4 for the line of transect and the text for explanations. Reverse basin modeling has been performed with Phil/BaSim® (PetroDynamics Inc., Houston; see Bowman & Vail, 1999).

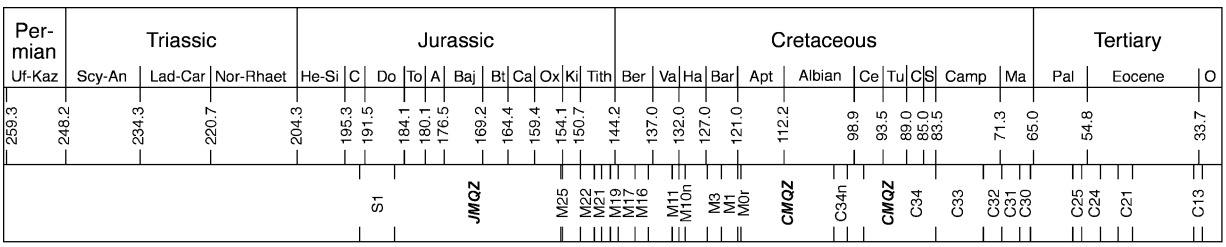

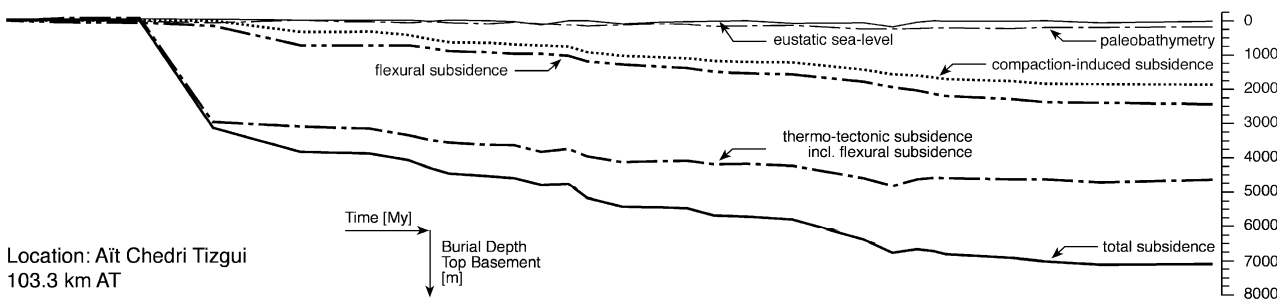

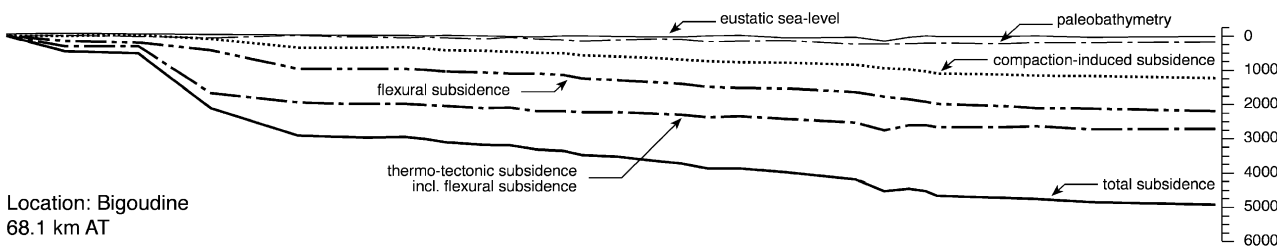

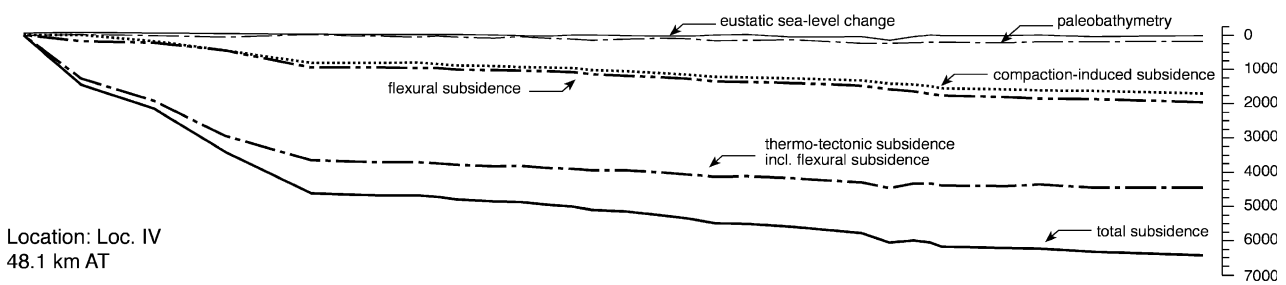

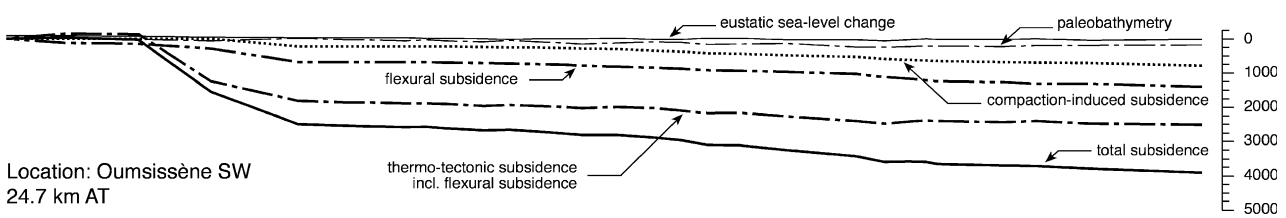

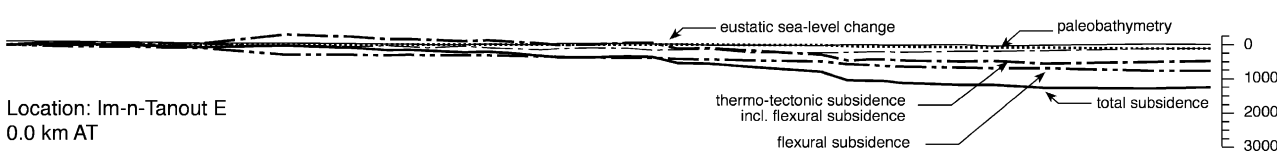

Fig. 12. Time/depth paths for the top of the Hercynian basement at five locations along the transect (see Figs. 4 and 8) derived from 2D reverse basin modeling, i.e. including flexural, compaction-induced and thermo-tectonic subsidence. Legend: km AT—kilometers along the transect of Fig. 4.

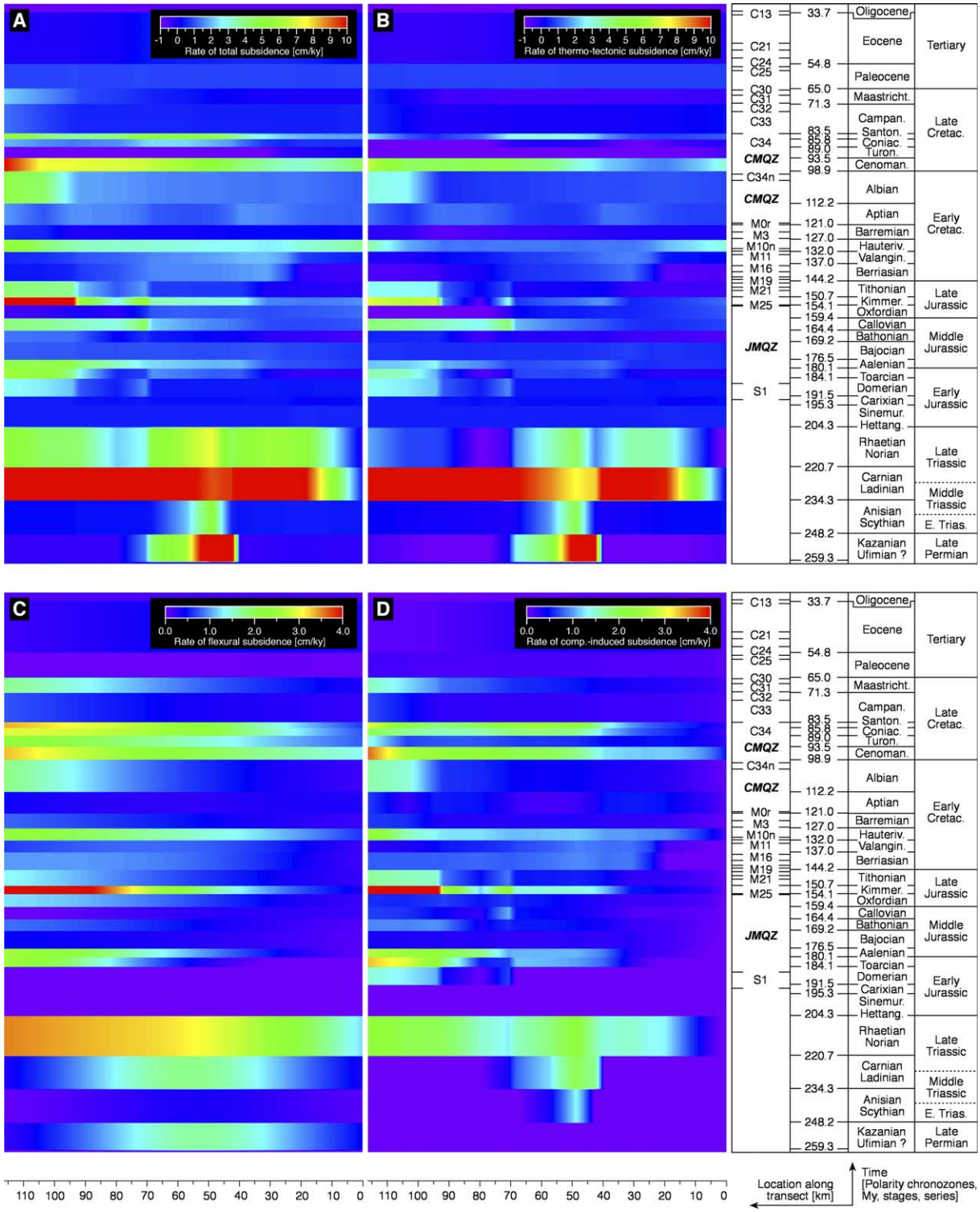

Fig. 13. Spectrogram indicating total, thermo-tectonic, flexural and compaction-induced subsidence rates along the southwestern to northeastern Agadir Basin transect (0–116 km AT). The range of rates indicated is −1 to 10 cm/kyr for total and thermo-tectonic subsidence and 0–4 cm/kyr for flexural and compaction-induced subsidence rates. Higher and lower rates (see below) have been cut in the color spectrum in order to better visualize changes in the medium range of values. Detailed maximum rates for subsidence components are listed in Table 2. Rates are interpolated for the time layers shown on the Late Permian to Eocene time scheme (right column). Absolute ages according to Berggren et al. (1995) and Gradstein et al. (1994); magnetic polarity chronozones according to Hardenbol et al. (1998). Absolute ages represent time steps in the reverse basin modeling. The *X*-axis indicates kilometers along transect (Fig. 4) from 0 km (NE) to 116 km (SW). The *Y*-axis indicates time in (Myr) full-scale. (A) Rates of total subsidence. (B) Rates of thermo-tectonic subsidence. (C) Rates of flexural subsidence. (D) Rates of compaction-induced subsidence.

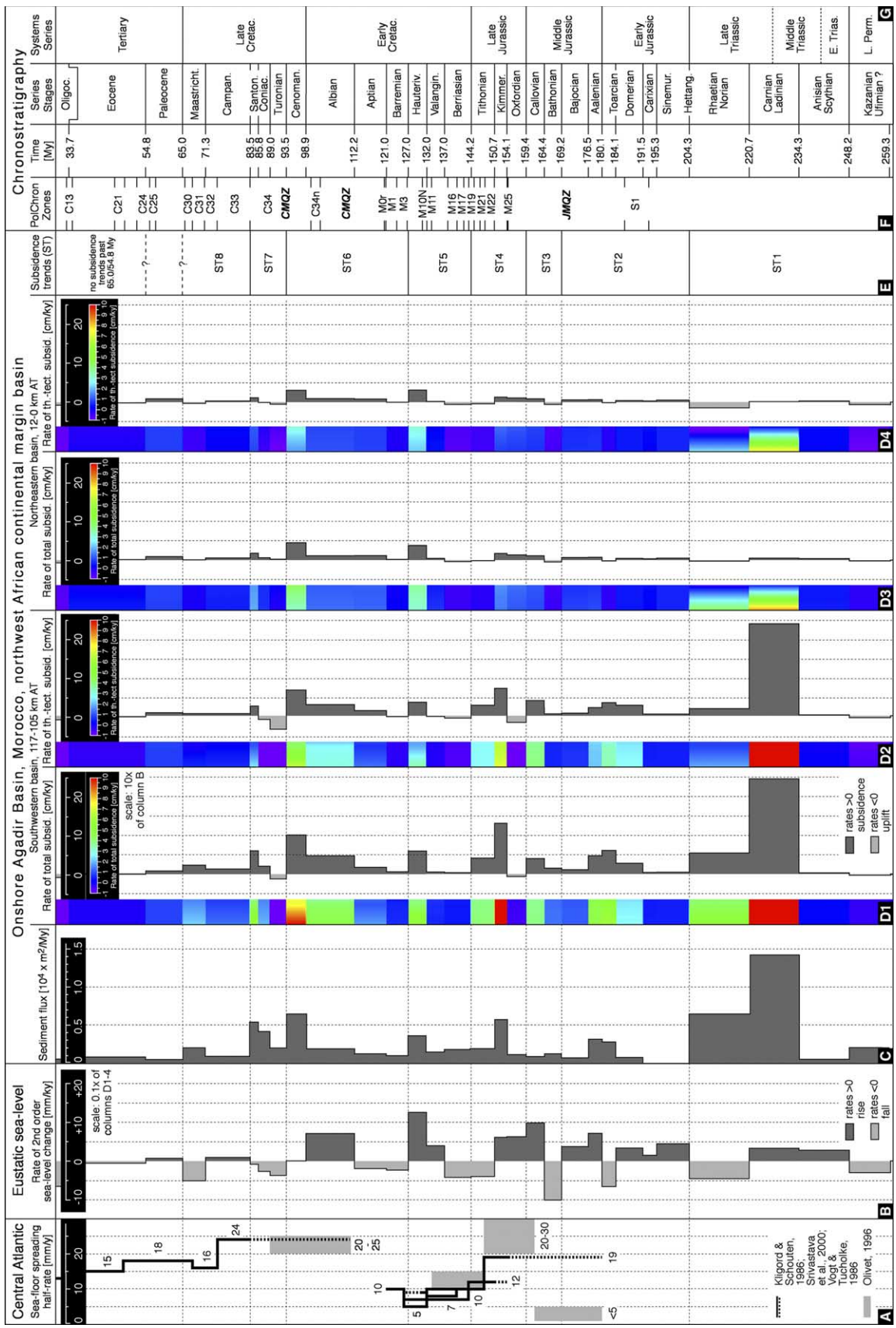
Onshore Agadir Basin, Morocco, northwest African continental margin basin
Central Atlantic
Sea-floor spreading half-rate [mm/y]
Eustatic sea-level
Rate of 2nd order sea-level change [mm/ky]
scale: 0.1x of columns D1-4
rates >0 rise
rates <0 fall
Sediment flux [10⁴ x m²/My]
Southwestern basin, 117-105 km AT
Rate of total subsid. [cm/ky]
Rate of th.-tect. subsid. [cm/ky]
Rate of total subsidence [cm/ky]
scale: 10x of column B
rates >0 subsidence
rates <0 uplift
Northeastern basin, 12-0 km AT
Rate of th.-tect. subsid. [cm/ky]
Subsidence trends (ST)
no subsidence trends past 65.0/54.8 My
Chronostratigraphy
PolChron Zones
Time [My]
Series Stages
Systems Series
Tertiary
Eocene
Paleocene
Late Cretac.
Maastricht.
Campan.
Santon.
Coniac.
Turonian
Cenoman.
Early Cretac.
Albian
Aptian
Barremian
Hauteriv.
Valangin.
Berriasian
Late Jurassic
Tithonian
Kimmer.
Oxfordian
Middle Jurassic
Callovian
Bathonian
Bajocian
Aalenian
Early Jurassic
Toarcian
Domerian
Carixian
Sinemur.
Hettang
Late Triassic
Rhaetian
Norian
Middle Triassic
Carnian
Ladinian
E. Trias.
Anisian
Scythian
L. Perm.
Kazanian
Ufimian ?
CMQZ
JMQZ
ST1
ST2
ST3
ST4
ST5
ST6
ST7
ST8
Kligord & Schouten, 1986; Srivastava et al., 2000; Vogt & Tucholke, 1986
Olivet, 1996

analyzed in Fig. 13(B)–(D), rates of eustatic sea-level change in Fig. 9(B). The application of CA-analysis is reasonably restricted to marine depositional settings of Toarcian to Eocene age (184.1–33.7 Myr), because they are directly controlled by base level changes. It is still a matter of dispute, to which extent continental depositional settings are directly controlled by base level changes in the marine realm. A direct control exists in coastal or delta plain areas but is uncertain for inner continental settings.

In the early drift basin stage (Toarcian to Tithonian, upper ST2–4, 184.1–144.2 Myr) accommodation space in the western to central Agadir Basin was primarily controlled by total subsidence which exceeded rates of eustatic sea-level rises (Aalenian to Bajocian, Callovian to Kimmeridgian). In the Late Toarcian, Bathonian and Tithonian, eustatic sea-level falls attenuated the overall increase in accommodation. In the eastern parts of the basin accommodation space became destroyed. At the very basin margin, tectonic uplift was the prevalent control, followed towards the central basin by a transitional zone of prevalent eustatic sea-level fall. In the western to central basin total subsidence continued to primarily control the long-term increase in accommodation space.

In the Berriasian to Hauterivian (mature drift basin stage, ST5, 144.2–127.0 Myr) and the Barremian to Cenomanian (ST6, 127.0–93.5 Myr) the composition of accommodation space in time follows the same scheme. At the lower part of each subsidence trend (Berriasian, Barremian) accommodation space was destroyed in the eastern to central basin, primarily by total uplift in the Berriasian and by eustatic sea-level fall in the Barremian. In the middle to upper part of ST5 and ST6 accommodation space increased primarily by total subsidence, which exceeded the rates of sea-level rise (Valanginian to Hauterivian, Albian to Cenomanian).

Within the Turonian to Santonian interval (mature drift with initial Atlasian deformation basin stage, ST7, 93.5–83.5), the Turonian represents the only time of basinwide destruction of accommodation space in the Early Jurassic to Eocene development of the Agadir Basin. Total uplift represented the dominant control in the western and central basin. For the first and only time, accommodation space in the eastern basin was primarily controlled by an eustatic sea-level fall. Subsequently, in the Coniacian to Santonian total subsidence represented the main control for the increase of accommodation space.

In the Campanian to Paleocene (mature drift with initial Atlasian deformation basin stage, ST8 and younger, 83.5–54.8 Myr) accommodation space continued to be primarily controlled by total subsidence. Eustatic sea-level rises and falls subordinately modulated the rate of increase. Only in the Maastrichtian of the eastern to central basin accommodation space was destroyed, primarily by eustatic sea-level fall. In the Eocene to Early Oligocene (mature drift basin stage, 54.8 to post-33.7 Myr) accommodation space, primarily triggered by total uplift, became increasingly destroyed from the west to the east.

CA-analysis reveals that changes in total subsidence acted as primary control on accommodation for most of the Meso- to Early Cenozoic development of the Agadir Basin. Second order eustatic sea-level changes were usually subordinate. Detailed results include:

(1) In the early drift to initial mature drift basin stage, predominant control by total uplift was almost exclusively restricted to the base of subsidence trends and to the eastern basin margin. In the mature basin stage, thermo-tectonic uplift as dominant control on accommodation space was not existent. The western basin during the Turonian is the only exception.
(2) Both in the early and mature drift basin stage, total subsidence almost exclusively acted as dominant control on accommodation in the middle to upper part of subsidence trends throughout the basin.
(3) In the mature drift basin stage, accommodation space in the eastern basin margin was only primarily destroyed by eustatic sea-level falls at the base of subsidence trends.
(4) In the western basin, total subsidence almost constantly exerted the dominant control on accommodation space during the Early Jurassic to Early Paleocene. This result most probably also applies to the Jurassic to Cretaceous continental shelf margin, although it is situated 5–15 km west of the onshore modeling transect of this study (Fig. 4). The only exceptions include the Berriasian and Turonian (base ST5 and base ST6).

Fig. 14. Specific patterns in the evolution of total and thermo-tectonic subsidence along the southwestern to northeastern Agadir Basin transect, compared to variations in sediment flux, second order eustatic sea-level changes and sea-floor spreading rates in the Central Atlantic. The *Y*-axis indicates time in Myr full-scale. (A) Sea-floor spreading halfrates in the Central Atlantic according to Klitgord and Schouten (1986), Olivet (1996), Srivastava, Sibuet, Cande, Roest, and Reid (2000), and Vogt and Tucholke (1986). (B) Rates of second order eustatic sea-level change according to Haq et al. (1987) and Hardenbol et al. (1998). Sea-level falls are indicated in light gray, sea-level rises in dark gray. Minimum sea-floor spreading halfrates in the Hauterivian correspond to the maximum rates of eustatic rise during Mesozoic times. Apart from this, there is no direct correlation between rates of sea-floor spreading in the Central Atlantic and second order rates of eustatic change (cf. Christie-Blick, Mountain, & Miller, 1990; Cloetingh, 1988; Dewey & Pitman, 1998; Harrison, 1990). The *Y*-axis scale is 0.1 × of the scale in columns D1–D4. (C) Sediment flux in the Agadir Basin. The unit of (m^2/Myr) is related to the 2D approach of the modeling. The main focus is on the relative variations of sediment flux between successive time layers (see text). (D) Total and thermo-tectonic subsidence rates along the southwestern (D1–2) to northeastern (D3–4) Agadir Basin transect. The *Y*-axis scale is identical for the columns D1–4, and 10 × of the scale in column B. (E) Subsidence trends (ST) in the Agadir Basin (see text). (F) Magnetic polarity chronozones according to Hardenbol et al. (1998). (G) Time scale of Berggren et al. (1995) and Gradstein et al. (1994).

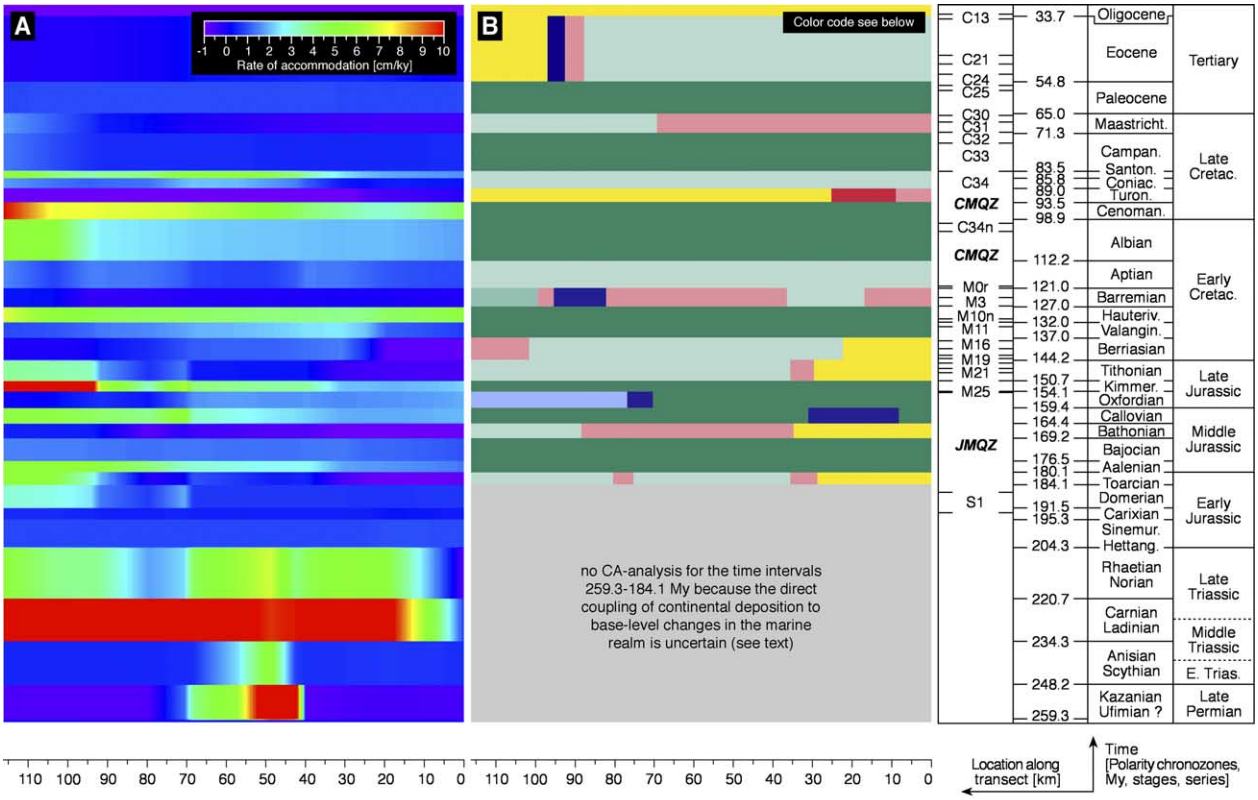

Config. code	Color code (see B)	Rates of total subsidence/uplift	Rate of eustatic sea-level change	Relative quantities	Resulting change in accommodation	Dominant control on accommodation space
+4		$R_{TSU} > 0$	$R_{SL} > 0$	$R_{TSU} > R_{SL}$	$R_{AC} > 0$	total subsidence
+3		$R_{TSU} > 0$	$R_{SL} > 0$	$R_{TSU} < R_{SL}$	$R_{AC} > 0$	eustatic sea-level rise
+2		$R_{TSU} \geq 0$	$R_{SL} \leq 0$	$(R_{TSU} + R_{SL}) > 0$	$R_{AC} > 0$	total subsidence
+1		$R_{TSU} \leq 0$	$R_{SL} \geq 0$	$(R_{TSU} + R_{SL}) > 0$	$R_{AC} > 0$	eustatic sea-level rise
-1		$R_{TSU} \geq 0$	$R_{SL} \leq 0$	$(R_{TSU} + R_{SL}) < 0$	$R_{AC} < 0$	eustatic sea-level fall
-2		$R_{TSU} \leq 0$	$R_{SL} \geq 0$	$(R_{TSU} + R_{SL}) < 0$	$R_{AC} < 0$	total uplift
-3		$R_{TSU} < 0$	$R_{SL} < 0$	$R_{TSU} > R_{SL}$	$R_{AC} < 0$	eustatic sea-level fall
-4		$R_{TSU} < 0$	$R_{SL} < 0$	$R_{TSU} < R_{SL}$	$R_{AC} < 0$	total uplift

Fig. 15. Compositional accommodation analysis (CA-analysis) of the Agadir Basin. (A) Rate of accommodation. (B) Relative ratios of the two parameters controlling accommodation rate: rates of total subsidence/uplift vs. rates of eustatic sea-level change. Eight indicative ratios have been defined based on the results of numerical reverse basin modeling (this project) and long-term eustatic sea-level changes according to Haq et al. (1987) and Hardenbol et al. (1998). Colors indicate: (1) blue, green: zero to increase in accommodation; (2) red, yellow: zero to decrease in accommodation; (3) blue, red: predominant control by eustatic sea-level rise, fall, respectively; (4) green, yellow: predominant control by total subsidence, total uplift, respectively. (C) Indicative parameter configurations in CA-analysis (R_{TSU} : rate of total subsidence/uplift; R_{SL} : rate of eustatic sea-level fall/rise; R_{AC} : resulting rate of accommodation).

7. Feedback processes in the Agadir Basin development

During initial rifting in the Late Permian to top Anisian, halfgrabens represented small-scale basins with local, diverging topographic gradients and sediment transport directions. Only in the sag basin stage (post-220.7 Myr) local basins had been completely filled and faulting was terminated. Basinwide deposition along large-scale topographic/depositional gradients dipping from approximately ENE to WSW was established. These gradients persisted for the sag, early drift and mature drift and mature drift with initial Atlasian compression basin stages until the Late Eocene to Early Oligocene (C13, post-34.7 Myr). They determined the direction of clastic input from the eastern source areas to the western shelf-interior depocenters and the continental slope to rise. Periods of significant carbonate deposition include the Late Toarcian, the Bathonian to Berriasian, the Aptian and the Late Albian to top Eocene. Large-scale shelf-interior progradation occurred from ENE–WSW. For most of its post-Early Jurassic development, the Agadir Basin received or produced sediment volumes, which were equal to or in excess of the accommodation space available. Since the start of subsidence trend ST2 in the Middle Hettangian, the temporal pattern of subsidence components and sediment flux in the Agadir Basin showed positive and negative backfeed processes between sediment input/production, lithospheric flexure and compaction. These backfeed processes were

controlled by changes in thermo-tectonic subsidence on the northwest African continental shelf triggered by plate-tectonic reconfigurations in the Atlantic, Tethyan and Atlasian domains.

The positive feedback process includes:

(1) Transfer of clastic sediment from ENE to WSW as well as carbonate production preferably in WSW increased the lithospheric load, resulting in increased flexural and consequently total subsidence in the western Agadir Basin.
(2) Increased total subsidence in the western basin and eustatic sea-level changes combined to increase long-term accommodation space. As sediment input and production were sufficiently high, large sediment volumes were accommodated. This process is especially important to carbonate deposition, because carbonate production, restricted to submarine environments, is directly coupled to changes in accommodation space.
(3) Large accommodated sediment volumes increased and accelerated compaction in the underlying time layers, resulting in higher compaction-induced subsidence. As a consequence total subsidence was further increased in the western basin.
(4) Additional sediment volume was accommodated, which further increased the lithospheric load and raised flexural and consequently total subsidence.

This positive feedback process between sediment input/production, flexural and compaction-induced subsidence produced exponentially increasing total subsidence rates until changes in the underlying plate-tectonic processes (re-)occurred. When thermo-tectonic subsidence rates on the continental shelf significantly decreased or turned negative (uplift), a negative feedback process started:

(1) The basinwide depositional gradient and the accommodation space available for deposition decreased.
(2) Clastic sediment bypassed the basin and less carbonate sediment was produced within the continental shelf basin.
(3) The incremental lithospheric load became reduced because sediment thicknesses were relatively small and water depths changed only subordinately. Flexural subsidence rates dropped and, in addition to minimum thermo-tectonic subsidence rates, caused an overall reduction in total subsidence.
(4) Because of the reduction in the sediment load, compaction in subsurface stratigraphic units slowed down and decreased thereby reducing compaction-induced subsidence. As a consequence total subsidence rates and accommodation space were further diminished.

In order to sustain these feedback processes the following requirements had to be met:

(1) Processes in the hinterland of the continental shelf were subordinate with respect to plate-tectonic reconfigurations in the Atlantic, Tethyan and Atlasian domains and flexural loading of marginal continental crust below the northwest African passive margin. This appears to be a warrant assumption for the sag, early drift and mature drift basin (with initial Atlasian compression) basin stages (subsidence trends ST2–8). During the early rift and rift climax basin stage, regional processes in the hinterland and faulting constituted the main control on subsidence trend ST1.
(2) Sediment input and production were at balance or in excess of the accommodation space created during each time interval. If, for climatic or paleoecological reasons, sediment input and production could not fill the accommodation space available within the stratigraphic interval considered, the coupled processes of sediment volume, flexure- and compaction-induced subsidence were delayed with regard to the triggering plate-tectonic process (i.e. the change in thermo-tectonic subsidence rates).
(3) During the periods in between plate-tectonic reconfigurations, the marginal continental lithosphere underlying the shelf-interior basin readjusted to the changed boundary conditions (sediment, water load) with an offset of one time layer at maximum.

Feedback processes similar to those described for the Agadir Basin in the subsidence trends ST2–8, can be expected to exist in other circum-Central Atlantic continental shelf basins.

8. Plate-tectonic reconfigurations in the Atlantic, Tethyan and Atlasian Domains

Plate-tectonic reconfigurations in the Atlantic and western Tethys domain have been compiled in Table 4 including key references. Major African–Eurasian plate motions and tectono-stratigraphic developments in the Atlasian domain are listed in Table 5. Temporal correlations between plate-tectonic reconfigurations in the Atlantic and Tethyan domains with subsidence trends in the Agadir Basin do not necessarily indicate a genetic relationship. A genetic model of the Agadir Basin development will be presented in the discussion.

Plate-tectonic reconfigurations in the Atlantic domain are tied to magnetic polarity chronozones. No magnetostratigraphic data exist from the Atlantic oceanic sea-floor prior to polarity chronozone M25 (Latest Oxfordian, pre-154.10 Myr; Jurassic Magnetic Quiet Zone, JMQZ). Time resolution is very limited during the Cretaceous Magnetic Quiet Zone (CMQZ, including M-1r, C34m, C33). Table 4

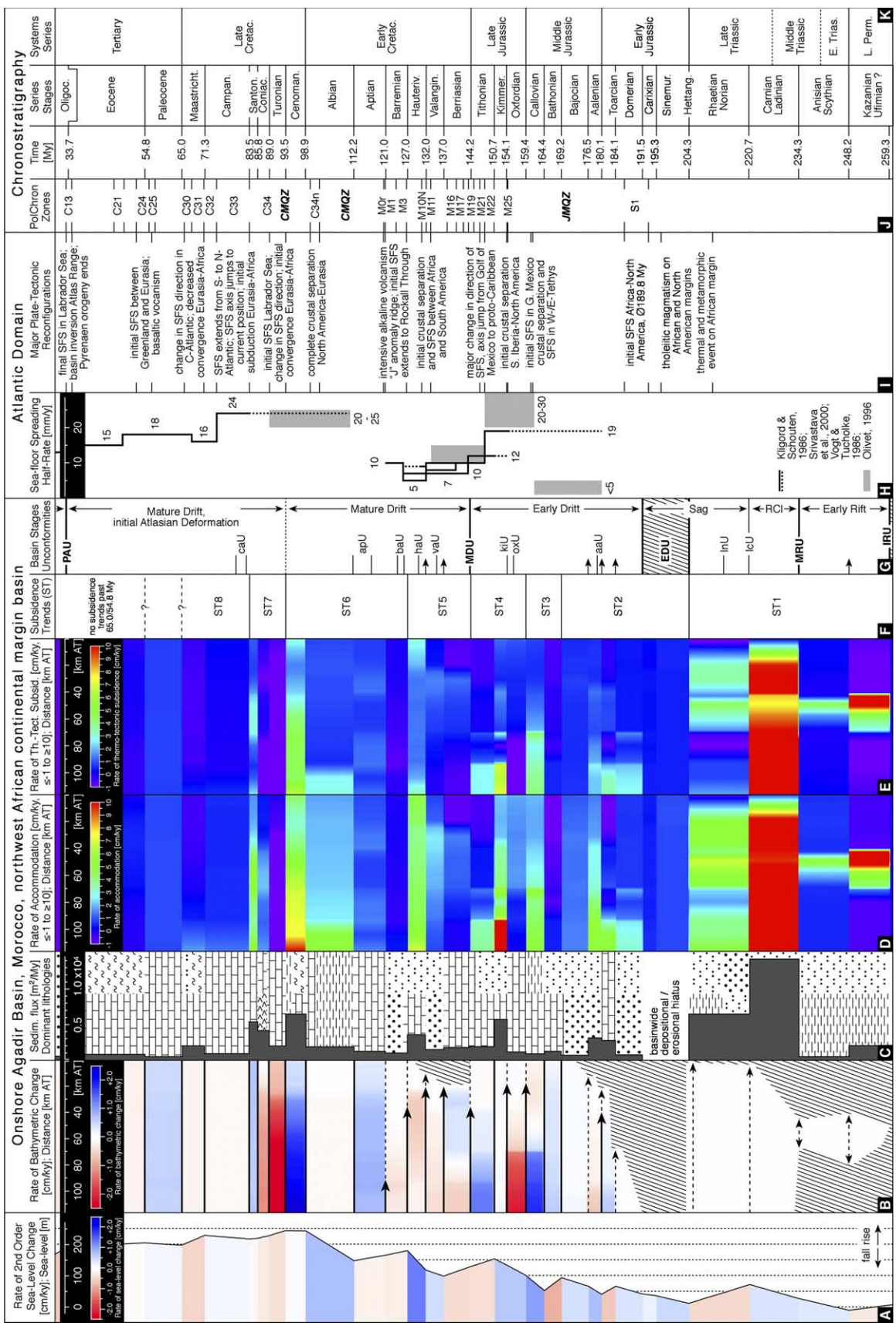
Onshore Agadir Basin, Morocco, northwest African continental margin basin
Atlantic Domain
Chronostratigraphy
Rate of 2nd Order Sea-Level Change [cm/ky]; Sea-level [m]
Rate of Bathymetric Change [cm/ky]; Distance [km AT]
Sedim. flux [m²/My]
Dominant lithologies
Rate of Accommodation [cm/ky]; ≤-1 to ≥10]; Distance [km AT]
Rate of Th.-Tect. Subsid. [cm/ky]; ≤-1 to ≥10]; Distance [km AT]
Subsidence Trends (ST)
Basin Stages
Unconformities
Sea-floor Spreading Half-Rate [mm/y]
Major Plate-Tectonic Reconfigurations
PolChron Zones
Time [My]
Series
Stages
Systems
Series
Mature Drift, initial Atlasian Deformation
Mature Drift
Early Dritt
Sag
RCI
Early Rift
PAU
MDU
EDU
MRU
IRU
caU
apU
baU
haU
vaU
kiU
oxU
aaU
lnU
lcU
ST1
ST2
ST3
ST4
ST5
ST6
ST7
ST8
basinwide depositional / erosional hiatus
no subsidence trends past 65.0/84.8 My
final SFS in Labrador Sea; basin inversion Atlas Range; Pyrenaen orogeny ends
initial SFS between Greenland and Eurasia; basaltic vocanism
change in SFS direction in C-Atlantic; decreased convergence Eurasia-Africa
SFS extends from S- to N-Atlantic; SFS axis jumps to current position; initial subduction Eurasia-Africa
initial SFS Labrador Sea; change in SFS direction; initial convergence Eurasia-Africa
complete crustal separation North America-Eurasia
intensive alkaline volcanism 'J' anomaly ridge; initial SFS extends to Rockall Through
initial crustal separation and SFS between Africa and South America
major change in direction of SFS, axis jump from Golf of Mexico to proto-Caribbean
initial crustal separation S. Iberia-North America
initial SFS in G. Mexico crustal separation and SFS in W-/E-Tethys
initial SFS Africa-North America, Ø189.8 My
tholeiitic magmatism on African and North American margins
thermal and metamorphic event on African margin
Kligord & Schouten, 1986; Srivastava, et al., 2000; Vogt & Tucholke, 1986; Olivet, 1996
CMQZ
JMQZ
Tertiary
Late Cretac.
Early Cretac.
Late Jurassic
Middle Jurassic
Early Jurassic
Late Triassic
Middle Triassic
E. Trias.
L. Perm.
Oligoc.
Eocene
Paleocene
Maastricht.
Campan.
Santon.
Coniac.
Turonian
Cenoman.
Albian
Aptian
Barremian
Hauterin.
Valangin.
Berriasian
Tithonian
Kimmer.
Oxfordian
Callovian
Bathonian
Bajocian
Aalenian
Toarcian
Domerian
Carixian
Sinemur.
Hettang.
Rhaetian
Norian
Carnian
Ladinian
Anisian
Scythian
Kazanian
Ufimian ?
fall rise
A
B
C
D
E
F
G
H
I
J
K

indicates that sea-floor spreading in the Central Atlantic started in the Early Pliensbachian. On Fuerteventura (Canary Islands, 550 km southwest of Agadir) N-MORB basalts are overlain by interbedded basalts, calciturbidites and pelagic sediments (Steiner, Hobson, Favre, Stampfli, & Hernandez, 1998; 'Basal Unit') of pre-Late Toarcian to Early Aalenian age. The only candidate for a carbonate ramp, which could shed these calciturbidites, is the Tamarout Fm. in the Agadir Basin (see Figs. 3 and 5) and its southern extension into the Tarfaya Basin. Therefore sea-floor spreading must have started before the Late Toarcian (184.1 Myr), but after the extrusion of rift-associated tholeiites up to the latest Sinemurian (approx. 195 Myr, see above). The S1 anomaly marks the approximate landward edge of oceanic crust off northwest Africa and is situated 400 km east of the magnetic anomaly M25, 45 km east of Fuerteventura (localities in Steiner et al. (1998)) and 100 km west of Cap Rhir (see Fig. 2). Applying existing estimates of spreading halfrates prior to 184.1 Myr (top Toarcian), initial sea-floor spreading in the Central Atlantic started between 193.1 and 186.5 Myr (Early Pliensbachian to Middle Toarcian, at an average of 189.8 Myr, latest Pliensbachian, Late Domerian). Previous models assumed that the initial separation of Africa from North America took place in the Early Bathonian around 169.2 Myr (175 Myr according to the time scale of Kent and Gradstein (1986)) (see Klitgord and Schouten (1986)). These models were based on a projection of post-M25 (latest Oxfordian) spreading halfrates of 19 mm/yr from base M25 to the S1 magnetic anomaly. However, the calculations presented above, absolute ages for tholeiites on both Central Atlantic margins and the sedimentary succession on Fuerteventura clearly favor the model of initial sea-floor spreading in the Early Pliensbachian to Middle Toarcian.

Plate-tectonic reconfigurations in the Tethys domain (e.g. Savostin, Sibuet, Zonenshain, le Pichon, & Roulet, 1986; in Dercourt et al. (2000)) are less constrained than in the Atlantic domain because magnetic polarity patterns within oceanic crust have not been preserved. Reconstructed plate positions and reconfigurations in time include considerable uncertainties.

Plate-tectonic reconfigurations in the Atlasian domain and African–Eurasian relative plate motions paths are well constrained. They were derived from magnetic anomalies in the Central Atlantic, plate rotation parameters as well as fracture zone, altimetry and gravity maps (Dewey, Helman, Turco, Hutton, & Knot, 1989).

9. Discussion

9.1. Sediment flux and paleobathymetry

Long-term changes in sediment flux in the Agadir Basin are not controlled by second order eustatic sea-level changes. Peak and high sediment flux (Fig. 14(C)) occurs during times of second order eustatic sea-level fall (ST2, Toarcian; ST7, Coniacian to Santonian), rise (ST2, Aalenian; ST4, Kimmeridgian; ST5, Hauterivian) and stationary sea-level (ST6, Cenomanian). In the early to mature drift basin stages, which were dominated by marine deposition, sediment flux varied for ratios of up to 1:6 between successive time layers with a duration of ∅6.5 Myr (min. 2.3 Myr, max. 16.4 Myr, Hettangian to Maastrichtian). Therefore, changes in paleobathymetry as indicated by facies analysis and deepening/shallowing upward trends cannot be equated with changes in accommodation (Fig. 17, columns A and B; cf. Le Roy et al., 1998). Transgressive/regressive trends in the Agadir Basin cannot be used for a basin scale sequence stratigraphic model or for time calibration by correlation to eustatic sea-level charts (Haq et al., 1987; Hardenbol et al., 1998) (Figs. 9(A) and (D) and 17(A), (F)–(H)). Stratal terminations and large-scale sediment geometries, e.g. in seismic lines, were influenced by changes in sediment input/production.

Fig. 16. Summary of key parameters for the Meso-/Cenozoic development of the Agadir Basin. All data are interpolated over the time layers indicated in column J (stage-level resolution). The *Y*-axis indicates time in (Myr) full-scale. (A) Rates of long-term eustatic sea-level change (Fig. 9(B)). Scale bar indicates sea-level in (m) compared to recent; (B) Rates of bathymetric change, coastal and continental onlap in the Agadir Basin (Fig. 9(D)). Scale bar indicates distances in (km AT) (see Fig. 4); (C) Sediment flux and dominant lithologies in the Agadir Basin (see Fig. 14). Scale bar indicates flux in (m^2/Myr); (D) Rates of accommodation in the Agadir Basin. The spectrum is cut at − 1 and 10 cm/kyr (Fig. 15(A)). Scale bar indicates distances in (km AT) (see Fig. 4); (E) Rates of thermo-tectonic subsidence in the Agadir Basin. The spectrum is cut at − 1 and 10 cm/kyr. Scale bar indicates distances in (km AT) (see Fig. 4); (F) Subsidence trends in the onshore Agadir Basin (Fig. 14(E)); (G) Basin stages (Table 1) defined on the basis of basin architecture, unconformities, onlaps (Fig. 8) and results of 2D reverse basin modeling. Unconformities at the resolution of time layers in bold capitals. Arrows indicate onlap of time layers against the unconformity (Fig. 9(A) and (D)). Unconformities below the resolution of time layers in small letters (see text); (H) Sea-floor spreading halfrates in the Central and northern Atlantic according to Klitgord and Schouten (1986), Srivastava et al. (2000), and Vogt and Tucholke (1986) (Fig. 14(A)); (I) Major plate-tectonic reconfigurations in the Atlantic and western Tethys domain (see Table 4 for a detailed list of reconfigurations). For an overview of paleo-climatic, paleo-oceanographic and paleo-biogeographic controls on depositional systems on circum-Atlantic continental shelves, see Gradstein et al. (1990). (J) Magnetic polarity chronozones in the Central and northern Atlantic according to Hardenbol et al. (1998); (K) Standard chronostratigraphy according to Berggren et al. (1995), Gradstein et al. (1994), and Hardenbol et al. (1998). Legend (sorted by columns): (B): km AT—kilometers along transect (see Fig. 2) (F): RCl—Rift Climax; IRU—Initial Rift Unconformity; MRU—Main Rift Unconformity; EDU—Early Drift Unconformity; MDU—Mature Drift Unconformity; PAU—Peak Atlasian Unconformity; lcU—Late Carnian unconformity; lnU—Late Norian to Rhaetian unconformity; aaU—Early Aalenian unconformity; oxU—Late Oxfordian unconformity; kiU—Early Kimmeridgian unconformity; vaU—Early Valanginian unconformity; haU—Early Hauterivian unconformity; baU—Early Barremian unconformity; apU—Late Aptian unconformity; caU—Early (?) Campanian unconformity; (H): N—North; S—southern; SFS—sea floor spreading; C—Central; (I): CMQZ—Cretaceous Magnetic Quiet Zone; ECMA—East Coast Magnetic Anomaly (Vogt, 1973); JMQZ—Jurassic Magnetic Quiet Zone; BMA—Brunswick Magnetic Anomaly (Klitgord et al., 1988); BSMA—Blake Spur Magnetic Quiet Zone (Vogt, 1973); S1—west African magnetic anomaly (Roeser, 1982).

Although the discrepancy between paleobathymetry and accommodation has only been quantified for the Agadir Basin in this study, it probably also applies to other northwest African Atlantic Basins.

Facies and paleobathymetry data in the Agadir Basin do not provide any indication for the subsidence trends ST3 and ST6. Depending on the locality within the basin, subsidence trends ST3 and ST4 would be interpreted as large-scale shallowing (eastern basin) or deepening upward succession (western basin) with serious consequences for correlations to eustatic sea-level charts. An interpretation of the Cretaceous basin fill based on large-scale shallowing/-deepening upward trends would produce a very different accommodation and subsidence/uplift model. Temporal and spatial variations in total/thermo-tectonic subsidence, like in the subsidence trends ST5–8, with their specific internal signature and relation to plate-tectonic reconfigurations in the Atlantic domain will not be disclosed.

In summary, qualitative facies analyses, the identification of large-scale transgressive/regressive trends and respective plots constitute important approaches and tools to reconstruct the facies architecture of continental shelves. However, they are not necessarily an appropriate methodology to analyze changes in accommodation and to develop genetic models of continental shelf development.

9.2. Total and thermo-tectonic subsidence

Maximum and average rates of subsidence components and their relative ratios are presented in Tables 2 and 3. All rates have been specified for individual geological stages until the Maastrichtian, well before peak compression, uplift and basin inversion started in the Late Eocene.

Average total and thermo-tectonic subsidence rates in the western basin decrease from 3.5 [2.2] cm/kyr (total subsidence [thermo-tectonic subsidence]) in the early drift to 2.7 [1.2] cm/kyr in the mature drift basin stage (Table 3). In the eastern onshore basin the respective values increase slightly from 0.6 [0.4] to 1.0 [0.6] cm/kyr. The long-term reduction in thermo-tectonic subsidence rates of the continental shelf between the early and mature drift stages reflect the thermal relaxation of adjacent oceanic crust with increasing age and distance from the spreading ridge. However, the reduction in thermo-tectonic subsidence is partly compensated for by increased flexural and compaction-induced subsidence. As a consequence, the reduction in total subsidence between the early and mature drift basin stages is smaller than the reduction in thermo-tectonic subsidence. Average rates of total subsidence decrease to 77% of the average early drift rates, compared to a decrease to 54% in average rates of thermo-tectonic subsidence. On average, total subsidence rates during the early drift stage are 1.6–1.7 times higher than tectonic subsidence rates. In the mature drift basin stage the factor increases to 1.7–2.3 times. The difference is accounted for by the increase in flexural and compaction-induced subsidence in time.

Reverse basin modeling reveals that total subsidence persisted in the Berriasian, Barremian and Coniacian and was zero in the Oxfordian. However, thermo-tectonic uplift prevailed in the Oxfordian, Barremian and Coniacian and was zero in the Berriasian (see Table 2, Fig. 14). Without numerical modeling, changes in the basin development as indicated by thermo-tectonic uplift in ST4–7 and their potential relation to changes in plate-tectonic reconfigurations in the Atlantic domain would be hard to recognize.

9.3. Accommodation

Sequence stratigraphic models commonly consider eustatic sea-level changes, and partly also subsidence, within limited stratigraphic intervals to qualitatively assess or quantitatively analyze changes in accommodation. Numerical basin modeling of this study shows that total subsidence rates have to be considered to adequately analyze changes in accommodation in sequence stratigraphic models. Furthermore, sequence stratigraphic studies focused on limited stratigraphic time intervals within sedimentary basins are likely to produce unrealistic approximations of changes in accommodation, because flexure and compaction in the underlying basin fill are not considered. All subsidence, necessary to accommodate the sedimentary series of interest, is commonly attributed to thermo-tectonic subsidence and/or sea level rise. Either the rates of thermo-tectonic subsidence will appear unrealistically high, leading to misinterpretation of structural or plate-tectonic reconfigurations on the regional to basin scale. Alternatively, a long-term sea level rise may be assumed, which did not actually exist.

Existing studies on the sequence stratigraphy of the Moroccan Atlantic Basins were primarily based on qualitative facies analyses. Very few previous studies have actually identified shallowing/deepening upward trends in 2D, i.e. in seismic lines (Tarfaya Basin: Le Roy, 1997; Todd & Mitchum, 1977; Vail, Mitchum, & Thompson, 1977) and/or by correlations between wells. In fact, all previous studies followed an allostratigraphic rather than a sequence stratigraphic approach (NACSN, 1983; Walker & James, 1992). They were based on the identification of (mappable) stratiform sediment units by their bounding discontinuities and their correlative conformities. In the majority of studies, shallowing/deepening upward trends were defined only in single vertical sections. The resulting pattern was compared to the sea-level chart of Haq et al. (1987), implying that shallowing/deepening upward trends directly and exclusively reflected changes in sea-level. Transgressive/regressive peaks in the sediment succession were tied to eustatic sea-level high- and lowstands in the Exxon sea-level chart and thereby time-calibrated.

Numerical basin modeling allows to quantitatively compare the peak and average rates of subsidence

Table 2
Maximum rates of subsidence/uplift components and total subsidence/uplift in different segments of the Agadir Basin

Subsid. Trend	Ages (Myr)	Geological stages	Accommodation and subsidence components, maximum rates: geological stages, basin segments (cm/kyr)														
			SW-Basin (116–80 km AT)					Central Basin (79–40 km AT)					NE-Basin (39–0 km AT)				
			Acc.	Total	Th-T.	Flex.	Com.	Acc.	Total	Th-T.	Flex.	Com.	Acc.	Total	Th-T.	Flex.	Com.
ST8	71.3–65.0	Maastrichtian	+1.8	+2.3	+0.5	+1.8	+1.6	+0.2	+0.8	+0.8	+1.2	+0.8	−0.4	+0.1	−0.5	+0.7	+0.3
	83.5–71.3	Campanian	+1.4	+1.3	+0.6	+0.7	+0.7	+0.6	+0.5	−0.5	+0.5	+0.3	+0.6	+0.5	+0.3	+0.4	+0.2
ST7	85.5–83.5	Santonian	+5.8	+5.9	+2.5	+3.4	+3.0	+5.5	+5.6	+3.0	+2.9	+2.5	+3.4	+3.5	+1.7	+1.8	+1.5
	89.0–85.5	Coniacian	+1.8	+2.0	−1.0	+3.0	+2.0	+2.1	+2.4	−0.1	+2.8	+1.9	+1.1	+1.3	−0.1	+1.9	+1.2
	93.5–89.0	Turonian	−1.6	−1.3	−3.6	+2.3	+1.5	−2.2	−1.3	−2.6	+1.9	+1.9	−0.2	+0.2	−0.6	+1.3	+0.5
ST6	98.8–93.5	Cenomanian	+10.1	+10.1	+6.8	+3.3	+3.7	+7.1	+7.1	+4.6	+2.5	+2.4	+4.5	+4.5	+3.1	+1.8	+1.3
	112.2–98.8	Albian	+5.5	+4.7	+2.9	+1.8	+1.7	+2.5	+1.7	+0.9	+1.0	+0.6	+2.1	+1.4	+1.0	+0.5	+0.4
	121.0–112.2	Aptian	+1.6	+1.8	+1.3	+0.4	+0.6	+1.4	+1.6	+1.3	+0.3	+0.5	+1.4	+1.6	+1.3	+0.4	+0.5
	127.0–121.0	Barremian	+0.4	+0.6	−0.2	+0.8	+0.6	−0.0	+0.2	−0.2	+0.6	+0.3	+0.0	+0.3	±0.0	+0.4	+0.3
ST5	132.0–127.0	Hauterivian	+7.2	+5.9	+3.6	+2.3	+2.4	+4.4	+3.2	+1.4	+1.8	+1.3	+5.0	+3.7	+3.1	+1.3	+1.0
	137.0–132.0	Valanginian	+1.6	+1.1	+0.3	+0.8	+0.6	+2.5	+2.1	+1.4	+0.8	+0.9	+2.5	+2.1	+1.5	+0.7	+0.9
	144.2–137.0	Berriasian	+0.6	+1.0	±0.0	+1.0	+0.8	+1.3	+1.7	+1.0	+1.0	+0.9	+1.3	+1.9	+1.3	+0.7	+0.9
ST4	150.7–144.2	Tithonian	+3.7	+4.1	+2.8	+1.4	+1.7	+1.4	+1.8	+1.0	+0.9	+0.9	+0.3	+0.7	+0.2	+0.5	+0.5
	154.1–150.7	Kimmeridgian	+13.7	+13.1	+7.3	+5.8	+5.4	+6.3	+3.4	+2.9	+1.3	+0.9	+3.5	+1.7	+1.3	+0.8	+0.5
	159.4–154.1	Oxfordian	+0.6	±0.0	−1.1	+1.3	+0.7	+1.8	+1.1	+0.6	+1.0	+1.5	+1.9	+1.3	+1.0	+0.5	+0.5
ST3	164.4–159.4	Callovian	+5.0	+4.0	+4.0	+0.2	+0.7	+5.4	+4.4	+4.2	+0.3	+1.1	+2.3	+1.3	+1.0	+0.3	+0.3
	169.2–164.4	Bathonian	+0.5	+1.4	+0.6	+0.8	+1.0	−0.7	+0.7	+0.1	+0.6	+0.6	−0.7	+0.2	−0.1	+0.3	+0.4
ST2	176.5–169.2	Bajocian	+1.5	+1.1	+0.7	+0.4	+0.4	+1.4	+1.0	+0.7	+0.4	+0.3	+1.4	+1.0	+0.8	+0.3	+0.3
	180.1–176.5	Aalenian	+5.5	+4.8	+2.7	+2.6	+2.7	+4.0	+3.3	+1.6	+1.8	+1.8	+2.7	+2.0	+1.3	+0.7	+0.9
	184.1–180.1	Late Toarcian	+5.4	+6.1	+3.5	+2.6	+3.3	+0.9	+1.7	+1.0	+1.2	+1.2	+0.5	+1.1	+1.0	+0.1	+0.8
	191.5–184.1	Dom. to Mid. Toarc.	+3.1	+2.8	+2.8	±0.0	+1.5	+1.9	+1.6	+1.6	±0.0	+0.7	+0.7	+0.4	+0.4	±0.0	±0.0
	195.3–191.5	Carixian	+0.6	+0.4	+0.4	±0.0	±0.0	+0.5	+0.4	+0.4	±0.0	±0.0	+0.5	+0.3	+0.3	±0.0	±0.0
	204.3–195.3	Mid. Hett. to Sinem.	+0.9	+0.5	+0.5	±0.0	±0.0	+0.9	+0.5	+0.5	±0.0	±0.0	+1.0	+0.5	+0.5	±0.0	±0.0
ST1	220.7–204.3	Norian to Early Hett.	+5.0	+5.5	+1.9	+3.6	+2.4	+6.9	+7.4	+4.4	+3.3	+2.2	+5.6	+6.1	+3.6	+2.8	+1.5
	234.3–220.7	Ladinian to Carnian	+24.9	+24.5	+24.3	+1.4	±0.0	+24.4	+24.1	+22.7	+1.8	+2.0	+12.9	+12.6	+11.1	+1.5	±0.0
	248.2–234.3	Scythian to Anisian	+0.6	+0.3	+0.2	+0.3	±0.0	+5.3	+5.0	+4.6	+0.4	+1.3	+0.7	+0.4	+0.3	+0.3	±0.0
	259.3–248.2	Late Permian	−0.6	−0.3	−0.6	+1.2	±0.0	+12.8	+13.1	+11.5	+1.7	±0.0	−0.7	−0.2	−0.7	+1.5	±0.0

See Fig. 13 for spectrograms cut at −1/+10 cm/kyr (total, thermo-tectonic subsidence) and ±0/+4 cm/kyr (flexural, compaction-induced subsidence). Legend: Subsid. Trend, subsidence trend; SW-Basin, south western basin; NE-Basin, northeastern basin; Hett. Hettangian; Sinem., Sinemurian; Dom. Domerian; Toarc., Toarcian; AT, along the transect; Total, total subsidence; Th-T., thermo-tectonic subsidence; Flex., flexural subsidence; Com., compaction-induced subsidence; positive values, subsidence; negative values, uplift. For abbreviations of unconformities see Fig. 6.

Table 3
Average rates for changes in accommodation, total and thermo-tectonic subsidence in the Agadir Basin

Basin stages	Accommodation, subsidence components, average rates: basin stages, segments (cm/kyr)					
	Accommodation		Total subsidence		Th.-Tect. subsid.	
	SW-Basin	NE-Basin	SW-Basin	NE-Basin	SW-Basin	NE-Basin
Early to mature drift (191.5–93.5 Myr)	+2.5	+0.8	+2.4	+0.7	+1.2	+0.4
Mature drift (144.2–93.5 Myr)	+2.8	+1.1	+2.7	+1.0	+1.2	+0.6
Early drift (191.5–144.2 Myr)	+3.7	+0.7	+3.5	+0.6	+2.2	+0.4
Early rift to sag (259.3–191.5 Myr)	+6.3	+0.2	+6.3	+0.1	+5.3	−0.3
Sag (220.7–191.5 Myr)	+3.2	−0.1	+3.2	+0.0	+1.3	−0.7
Early rift to rift climax (259.3–220.7 Myr)	+8.7	+0.3	+8.6	+0.2	+8.4	−0.1
Ratios [ ]	SW-Basin	NE-Basin				
∅Total subsid.:∅Therm.–tect. subsid.						
Mature drift (144.2–93.5 Myr; max., min.)	2.28	1.70				
Early drift (191.5–144.2 Myr; max., min.)	1.62	1.70				

Rates are grouped for the northeastern and southwestern basin (table header) and the early rift to sag and the early to mature drift basin stages (left column). The basinwide depositional hiatus between 204.3 and 191.5 Myr has been added to the early rift to sag basin stages.

components, accommodation and long-term eustatic sea-level changes during the Meso-/Cenozoic development of the Agadir Basin. The following ratios between specific controls refer to the whole Meso-/Cenozoic development of the western onshore Agadir Basin. Fig. 17 shows spectrograms of bathymetric change, accommodation and thermo-tectonic subsidence rates for the Agadir Basin as well as rates of eustatic change at the same scale (−2.0 to +6.0 cm/kyr).

Ratios of subsidence rates vs. rates of eustatic sea-level rise (accommodation space created):

(1) peak total subsidence rates : peak thermo-tectonic subsidence rates: 1.5–1.8 ×
(2) peak total subsidence rates : rates of second order eustatic sea-level rises: 8.0–13.2 ×
(3) peak thermo-tectonic subsidence rates : peak second order eustatic sea-level rises: 5.4–7.3 ×

Ratios of uplift rates vs. rates of eustatic sea-level falls (accommodation space destroyed):

(1) peak thermo-tectonic uplift rates : effective peak total uplift rates: 2.8–3.4 ×
(2) peak thermo-tectonic uplift rates : peak second order eustatic sea-level falls: 2.0–7.0 ×
(3) peak total uplift rates : rates of second order eustatic sea-level falls: approximately same range

Thermo-tectonic uplift was significantly attenuated to counteracted by compaction-induced and flexural subsidence. The interactions between (1) compaction-induced and flexural subsidence and thermo-tectonic subsidence to produce total subsidence and (2) total subsidence and eustatic sea-level to produce accommodation space, have serious implications for basin analysis. Although thermo-tectonic uplift occurs, moderate to low total subsidence prevail in basins with thick, compactible successions. Accommodation space may still be created. Facies may indicate constant to increasing paleowater depths.

Close to the continental margin, i.e. in the westernmost onshore Agadir Basin, where accommodation space was almost permanently created between the Pliensbachian to Maastrichtian, rates of total subsidence were one dimension higher than rates of second order eustatic sea-level rise. In general, changes in accommodation over time intervals of 2.3–13.4 Myr in the Agadir Basin were primarily controlled by total subsidence and not by second order eustatic sea-level changes. Therefore, long-term transgressive–regressive cycles analyzed by qualitative facies analysis in previous studies reflected subsidence trends controlled by plate-tectonic reconfigurations in the Atlantic domain rather than eustatic sea-level changes.

In summary, incorporating changes of sediment flux into a sequence stratigraphic model and building a genetic model of the basin development requires a quantitative approach. Reverse numerical basin modeling can be applied to build genetic models with second order time resolution (3–10 Myr, stage level). Genetic models at third order time resolution (sequences, 1–3 Myr) will require forward stratigraphic modeling. Realistic approximations on changes in accommodation within a limited stratigraphic interval have to consider flexure and compaction in the complete underlying sedimentary series.

9.4. Genetic model of the Agadir Basin development

The correlation of subsidence trends and sediment flux in the Agadir Basin to plate-tectonic reconfigurations in the Atlantic and adjacent domains indicates, that four types of plate-tectonic reconfigurations controlled the long-term development of continental shelf basins bordering the Central Atlantic (Figs. 16 and 18):

Table 4
Early Jurassic to Paleogene major plate-tectonic and structural developments in the Atlantic and western Tethyan domains

Plate-tectonic developments	Ages (Myr)		Atlantic and western Tethys domain (Jurassic to Oligocene)	Key references	Subsid. trends
	From	To			
Plate-tectonic reorganization	34.7, Latest Eoc., C13	33.1, Earliest Oligoc., C13	Final SFS in the Labrodor Sea	Klitgord and Schouten (1986)	
			Final major compression ("orogenies") in the Pyrenees and the Caribbean		
			Major plate convergence African–Eurasian plates with compression uplift and basin inversion in the Atlas Range (post-C13, post-latest Eocene)	Gomez et al. (2000)	
Change in sea floor spreading direction	49.0, Middle Eoc., C21	46.3, Middle Eoc., C21	Change in Central Atlantic SFS directions	Klitgord and Schouten (1986)	No subsid trends past 65.0/54.8 Myr
			Peak collision African/Apulian and Eurasian plates and uplift of peri-Tethyan domains/platforms (Middle–Late Eocene, 49.0–33.7 Myr)		
			N directed propagation of subduction, thrusting and foredeep development in the present western Alpine domains	Meulenkamp et al. (2000a)	
			Renewed strong NE to N motion of African against Eurasian plate (post-Early Eocene, post-C24, post-52.4 Myr)	Dewey et al. (1989)	
Plate-tectonic reorganization	57.5, Late Paleoc., C25	52.4, Early Eoc., C24	Initial SFS in the Norwegian-Greenland-Arctic Sea	Roest and Srivastava (1989)	---54.8---
			Change in plate motion of Greenland (from ENE- to NNW-direction) (relative to Eurasia and North America)		
			Basaltic volcanism W-/E-Greenland and Scotland ridges	Srivastava and Tapscott (1986)	
			Peak collision of Iberian microplate and Eurasian plate (nappe piling in the Pyrenees, formation of N and S foreland basins)	Meulenkamp et al. (2000b)	
			Uplift of northern and southern Peri-Tethys domains		
Plate tectonic reorganization	67.6, Late Maastricht., C30	65.6, Late Maastricht., C30	Change in SFS directions in the Central Atlantic	Klitgord and Schouten (1986)	---65.0---
			Increased collision of Apulian and Eurasian plates	Philip and Floquet (2000a)	
			Former oceanic W-Tethys domains completely subducted		
			Strong decrease in convergence rates between African and European plates (post-C30, post-65.6 Myr)	Dewey et al. (1989)	

(*continued on next page*)

Table 4 (*continued*)

Plate-tectonic developments	Ages (Myr)		Atlantic and western Tethys domain (Jurassic to Oligocene)	Key references	Subsid. trends
	From	To			
Change in sea floor spreading velocity	74.5, Late Campanian C32	71.0, Late Campanian C32	Decrease in Central Atlantic SFS halfrates, 24 mm/ky to 16 mm/ky Change of motion between Eurasia and North America	Klitgord and Schouten (1986) Srivastava, Verhoef, and Macnab (1988)	ST8
Sea floor spreading shift	83.5, Early Campan., C33	74.5, Mid. Campan., C33	Spreading axis jump from the proto-Caribbean to the curent position SFS extends from the South Atlantic (Falkland Fault Zone) over the Central Atlantic to Northern Atlantic (Labrador Sea) SFS in the Bay of Biscay ceases Compression Africa–Eurasia advances from strike-slip to subduction at N-Iberia and Eurasia margins	Klitgord and Schouten (1986)	
Plate-tectonic reorganization	84.6, Late Santon., C34/CMQZ	83.5, Late Santon., C34/CMQZ	Change in the rotation pole for Atlantic opening triggers compression in Western Tethys and European domains (terminates C34, CMQZ) Increased NW drift of Apulian and Iberian microplates Ligurean Ocean largely subducted	Guiraud and Bosworth (1997) Philip and Floquet (2000b) Stampfli (1993)	---83.5--- ST7
Extension of sea-floor spreading	93.5, Turonian, C34/CMQZ	89.0, Turonian, C34/CMQZ	Change in SFS directions in the Central Atlantic Initial SFS in the Labrador Sea Initial NE directed convergence between Eurasian and Africa plates	Olivet (1996) Roest and Srivastava (1989) Dewey et al. (1989)	---93.5---
Plate-tectonic reorganization	102.8, Middle Albian, C34n	100.2, Late Albian, C34n	Complete crustal separation North America-Europe Initial closure of Ligurian/Piemont Ocean	Srivastava et al. (1988) Olivet (1996)	
Peak high sea-floor spreading velocity	121.0, earliest Aptian M0r	93.5, Cenomanian, CMQZ	Sea floor spreading halfrates 20-25 mm/yr (Central Atlantic) Sea floor spreading halfrates 24 mm/yr (Central Atlantic)	Olivet (1996) Klitgord and Schouten (1986)	ST6
Mid-plate alkaline volcanism	121.0, earliest Aptian, M0r	120.4, earliest Aptian, M0r	"J" anomaly ridge between North American Margin, Iberia and Africa Intensive alkaline volcanism in Newfoundland Fracture Zone Initial rifting Bay of Biscay and Norwegian Sea Initial collision Iberian and Apulian microplates ∅ final SFS in the Ligurian/Piemont Ocean See 146.0–142.0 Myr (Thierry, 2000d)	Gradstein et al. (1990) Srivastava and Verhoef (1992) Klitgord and Schouten (1986) Olivet (1996)	
Extension of sea-floor spreading	126.7, Early Barremian, M3	120.4, Late Barremian, M0	SFS extends into North Atlantic between Grand Banks and Iberia Initial SFS in Bay of Biskay and Rockall Trough Uplift of Central Atlantic continental margins Complete separation Africa-South America	Boillot, Mougenot, Girardeau, and Winterer (1989) Jansa and Wade (1975) Olivet (1996)	---127.0---

Peak low sea-floor spreading velocity	132.1, Latest Valangin, M10N	124.1 Middle Barrem. M3	Sea-floor spreading halfrates 5 mm/yr (Central Atlantic) Sea-floor spreading halfrates 7 mm/yr (Central Atlantic) Sea-floor spreading halfrates 9 mm/yr (Central Atlantic)	Olivet (1996) Klitgord and Schouten (1986) Vogt and Tucholke (1986)	
Initial sea-floor spreading outside the Central Atlantic	133.4 Late Valangin M11	130.9, Early Hauteriv., M10N	Initial rifting in North Atlantic (Maghreb Fault Zone to Rockall Through) Initial SFS between Africa and South America (Benué Tr. to Falkland FZ) Crustal separation Africa and South America (south of Falkland FZ)	Klitgord and Schouten (1986)	ST5
	132.0, Early Hauteriv. M10N	129.9, Early Hauteriv. M9	∅ Compression North–South America and African/Arab Block-Eurasia See 93.5–89.0 Myr (Dewey et al., 1989) ∅ Initial compression in Tethys domain with flysch development See 146.0–142.0 Myr (Thierry, 2000d)	Bulot (2000)	
Plate-tectonic reconfiguration	146.0, Late Tithonian M20	142.0 Early Berrias. M17	Initial sinistral rotational translation of Eurasia relative to Gondwana ("Neo-Cimmerian unconformity/phase" on European plate) Termination of SFS in the westernmost Tethys (Ligurian Ocean) Initial obduction of Dinarid/Hellenid domains in the western Tethys Initial collision of Apulian plate against Eurasian plate in the W-Tethys Initial sinistral displacement/separation of Iberian microplate from the European plate, pull-apart basins in future Bay of Biscay rift	Thierry (2000d) Olivet (1996) and Thierry (2000d)	---144.2---
Sea-floor spreading shift	148.1 Middle Tithon M21	143.6 earliest Berrias. M19	Gulf of Mexico to the proto-Caribbean spreading axis jump (M21) Decrease in Central Atlantic SFS halfrates (M21-M19) 20–30 mm/yr to 10–15 mm/yr, 19 mm/yr to 10 mm/yr, 12 mm/yr to 7 mm/yr	Klitgord and Schouten (1986) Olivet (1996) Klitgord and Schouten (1986) Vogt and Tucholke (1986)	ST4
First major northward extension of crustal separation	154.4 Latest Oxford. M25	152.6 Early Kimm. M24	Initial crustal separation of southern Iberia from North America (M25) Crustal separation beyond subsequent East Azores/Gloria and Pico Fracture Zones High subsidence rates and abundant terrigenous input in the Western High Atlas (159.4-144.2, Oxfordian to Tithonian)	Srivastava and Verhoef (1992) Srivastava et al. (1990) and Mauffret et al. (1989) Thierry (2000c) and Labassi et al. (2000)	
Plate-tectonic reconfiguration	161.3 Middle Callov. JMQZ	160.8 Middle Callov. JMQZ	Initial SFS in the Gulf of Mexico Ceased rifting in Atlasic domain, simple extension (Middle Callovian) Crustal separation in the western, SFS in the eastern Ligurian domain Final compression of Vardar Ocean at northern Tethys margin Maghreb transfer zone links Atlantic and eastern Ligurian ridges	Thierry (2000b) Ziegler, Cloetingh, Guiraud, and Stampfli (2001)	---159.4--- ST3
	172.9 Late Bajocian JMQZ	167.9 Early Bathonian JMQZ	∅ Initial formation of a Mid-oceanic ridge in the Central Atlantic ∅ Initial SFS in Central Atlantic, Gulf of Mexico and Ligurian Tethys (175 Myr in time scale of Kent and Gradstein (1985)) See 193.1-186.5 Myr (Steiner et al., 1998; this study/see text)	Thierry (2000b) Klitgord and Schouten (1986) and Speed (1994)	---169.2---

(*continued on next page*)

Table 4 (*continued*)

Plate-tectonic developments	Ages (Myr)		Atlantic and western Tethys domain (Jurassic to Oligocene)	Key references	Subsid. trends
	From	To			
Continental separation in the western Tethys domain	186.8 Middle Toarc. JMQZ	185.3 Middle Toarc. JMQZ	Continental separation in the western Tethyan domain (Ligurian Basin) (oceanic deep sea-areas propagate W, e.g. Vardar, Bükk furrows) Pull-apart basins due to NW–SE synrift extension in W-Morocco basins Major subsidence, general rifting and active extension in western Tethys basins (Sinemurian/Pliensbachian to Callovian, "Ligurian Cycle")	Thierry (2000a) Jacquin and de Graciansky (1998)	
Initial sea-floor spreading in the Central Atlantic	193.1 Early Pliensb. JMQZ	186.5 Middle Toarc. JMQZ	Initial SFS in the Central Atlantic (∅ 189.8 Myr, latest Pliensbachian, latest Domerian) N-MORB basalts overlain by pelagic sediments (pre-Late Toarcian to Early Aalennian) Sea floor spreading halfrates 5 mm/yr Sea floor spreading halfrates 19 mm/yr	(this study, see text) Steiner et al. (1998) Olivet (1996) Klitgord and Schouten (1986)	ST2
Early magnetic anomalies	pre-184.1/Late Toarcian, post-195.0/latest Sinemurian JMQZ		S1 and Blake Spur Magnetic Anomaly (BSMA), assumed landward edges of oceanic crust off NW-Africa and North America Mojave-Sonora megashear	Roeser (1982) and Roest, Danobeitia, Verhoef, and Collette (1992) Klitgord and Schouten (1986)	
Magmatism and thermal uplift in future Central Atlantic domain	204.3 Middle Hettang., 210.4 ± 2.1 196.1 ± 7.5, 200.4 ± 0.2 202.0 Late Hettangian JMQZ	195.3 latest Sinemur. 196.3 ± 1.2, 196.0 ± 5.7, 194.8 ± 0.5, 201.0 Late Hettangian JMQZ	Widespread basaltic flows on African and North American margins Basalts in Central/High Atlas with anorogenic geochemical signature Tholeiites, High/Middle Atlas ($^{40}Ar/^{39}Ar$ ages, latest Norian to Sinem.) Tholeiites on Guayana margin ($^{40}Ar/^{39}Ar$ ages, latest Sinemurian) Tholeiites on Guinea margin ($^{40}Ar/^{39}Ar$ ages, Early Sinem. to Early Pliensb.) Unaltered granophyric veins and feeder intrusions in North American Rift Basins (e.g. Fundy, Newark Basins) (average U/Pb, $^{40}Ar/^{39}Ar$ ages)	Olsen (1997) Aït Chaye et al. (1998) Fiechtner et al. (1992) Deckart et al. (1997) Deckart et al. (1997) Olsen (1997) and Sutter (1988)	---204.3--- ST1 259.3

Subsidence trends in the Agadir Basin are indicated for comparison (Figs. 14 and 17).

(1) major shifts in the location of the sea-floor spreading axis in the Central Atlantic;
(2) major changes in sea-floor spreading rates in the Central Atlantic;
(3) the northward migration of crustal separation and sea-floor spreading in the Central and the southern North Atlantic;
(4) relative motions between the African and Eurasian plates.

The following genetic models are based on:

(1) the positive and negative feedback processes between thermo-tectonic subsidence, sediment input/production, flexural and compaction-induced subsidence in the Agadir Basin;
(2) temporal correlations to plate-tectonic reconfigurations in the Atlantic domain;
(3) general plate force-balance models (Bott, 1982);
(4) paleostress fields of the Atlantic Basins of Morocco derived from microtectonic data (Aït Brahim et al., 2002).

Models allow for offsets of up to one time interval (geological stage, 2.3–13.4 Myr) between a plate-tectonic reconfiguration and the resulting shift in thermo-tectonic subsidence in the Agadir Basin. These offsets represent lag-times, in which the positive and negative feedback processes established or readjusted to a new plate-tectonic settings. The different plate-tectonic processes were probably coupled or interfered with each other to produce a specific thermo-tectonic subsidence development on the Agadir continental shelf.

The development of the Central Atlantic shows two major shifts of the spreading center. The first shift from the Gulf of Mexico to the proto-Caribbean occurred in the Late Tithonian (M21). It was associated with a reduction in spreading halfrates and triggered the transition from ST4 to ST5 in the Agadir Basin. The spreading axis jump predated the turnover to minimum thermo-tectonic subsidence rates in the Agadir Basin for 3.9–2.5 Myr or half the Tithonian time interval at maximum. The second shift from the proto-Caribbean to the current position occurred in the Early/Mid-Campanian (C33) and controlled the reduction in tectonic subsidence from ST7 to ST8. This spreading axis jump is superimposed on the gradually increasing NE-directed convergence between the African and Eurasian plates, which had been initiated at the Turonian/Cenomanian boundary (see below). In general, major shifts in the spreading center of the Atlantic controlled low tectonic subsidence rates at the base of the subsidence trends in the Agadir Basin (or the respective transitions to them).

Two major changes in sea-floor spreading halfrates occurred in the Jurassic to Cretaceous of the Central Atlantic. A reduction of halfrates to 50–60% of the previous rates, occurred between the Middle Tithonian (M21) and the earliest Barremian (M4). It controlled moderate to high tectonic subsidence rates in the upper subsidence trend ST4. Peak low sea-floor spreading rates existed in the Hauterivian and triggered maximum thermo-tectonic subsidence rates in the upper subsidence trend ST5. The moderate or small decrease in sea-floor spreading rates in the Late Campanian to Maastrichtian (C32–31/30) is not reflected in the thermo-tectonic subsidence development of the Agadir Basin, because it was overprinted by African–Eurasian plate convergence. Increases in sea-floor spreading halfrates are little constrained. They potentially occurred in the Jurassic and Cretaceous Magnetic Quiet Zones (JMQZ, CMQZ), where existing estimates (Figs. 14 and 16) represent an interpolation between C33–M0r (CMQZ) and a projection of post-M25 (JMQZ) spreading rates to the Early Jurassic. The only pronounced increase in sea-floor spreading halfrates within the M- and C-series occurred in the Barremian to earliest Aptian (M3–M0r). It controlled low thermo-tectonic subsidence rates in the lower subsidence trend ST5 in the Agadir Basin. Whether peak high tectonic subsidence rates during the upper subsidence trends ST6 and ST3 were actually controlled by reduced sea-floor spreading halfrates or other plate-tectonic reconfigurations remains speculative. In general, major reductions in sea-floor spreading halfrates in the Atlantic controlled moderate to high thermo-tectonic subsidence rates at the top of subsidence trends in the Agadir Basin. Major increases in sea-floor spreading probably resulted in low thermo-tectonic subsidence rates because higher intra-plate forces (ridge-push) prevailed (see below).

The development of crustal separation and sea-floor spreading in and beyond the Central Atlantic did not produce consistent changes in the thermo-tectonic subsidence development in the Agadir Basin. The base of ST1 and low thermo-tectonic subsidence rates are controlled by magmatism and thermal uplift of the future Central Atlantic. Initial sea-floor spreading at 193.5–186.5 Myr triggered increasing thermo-tectonic subsidence rates in the Agadir Basin. It preceded peak high rates in the Late Toarcian for 2.4–9 Myr. The first major northward extension of the Atlantic occurred in latest Oxfordian times (M25), when crustal separation developed between Iberia and North America. The second major extension included the transition from crustal extension to sea-floor spreading in the southern North Atlantic during the Late Valanginian to Early Hauterivian (M11–M10N). Both plate-tectonic reconfigurations triggered the onset of high thermo-tectonic subsidence in middle ST4 and late ST5. Lag times amount to 1.4 Myr at maximum. In Early Jurassic to Hauterivian times, the extension of crustal separation and sea-floor spreading in the Atlantic triggered moderate to high thermo-tectonic subsidence rates in the middle to upper part of ST2–ST5 in the Agadir Basin. This genetic coupling is not confirmed for post-Hauterivian times, when sea-floor spreading in the Atlantic extended to more than 500–800 km north (Masse, 2000)

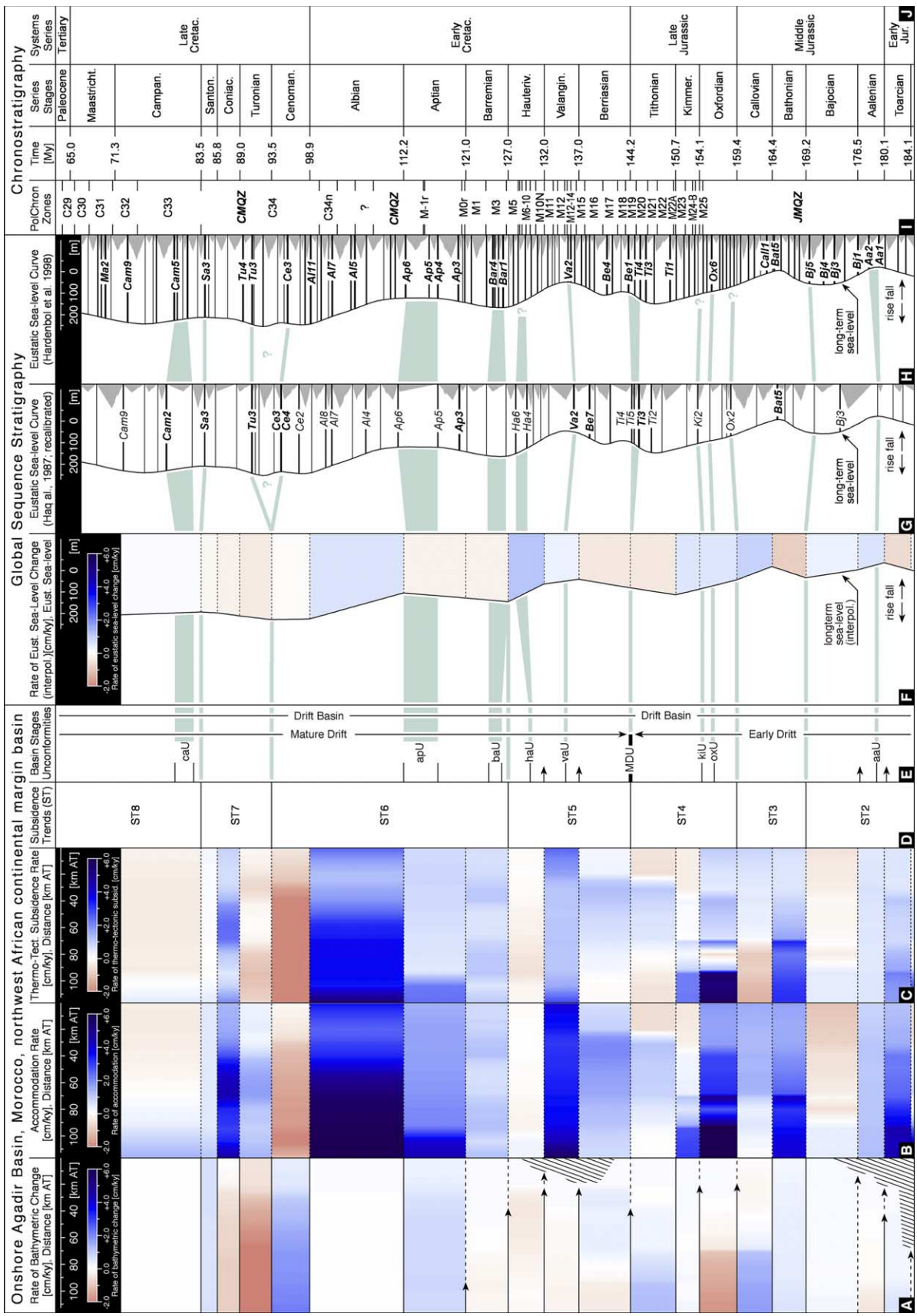
Onshore Agadir Basin, Morocco, northwest African continental margin basin
Rate of Bathymetric Change [cm/ky], Distance [km AT]
Accommodation Rate [cm/ky], Distance [km AT]
Thermo-Tect. Subsidence Rate [cm/ky], Distance [km AT]
Subsidence Trends (ST)
Basin Stages Unconformities
Global Sequence Stratigraphy
Rate of Eust. Sea-Level Change (interpol.)[cm/ky], Eust. Sea-level
Eustatic Sea-level Curve (Haq et al., 1987; recalibrated)
Eustatic Sea-level Curve (Hardenbol et al. 1998)
Chronostratigraphy
PolChron Zones
Time [My]
Series Stages
Systems Series
Drift Basin
Mature Drift
Early Dritt
caU
apU
baU
haU
vaU
MDU
kiU
oxU
aaU
ST8
ST7
ST6
ST5
ST4
ST3
ST2
long-term sea-level
rise fall
longterm sea-level (interpol.)
Paleocene
Maastricht.
Campan.
Santon.
Coniac.
Turonian
Cenoman.
Albian
Aptian
Barremian
Hauteriv.
Valangin.
Berriasian
Tithonian
Kimmer.
Oxfordian
Callovian
Bathonian
Bajocian
Aalenian
Toarcian
Late Cretac.
Early Cretac.
Late Jurassic
Middle Jurassic
Early Jur.
Tertiary
CMQZ
JMQZ
A
B
C
D
E
F
G
H
I
J

of the Azores Fracture Zone into the North Atlantic. The extension of sea-floor spreading to the area between Grand Banks and the Iberian plate coincides with peak low subsidence rates at the base of subsidence trend ST6. It is unlikely that the extension of sea-floor spreading further to the north, e.g. to the Labrador Sea (late C34, base ST7) or to the Norwegian-Greenland Sea (C25–24) influenced the northwest African continental margin in its mature drift stage.

Atlasian compression and uplift constitute a potential control on the Cretaceous to Tertiary accommodation development in the Agadir Basin. The timing of initial Atlasian compression, folding and/or uplift as proposed by existing studies varies between the Late Cretaceous to Paleogene (Table 5). Reconstructed plate motion paths (Dewey et al., 1989) provide good indication, that (1) oblique strike-slip motion between the African and Eurasian plates changed to NE directed convergence some time between the Early Aptian (M0r, 121.0 Myr) and the Santonian (C34, 83.5 Myr); (2) convergence strongly decreased in the latest Maastrichtian (post-C30, post-65.6 Myr); (3) renewed strong convergence occurred in the Early Eocene (post-C-24, post-52.4 Myr). Major intra-plate compression and basin inversion in the Atlasian domain only started after the latest Eocene (post-34.7 Myr; e.g. Gomez et al., 2000). However, existing studies disagree at which time during the Cretaceous to Early Tertiary, African–Eurasian plate convergence actually resulted in early uplift and intra-plate deformation in the western Atlasian domain. Seismostratigraphic studies (Hafid et al., 2000) have described submarine erosional unconformities of Middle (sic) Cretaceous age on top of nascent folds in the offshore Essaouira Basin. They were interpreted as indication for Early Atlasian deformation. However, the timing of these unconformities is loosely constrained. In the onshore area, initial Late Cretaceous uplift is disputed. Small-scale unconformities were either interpreted as related to large-scale mild compression in the Atlas domain (Amrhar, 1995) or as entirely local features, which do not indicate a compressive regime (Giese & Jacobshagen, 1992). Other assumptions depend entirely on transgressive or regressive sedimentary successions, which are not necessarily indicative of tectonic uplift, reduced or continuous subsidence.

The thermo-tectonic subsidence rates calculated in this study parallel the African–Eurasian plate motions and convergence rates as described by Dewey et al. (1989). Thermo-tectonic uplift in the onshore Agadir Basin occurred at the base of subsidence trend ST7 (upper CMQZ) in the Turonian. This complies exactly with the average age assumed by Dewey et al. (1989) for initial NE-directed convergence between the Eurasian and African plates based on the coeval onset of high-pressure metamorphism in the western Alpine domain (Ernst & Dal Piaz, 1978). On a low level, thermo-tectonic subsidence rates in the Agadir Basin increased in the earliest Paleocene, after subsidence trend ST8. At the same time, plate motion paths indicate decreased convergence rates between the African and Eurasian plates. Subsequent to the Paleocene, tectonic uplift predominates in the Agadir Basin. With an offset for max. 1.6 Myr, this turnover corresponds to the renewal of strong plate convergence proposed by Dewey et al. (1989) for post-52.4 Myr times. In summary, post-Cenomanian variations in thermo-tectonic subsidence in the Agadir Basin were controlled by African–Eurasian plate-motion changes and convergence rates.

Plate-tectonic reconfigurations in the western Tethys might have subordinately influenced the Agadir Basin development. During the Jurassic to Early Late Cretaceous, the spreading axis in the westernmost Tethys trended NW–SE and turned to

Fig. 17. Rates of changes in bathymetry, accommodation and tectonic subsidence rates in the onshore Agadir Basin compared to eustatic sea-level changes (sequence stratigraphic charts of Haq et al. (1987) and Hardenbol et al. (1998)). All rates are shown with identical scale (−2 to +6 cm/kyr, color code). (A) Rates of bathymetric change as well as coastal and continental onlap in time (Wheeler Diagram) in the onshore Agadir Basin (Fig. 9(A) and (D)). Increases in bathymetry (transgressions) are shown in blue, decreases in bathymetry (regressions) in red. (B) Accommodation rates in the onshore Agadir Basin. Positive rates (development of accommodation space) are shown in blue, negative rates (destruction of accommodation space) in red. (C) Thermo-tectonic subsidence rates in the onshore Agadir Basin. Positive rates (net subsidence) are shown in blue, negative rates (net uplift) in red. (D–H) Relation of subsidence trends and bounding unconformities in the onshore Agadir Basin to long-term eustatic sea-level changes. Potential correlations are indicated by the green bars. See text for discussion. (D) Subsidence trends in the onshore Agadir Basin (Fig. 14(E)). (E) Basin stages and unconformities of this study (Table 1). (F) Rate of eustatic sea-level changes as interpolated over geological stages for reverse basin modeling in this study. Rates are based on the eustatic sea-level curve of Hardenbol et al. (1998, chart 1) (Fig. 9(B)). (G) Long-term, second order eustatic sea-level curve and third order sequence boundaries of Haq et al. (1987) as recalibrated to the time scale of Gradstein et al. (1994) by Hardenbol et al. (1998, chart 1). Legend: gray, schematic condensed section indicating the position of maximum flooding and transgressive surfaces; thick lines, major sequence boundaries; medium lines, medium sequence boundaries; thin lines, minor sequence boundaries (sensu Hardenbol et al., 1998). Only major (bold-typed italics) and medium (normal-typed italics) sequence boundaries have been labeled. (H) Long-term, second order eustatic sea-level curve and third order sequence boundaries of Hardenbol et al. (1998, chart 1). For legend see column G. Only major sequence boundaries have been labeled (bold-typed italics). (I) Magnetic polarity chronozones in the Central and northern Atlantic according to Hardenbol et al. (1998); (J) Standard chronostratigraphy according to Gradstein et al. (1994) and Hardenbol et al. (1998). Legend (sorted by columns): (A–C) km AT—kilometers along transect (D) MDU—Mature Drift Unconformity; aaU—Early Aalenian unconformity; oxU—Late Oxfordian unconformity; kiU—Late Kimmeridgian unconformity; vaU—Early Valanginian unconformity; haU—Late Hauterivian unconformity; baU—Early Barremian unconformity; apU—Late Aptian unconformity; caU—Early (?) Campanian unconformity; (G,H) sequence boundary abbreviations according to Hardenbol et al. (1998, chart 1), e.g. Bat5—fifth consecutive sequence boundary in the respective geological stage (Bathonian). (I) CMQZ—Cretaceous Magnetic Quiet Zone; JMQZ—Jurassic Magnetic Quiet Zone.

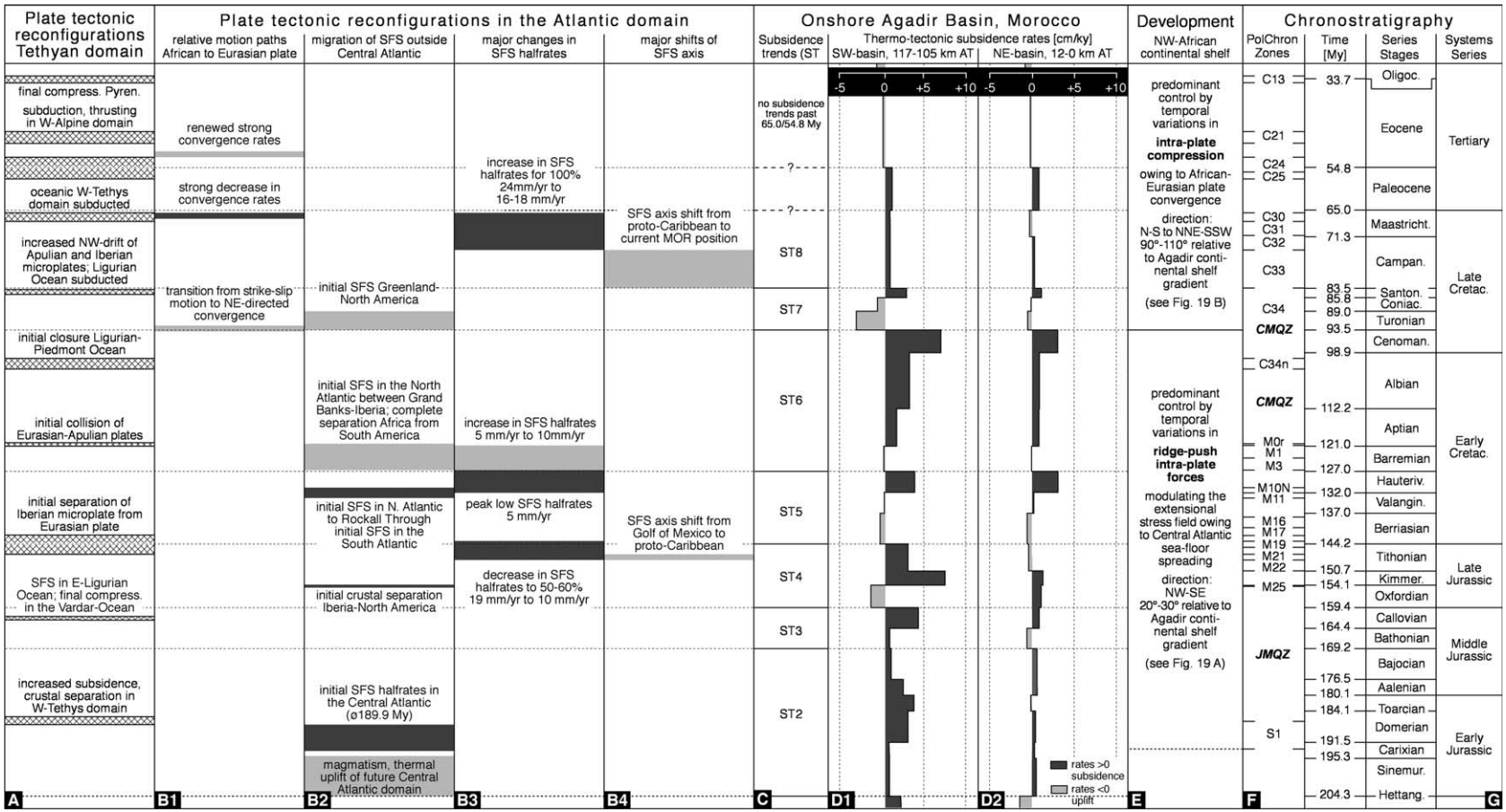

Fig. 18. Genetic model of the Agadir Basin development differentiated for specific plate-tectonic parameters and stress fields during the Meso-/Cenozoic. (A) Time intervals of major plate-teconic reconfigurations in the Tethyan domain (cross-hatched bars). The genetic model for the eastern Central Atlantic continental shelf (Agadir Basin) does not propose direct, major control by plate-tectonic reconfigurations in the Tethyan domain. (B1–B4) Plate-tectonic reconfigurations in the Atlantic domain controlling the Agadir Basin development. Dark gray bars indicate reconfigurations triggering (relatively) low thermo-tectonic subsidence rates or uplift (lower part of subsidence trends). Light gray bars indicate reconfigurations triggering (relatively) high thermo-tectonic subsidence rates (upper part of subsidence trends). The model includes an offset of up to one time layer between the triggering plate-tectonic reconfiguration and the resulting subsidence/uplift change in the Agadir Basin. The effects of different isochronous plate-tectonic reconfigurations may have interfered to produce a specific subsidence/uplift signal in the Agadir Basin. (D1–D2) Thermo-tectonic subsidence rates in the southwestern and northeastern parts, respectively, of the Agadir Basin (Fig. 14(D2) and (D4)). (E) Predominant plate-tectonic forces and paleo-stress fields governing the development of the northwest African continental shelf (see text, Aït Brahim et al., 2002; Jimenez-Munt & Negred, 2003). (F) Magnetic polarity chronozones in the Central and northern Atlantic according to Hardenbol et al. (1998). (G) Standard chronostratigraphy according to Gradstein et al. (1994) and Hardenbol et al. (1998).

N–S along the eastern margin of the African plate including the Arabian platform. The western (Atlantic) and eastern (Tethyan) passive margins of Africa were separated by at least 3000–6000 km of stable continental crust (Dercourt et al., 2000). It is unlikely, that ridge-push or other plate forces, triggered by plate-tectonic reconfiguration in the Tethyan domain, were transmitted by far-field stress propagation to the Atlantic passive margin of the African plate.

Decreases and increases in accommodation and total subsidence in continental shelf basins may be influenced or controlled by local processes such as salt tectonics. In the onshore Agadir Basin, the amount of evaporites in the Late Triassic to Early Jurassic basin fill (rift to sag basin stages) is very small. This is in clear contrast to the northerly adjacent onshore Doukkala and Essaouira Basins (see Fig. 1), where the Late Triassic succession includes thick evaporite intervals (Le Roy & Piqué, 2001; Piqué & Laville, 1995). Major salt tectonics with the development of salt pillows and diapirs occurred in the Jurassic to (?) Early Cretaceous (Hafid, 2000; Le Roy & Piqué, 2001). A north- to southward decrease in evaporites as between the Essaouira and Agadir Basins of northwest Africa also exists on the conjugate segment of the North American continental shelf margin. Haworth, Keen, and Williams (1994), Jansa, Bujak, and Williams (1980), Olsen (1997), and Wade and MacLean (1990) described the lateral distribution of Late Triassic to Early Jurassic evaporites along the Grand Banks and Nova Scotia to Maine margins. Evaporites are up to 2 km thick on the Grand Banks and Nova Scotian margin segments, but thin and lacking on the Maine margin. The Georges Bank Basin on the Maine margin marks the southwestern extent of Mesozoic evaporites on the Scotian margin (Wade & MacLean, 1990, p. 200). Rift basins close to the continent like the Fundy Basin feature up to 4 km of non-marine clastic sediment instead of evaporites as the more oceanward subbasins (Wade & MacLean, 1990). This spatial distribution of evaporites along a proximal to distal continental shelf basin transect is confirmed by the rift basin exposed in the Argana valley of the Moroccan margin. It was situated immediately northwest of the African craton and received terrigenous clastics in thicknesses of up to 2.5 km. Minimal amounts of evaporites are documented by molds within mudstones of the Bigoudine Formation (Tourani et al., 2000). The in- or outflow of subsurface salt, provided it exists in a continental shelf basin, can hardly produce rhythmic increases or decreases in basin-wide accommodation over periods of 10–35 Myr as in the case of the subsidence trends ST2–8 in the Agadir Basin. The development of salt pillows to diapirs would have resulted in stationary areas with a steady decrease in paleobathymetry and/or accommodation surrounded by areas with a steady increase in paleobathymetry and/or accommodation. The reconstructed basin architecture (Fig. 8) and paleobathymetry (Fig. 9) as well as the results of reverse basin modeling (Figs. 11 to 13) exclude salt tectonics as a significant control on the accommodation history of the onshore Agadir Basin.

The Pliensbachian to Recent development of the Agadir Basin featured two long-term periods with different large-scale stress fields and plate-tectonic settings (Figs. 18 and 19): (1) the Early Pliensbachian/Middle Toarcian (193.5/186.5 Myr) to Cenomanian (93.5 Myr, intra-C34); (2) the Turonian (93.5, intra-C34) to Recent.

In Early Pliensbachian/Middle Toarcian to Cenomanian times (Fig. 19, A1), thermo-tectonic subsidence in the Agadir Basin was predominantly controlled by temporal variations in intra-plate ridge-push forces (Bott, 1982; Turcotte & Schubert, 2002). They acted in NW–SE paleodirection, orthogonally from the spreading axis to the northwest African continental margin. Temporal variations in ridge-push forces modulated the overall extensional stress field of Central Atlantic plate drifting. In general, ridge-push forces depend primarily on the topographic elevation of the ridge, which is due to the greater buoyancy of the thin, hot lithosphere near the axis of accretion at the ridge crest (Turcotte & Schubert, 2002). Ridge-push forces in the two diverging oceanic lithospheric plates depend on the volume of mantle rock accreted to the two diverging plate boundaries, i.e. on sea-floor spreading velocities. A decrease in sea-floor spreading velocities, like in the Middle Tithonian to Early Barremian, resulted in a reduction of intra-plate ridge-push forces applied to the northwest African continental shelf. This triggered relatively high thermo-tectonic subsidence rates in the Agadir Basin. Westward shifts in the spreading axis increased ridge-push forces on the northwest African continental shelf triggering reduced thermo-tectonic subsidence or thermo-tectonic uplift. Temporal variations in ridge-push forces were also triggered by (1) the migration of crustal separation and sea-floor spreading beyond the Central Atlantic; (2) changes in the Central/North Atlantic spreading vector expressed as changes in the sea-floor spreading direction (cf. North Atlantic, Tertiary; Boldreel & Andersen, 1998; Dore et al., 1999; Vågnes, Gabrielsen, & Haremo, 1998). It is feasible, that net intra-plate forces on the northwest African continental margin were subordinately influenced by plate-tectonic reconfigurations in the western Tethys.

Since the Turonian (post-93.5 Myr, intra-C34), the Atlantic paleo-stress field progressively changed towards the recent stress field (Mueller, Reinecker, Heidbach, & Fuchs, 2000; Zoback, 1992; Fig. 19 B1–3). The onset of African–Eurasian plate convergence (Dewey et al., 1989) triggered intra-plate compression, which replaced orthogonal ridge-push forces as the principal control on the northwest African continental shelf development. In the Turonian to Recent stress field, spreading on the Mid-Atlantic ridge has negligible influence on the Iberian–Eurasian and African plate interior (Jimenez-Munt & Negredo, 2003). WNW–ESE directed ridge-push forces are transmitted by dextral strike-slip and thrust forces along the Eurasian–African plate boundary (Terceira Ridge, Gloria Fault Zone, Rif Thrust

Front) to produce principal stress directions between N–S and NE–SW in the WHA domain (Fig. 19). The major change in plate-forcing from ridge-push to intra-plate compression at the Cenomanian/Turonian boundary is well reflected in the results of CA-analysis. The Turonian, was the only time interval in the Jurassic to Cretaceous, when accommodation space in the Agadir Basin was primarily controlled by thermo-tectonic uplift.

This genetic model of the basin development is in agreement with reconstructed paleostress fields for northern and western Morocco (Äit Brahim et al., 2002). Paleostress data are based on striations measurements and relative chronology criteria such as fossilized structures and superimposed slickensides for successive tectonic events. Striations measurements indicate two long-term stress fields. In the Late Triassic to Early Cretaceous, NW–SE

Table 5
Late Cretaceous to Tertiary African–European plate motions and tectono-stratigraphic developments in the Atlasian domain

Key references	Ages (Myr)	Plate motions and tectonostratigraphic developments in the Atlasian domain (Cretaceous to Tertiary)
Gomez et al. (2000)	Post-9.7	~ 50 km of African–Eurasian plate convergence (post-C5; Late Miocene to Recent)
	19.0–97.0	30–40 km of African–Eurasian plate convergence (C6–C5; Early to Late Miocene)
	34.7–19.0	70–80 km of African–Eurasian plate convergence (C13–C6; latest Eoc. to Early Mioc.)
	Post-23.8	Main uplift episode of the Moroccan High Atlas (Oligocene to recent)
Hafid (2000)	Post-65.0	NNW–SSE compression leads to western High Atlas formation (Tertiary to recent)
Hafid (1999) and Hafid et al. (2000)	Post-98.9	Folding of Cap Tafelney folded belt (Mid-Cretaceous to Neogene) (submarine erosional unconformities on nascent folds in the offshore Essaouira Basin)
Olivet (1996)	Post-55.9	Initial north-directed compression in the NW-African and southern Iberian domains (Early Eocene, C24)
	Post-89.0	Initial compression in the western Mediterranean (Ligurian–Piemont domain) (Late Turonian/Early Coniacian, C34)
	Post-98.9	Left-lateral oblique convergence Africa–Eurasia (post-Albian/Cenomanian boundary)
El Harfi, Lang, and Salomon (1996)	37.0–23.8	Minor local uplift along the southern margin of the Central High Atlas (Late Eocene to Oligocene)
Medina (1994, 1995)	Post-1.8	WNW–ESE compression in the western High Atlas (post-Pliocene)
Amrhar (1995)	Post-33.7	NNE–SSW compression in the western High Atlas (post-Eocene)
	Post-98.9	Local unconformities in the western High Atlas indicate mild compression (upward convergence of Jurassic beds on anticlinal crests; Late Cretaceous)
Zouine (1993)	65.0–23.8	Sedimentation in the Atlas domain mostly reflects eustatic fluctuations (Paleogene)
Giese and Jacobshagen (1992)	Post-37.0	Initial inversion and uplift of the High Atlas (Late Eocene) Local unconformities are restricted to the northern margin of the western High Atlas and do not represent general inversion of the Atlas domain (Amrhar, 1995)
Brede, Hauptmann, and Herbig (1992)	23.8–1.8	Peak compressional deformation and uplift in the High Atlas (Miocene to Pliocene)
	Post-41.3	Initial uplift in the High Atlas (Late Middle Eocene to Late Eocene)
	Post-89.0	Initial wide-arched updoming within High Atlas realm (Senonian) Tectonic quiescience in spite of "epirogenetic" uplift of High Atlas (Senonian to Early Paleogene)
Dewey et al. (1989)	Post-52.4	Renewed strong NE to N motion of African plate (post-C24, post-Early Eocene)
	65.6–52.4	Strong decrease in convergence rates (C30–C24, Late Maastrichtian to latest Paleocene/Early Eocene)
	93.5–65.6	NE directed convergence between African and Eurasian plates (C34–C30, Cenomanian–Turonian boundary to Late Maastrichtian)
	Pre-93.5	Left lateral strike-slip motion between African and Eurasian plates (pre-C34, Cenomanian–Turonian boundary) Smooth change from strike-slip motion to convergence and compression
Goerler et al. (1988)	Post-16.4	Initiation of main uplift and erosion episode (Middle to Late Miocene) See also Chellai and Perriaux (1996)
Jacobshagen, Brede, Hauptmann, Heinitz, and Zylka (1988)	Post-23.8	Initial main inversion and uplift of the Atlas domain (Oligocene to recent)
	Pre-54.8	Conformable succession (Cenomanian/Turonian boundary to Eocene) Moderate subsidence in the Central High Atlas domain
Froitzheim, Stets, and Wurster (1988)	Post-89.0	Local unconformities giving first indication of uplift and inversion in the High Atlas (Turonian/Coniacian boundary to Tertiary)
Schaer (1987)	49.0–16.4	Folding in the Atlas domain (Middle Eocene to Burdigalian) Apart from differential subsidence no pre-Tertiary deformation (western High Atlas)
Klitgord and Schouten (1986)	83.5–76.1	Initial northern Iberian-African plate boundary subduction (Early to Middle Campanian, C33)

Existing studies vary as for the onset of compression and tectonic uplift in the Central and western High Atlas of Morocco (Cretaceous, Paleogene ?). Most studies agree, that peak compression and basin inversion occurred between the Late Eocene and Miocene.

to N–S extension prevailed. During the Late Cretaceous to present compression and tectonic inversion varied widely in time and space from N–S, NE–SW, NW–SE and E–W. Significant directions of major compression in the Agadir–Essaouira Basins of western Morocco include N–S in the Eocene and NNW–SSW to NE–SW during the Oligocene to Middle Miocene (Äit Brahim et al., 2002).

10. Sequence stratigraphic methodology and eustatic sea-level changes

The positions and the migrations of coastal onlaps at passive continental margins, analyzed within a rigid bio-/chronostratigraphic framework, have been interpreted as eustatic sea level variations of varying frequencies and amplitudes (sea-level charts of Haq et al. (1987) and Hardenbol et al. (1998)). The Meso- to Cenozoic circum-Atlantic continental passive margins have been regarded as one of the best settings to analyze eustatic sea-level changes and their amplitudes (Haq et al., 1987; Vail et al., 1977). In recent years, additional sequence stratigraphic data from a variety of other sedimentary basins, e.g. in Europe (de Graciansky, Hardenbol, Jacquin, & Vail, 1998), have allowed to increase the resolution models of eustatic sea-level changes during the Meso-/Cenozoic. Until today, sea-level charts are often used as a predictive tool to:

(1) date biostratigraphically unconstrained sediment packages based on an inferred relative sea-level position which controlled them;
(2) identify sequence boundaries, maximum flooding and transgressive surfaces, when indicative stratal patterns and facies stacking patterns are lacking.

According to Posamentier et al. (1989), the conceptual framework of sequence stratigraphy is based on two assumptions (sic):

(1) indicative stratal patterns at seismic resolution in the subsurface, controlled by wells to varying degrees, are exclusively controlled by changes in accommodation. In fact, sediment supply changes on real-world continental margins. This was supposed to affect primarily the seaward extent of deposition. Thus, the stratal pattern on the landward side of identical basins should be the same regardless of sediment supply, because sea-level and its global eustatic variations constituted the main controlling factor. Thorne and Swift (1991) for clastic and Schlager (1993) for carbonate depositional systems stressed the importance of changes in sediment supply and production for stratal geometries. However, sediment supply is commonly assumed to be constant in the overwhelming number of sequence stratigraphic studies. This is mainly due to the fact, that changes in sediment supply and their influence on stratal patterns are difficult to consider by qualitative sequence stratigraphic approaches.
(2) changes in accommodation are primarily controlled by eustatic sea-level changes. Passive continental margins are subject to subsidence rates, which are constant in any single location, because subsidence is primarily a function of lithospheric cooling and loading. Posamentier et al. acknowledged, that this assumption may be valid only over a limited time interval and depends on the relative frequency of the eustatic to subsidence variations considered. However, subsequent studies of real-world passive continental margins (and other sedimentary basins) have often disregarded the influence of changes in subsidence on accommodation development.

Fig. 17 shows temporal correlations of the subsidence trends ST2–ST8 in the onshore Agadir Basin to long-term sea-level changes according to the global sea-level charts of Haq et al. (1987) and Posamentier et al. (1989). Subsidence trend boundaries and unconformities do not show a specific genetic relation to long-term sea-level positions. Three subsidence trend boundaries (ST4–5, ST5–6, ST6–7) correlate to long-term stationary high to falling sea-level. A single boundary each correlates to falling (ST2–3) and rising sea level (ST3–4). The MDU coincides with long-term stationary high and falling sea level. Three unconformities below the resolution of time layers (aaU, vaU, apU) correlate with stationary low sea level, four unconformities (oxU, kiU, haU, caU) with rising sea-level and one unconformity (baU) with stationary high sea-level.

For the large majority of geological stages during the Toarcian to Maastrichtian and in most basin segments, eustatic sea-level changes occurred at considerably lower rates than thermo-tectonic or total subsidence (see CA-analysis; Figs. 15 and 16). They did not represent the principal control on the development of accommodation space. Temporal correlations of subsidence trend boundaries and unconformities in the Agadir Basin to eustatic sea-level changes (third and second order lowstands) are speculative (Fig. 17, green lines/bars). Reasons include:

(1) considerable differences in the timing and in the amplitudes of third order sequence boundaries in the charts of Haq et al. (1987) and Hardenbol et al. (1998). The first chart includes a global sequence stratigraphic database, the second chart additionally includes detailed data from European sedimentary basins.
(2) the stratigraphic resolution in the Jurassic and Cretaceous succession of the Atlantic realm is partly insufficient for reliable high-resolution correlations to both sea-level charts.
(3) the restricted available biostratigraphic resolution for the Mesozoic northwest African continental margin and the high number of sequence boundaries in the chart of Hardenbol et al. (1998) result in a large

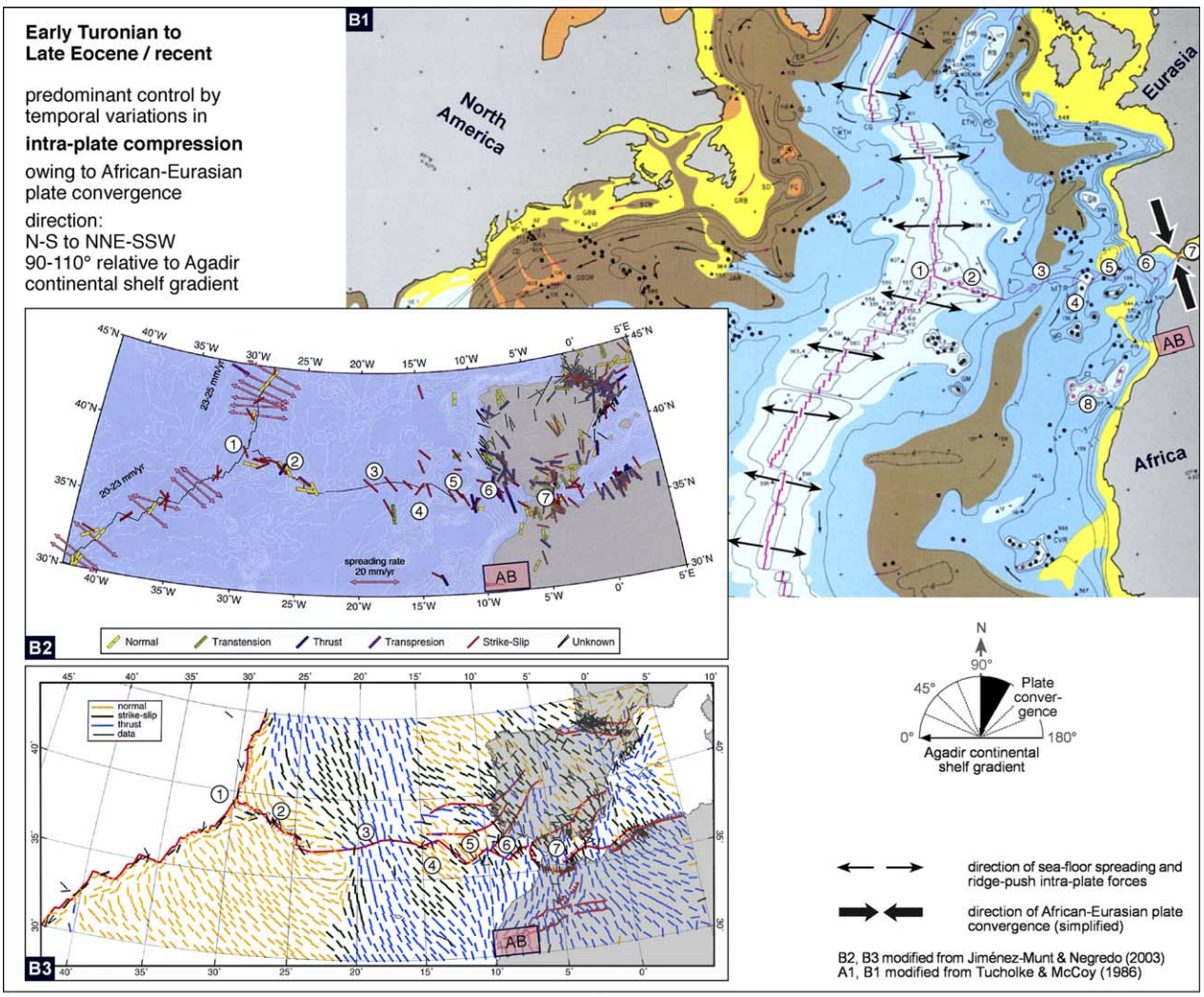
Early Turonian to
Late Eocene / recent
predominant control by
temporal variations in
intra-plate compression
owing to African-Eurasian
plate convergence
direction:
N-S to NNE-SSW
90-110° relative to Agadir
continental shelf gradient
B1
North America
Eurasia
Africa
AB
B2
23-25 mm/yr
20-23 mm/yr
spreading rate
20 mm/yr
Normal
Transtension
Thrust
Transpresion
Strike-Slip
Unknown
B3
normal
strike-slip
thrust
data
N
90°
45°
Plate
conver-
gence
0°
180°
Agadir continental
shelf gradient
direction of sea-floor spreading and
ridge-push intra-plate forces
direction of African-Eurasian plate
convergence (simplified)
B2, B3 modified from Jiménez-Munt & Negredo (2003)
A1, B1 modified from Tucholke & McCoy (1986)

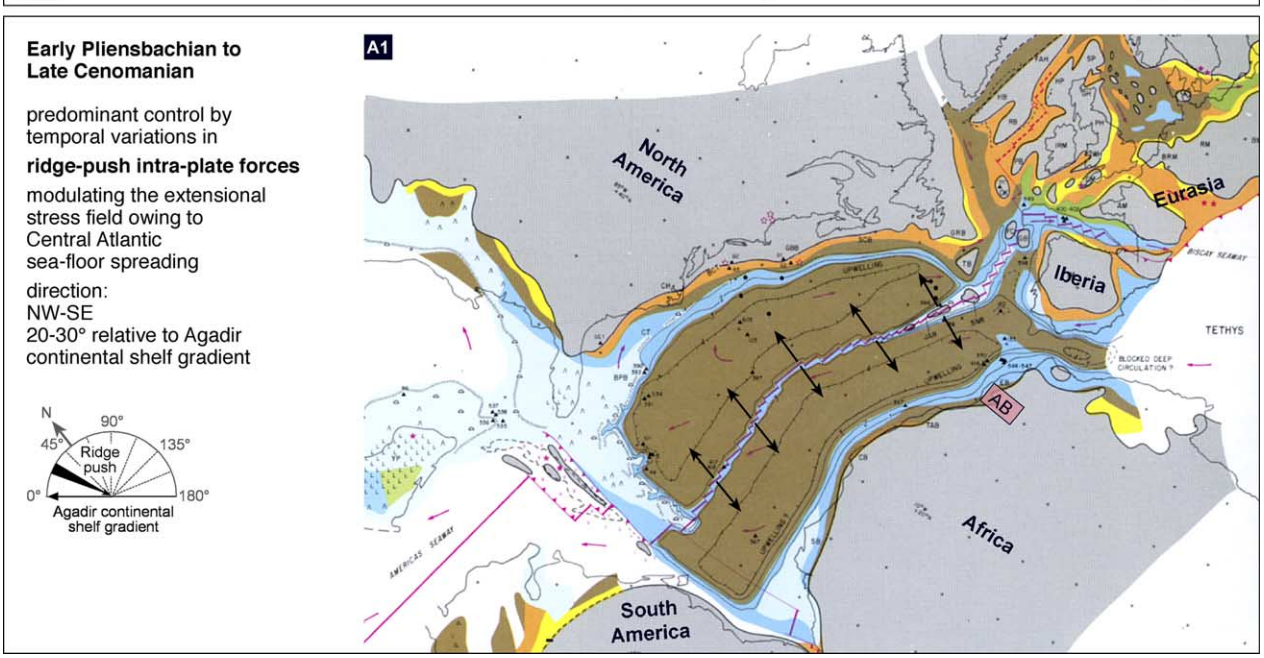
Early Pliensbachian to
Late Cenomanian
predominant control by
temporal variations in
ridge-push intra-plate forces
modulating the extensional
stress field owing to
Central Atlantic
sea-floor spreading
direction:
NW-SE
20-30° relative to Agadir
continental shelf gradient
N
90°
45°
135°
Ridge
push
0°
180°
Agadir continental
shelf gradient
A1
North America
Eurasia
Iberia
TETHYS
AB
Africa
South America

number of potential correlations. This refers especially to the Bathonian to Barremian time interval.

Any conceptual approach including changes in accommodation depends on the reliability and resolution of available eustatic sea-level data. On a qualitative scale only those major transgressive/regressive cycles which can be shown to appear isochronously in various sedimentary basins of different, uncoupled plate-tectonic settings represent sufficiently reliable indicators for long-term eustatic sea-level changes (Rüffer & Zühlke, 1995). Requirements include, that sediment production and input did not significantly change due to globally active processes, e.g. increased erosion rates in continental hinterlands caused by major global changes in climate or reduced carbonate production rates caused by associated paleo-ecological changes.

The model for the Agadir Basin development includes the second order sea-level data of Haq et al. (1987) and Hardenbol et al. (1998) as input parameters. Reverse basin modeling shows that the basin development was primarily controlled by total subsidence/uplift. This includes a significant thermo-tectonic component, which was in turn controlled by plate-tectonic processes. Total subsidence/uplift rates varied considerably, over a range of 13.1 to −1.3 cm/kyr during the early and mature drift basin stages. Within individual time layers significant differential subsidence occurred. The generally held assumption, that thermo-tectonic and total subsidence/uplift rates of passive continental margins were largely constant or followed a steady trend of exponentially decreasing thermo-tectonic subsidence, cannot be sustained—at least not for the eastern Central Atlantic continental shelf of northwest Africa. Passive continental margins do not necessarily represent well-suited settings to directly infer global, eustatic sea-level changes. Models of second order and third order sea-level changes require a comparison of coastal onlap and other indicative stratal termination data from more than a single oceanic basin and its passive margins. As plate-tectonic reconfigurations within oceanic basins influence adjacent continental margins by intra-plate ridge-push forces and coupled motions of different plates, accommodation data from conjugate margins of the same oceanic basin may still not exclusively reflect eustatic sea-level changes. Improved approximations of amplitudes of eustatic sea-level fluctuations require the application of both reverse basin and forward stratigraphic modeling techniques and a more rigid bio-/chronostratigraphic framework than currently applied for many settings.

In summary, the results of our study show, that the explanation of typical stratigraphic sequences (based on unconformities, stratal geometries, facies trends) as caused predominantly by sea-level fluctuations, and rough assumptions on sediment input/production and subsidence, is not necessarily applicable to passive continental margin settings. CA-analysis represents a more refined and quantitative analytical tool for basin research. The methodological approach applied in this study for the Agadir segment of the northwest African shelf—numerical basin modeling and CA-analysis—allows to develop a more rigorous genetic model for the development of passive continental margins. The combination with forward stratigraphic modeling will have the potential to significantly increase the reliability of predictive passive continental margin models.

11. Summary

Approach—This contribution is based on lithofacies, thickness and biostratigraphic data from 15 synthetic vertical sections. In addition, large-scale depositional geometries, stratal terminations like coastal and continental onlap and erosional/angular unconformities have been analyzed. All data have been projected into a 116 km long transect through the Agadir Basin, which covers the largest part of the eastern Central Atlantic continental shelf in

Fig. 19. Principal plate-tectonic forces and stress fields in the eastern Central Atlantic in Early Jurassic to Recent times. At the Cenomanian–Turonian boundary, the plate-tectonic configuration changed from African–Eurasian left-lateral strike-slip to N–S convergence. Paleogeographic maps (A1, B1) have transverse-mercator projection and grids indicate modern longitudes/latitudes on respective plates. Stress maps (B2–3) have conic projection. (A1) Middle Pliensbachian to Late Cenomanian configuration with dominant ridge-push intra-plate forces. The paleogeographic map depicts the Early Aptian setting (M0, 121.0–120.4 Myr; paleogeographic map from Tucholke and McCoy (1986); © The Geological Society of America, Inc.). The length of arrows does not represent sea-floor spreading halfrates (Figs. 14 and 16). (B1) Early Turonian to Late Eocene/Recent configuration with dominant intra-plate compression by African–Eurasian convergence. The paleogeographic map depicts the Holocene setting (post-0.01 Myr; paleogeographic map from Tucholke and McCoy (1986); © The Geological Society of America, Inc.).The length of arrows does not represent sea-floor spreading halfrates (Figs. 14 and 16) or convergence rates (Dewey et al., 1989; see Tables 4 and 5). (B2) Directions of the most compressive horizontal principal stress in the eastern Central Atlantic (based on Mueller et al. (2000); map from Jiménez-Munt and Negredo (2003)) (© Elsevier Science B.V.). The colors of the symbols indicate structural regime and their length data quality. (B3) Numerical model of most compressive horizontal principal stress direction in the eastern Central Atlantic after Jiménez-Munt and Negredo (2003) (© Elsevier Science B.V.). Colors indicate structural regime. Legend: Abbreviations/numbers: AB—Agadir Basin; 1—Azores Triple Junction; 2—Terceira Ridge; 3—Gloria Fault Zone; 4—Madeira Tore; 5—Gorringe Bank; 6—Golf of Cadiz; 7—Gibraltar Arc and Alboran Ridge (unspecified); 8—Canary Bank. Colors (A1, B1): light blue—limestone, dolomite, calcareous ooze; blue—shaley limestone, marl; green—sandy shaley limestone; brown—shale (clay, silt); orange—shale, sandstone; yellow—sandstone, conglomerate; gray—exposed land; white—no data; red lines—Mid-ocean ridge, transform faults, thrust zones; red asteriks—igneous, volcanic rocks; black lines—paleocoastlines; gray lines—modern coastlines. (A1) and (B1) (Background paleogeographic maps) reprinted with permission from The Western North Atlantic region, The Geology of North America, Volume M, Tucholke, B. E. & McCoy, F.W., and Paleogeographic and paleobathymetric evolution of the North Atlantic Ocean. In P. R. Vogt, & B. E. Tucholke (Eds.), pp. 589–602, Copyright (1986), with permission from Geological Society of America. Figures 19(B2) and 19(B3) (stress maps) reprinted from: *Earth and Planetary Science Letters. Volume 205,* Jimenez-Munt, I. & Negredo, A. M., Neotectonic modelling of the western part of the Africa–Eurasia plate boundary; from the Mid-Atlantic Ridge to Algeria, pp. 257–271, Copyright (2003), with permission from Elsevier.

the direction of post-Early Hettangian long-term sediment transport and progradation.

Basin development stages—Unconformities, the overall basin architecture, the results of 2D numerical reverse basin modeling and the biostratigraphic correlation to polarity chronozones in the Central Atlantic sea-floor allow a subdivision of the shelf development into eight stages: (1) early rift, Late Permian to top Anisian, 259.3–234.4 Myr; (2) rift climax, Ladinian to top Carnian, 234.4–220.7 Myr; (3) sag, Norian to top Early Pliensbachian, 220.7–191.5 Myr; (4) early drift, Late Pliensbachian to top Tithonian, 191.5–144.2 Myr, S1 magnetic anomaly to chronozone M19; (5) mature drift, Berriasian to top Cenomanian 144.2–93.5 Myr, M19 to intra-C34; (6) mature drift with initial Atlasian deformation, 93.5–34.7 Myr, Turonian to Late Eocene, intra-C34 to C13; (7) Atlasian deformation, 34.7–19.0 Myr, Late Eocene to Early Miocene, C13–C6; (8) Atlasian uplift and basin inversion; 19.0–0.0, Early Miocene to Recent, post-C6. In combination with data from the literature, the onset of crustal accretion in the Central Atlantic can be inferred to have started between 193.1 and 186.5 Myr (Early Pliensbachian to Middle Toarcian; ∅189.8 Myr, latest Pliensbachian).

Numerical basin modeling, subsidence trends—2D numerical basin modeling (reverse modeling) was performed at stage-level time resolution (29 time layers, 2.3–13.4 Myr each) for the Late Permian to Eocene. The quantitative model includes the three components of total subsidence: thermo-tectonic, flexural and compaction-induced subsidence. In addition, changes in accommodation space and sediment flux are calculated for each time layer. The tectonic subsidence history of the basin shows eight trends of 10–35 Myr duration which are characterized by (1) initially low to zero subsidence or uplift; (2) a gradual increase in subsidence to maximum rates; (3) in some trends a final moderate decrease in rates. Eight subsidence trends exist: (1) ST1, Late Permian to Early Hettangian, 259.3–204.3 Myr; (2) ST2, top Early Hettangian to top Bajocian, 204.3–169.2 Myr; (3) ST3, top Bajocian to top Callovian, 169.2–159.4 Myr; (4) ST4, top Callovian to top Tithonian, 159.4–144.2 Myr; (5) ST5, top Tithonian to top Hauterivian, 144.2–127.0 Myr; (6) ST6, top Hauterivian to top Cenomanian, 127.0–93.5 Myr; (7) ST7, top Cenomanian to top Santonian, 93.5–83.5 Myr; (8) ST8, top Santonian to top Campanian/Maastrichtian, 83.5–71.3/65.0 Myr.

Compositional accommodation analysis (CA-analysis)—CA-analysis is a new tool for quantitative basin analysis. It compares (1) the relative quantities of changes in total subsidence and eustatic sea-level; (2) positive/negative domains of total subsidence/uplift and eustatic sea-level rise/fall; (3) the resulting change in accommodation. CA-analysis of the Agadir Basin reveals, that total subsidence acted as primary control on accommodation for most of the Meso-/Cenozoic basin development. Eustatic sea-level changes of second order were usually subordinate for the development of accommodation space. In the early drift to initial mature drift stage, total uplift as dominant control was restricted to the base of subsidence trends and to the eastern basin margin. In the mature drift basin stage decreases in accommodation were only triggered by eustatic sea-level falls, not by total uplift. Only in the Turonian, when African–Eurasian convergence was initiated, thermo-tectonic uplift represented the main control on accommodation development.

Feedback processes—Changes in thermo-tectonic subsidence, induced by plate-tectonic reconfigurations in the Atlantic domain triggered positive and negative feedback processes between sediment flux, flexural and compaction-induced subsidence. These feedback processes controlled the development and the specific signature of the subsidence trends ST2–8. Changes in sediment flux parallel individual subsidence trends.

Sediment flux, thermo-tectonic subsidence, accommodation—Major changes in sediment flux occurred with ratios of 1:6 between successive time intervals of ∅6.5 Myr duration. Changes in sediment flux were not coupled to eustatic sea-level changes. The reduction in thermo-tectonic subsidence of the northwest African shelf by progressive thermal relaxation of adjacent oceanic crust is to a large degree compensated for by increased flexural and compaction-induced subsidence. Although thermo-tectonic uplift occurs in the mature drift basin stage, moderate total subsidence prevailed and accommodation space was still created. The identification of transgressive/regressive trends derived from facies analysis does not provide sufficient indication to analyze long-term changes in accommodation and to develop genetic models of continental margin basins. This can only be achieved by numerical modeling of the complete basin fill.

Genetic basin model—Changes in thermo-tectonic subsidence in the Agadir Basin correlate with major plate-tectonic reconfigurations in the Central and North Atlantic domain: (1) major shifts of the sea-floor spreading axis; (2) major changes in sea-floor spreading halfrates; (3) the stepwise migration of crustal extension and sea-floor spreading to the North Atlantic and; (4) relative motions of the African and Eurasian plates since the Turonian. Shifts of the sea-floor spreading axis (Late Tithonian, M21; Early/Middle Campanian, C33) triggered a change to low thermo-tectonic subsidence rates. Major reductions in sea-floor spreading halfrates (Middle Tithonian to earliest Barremian, M21–M4; Late Campanian to Maastrichtian, C32–C30) controlled moderate to high thermo-tectonic subsidence rates. Until the Hauterivian, stepwise northward extensions of crustal separation and sea-floor spreading from the Central to the southern North Atlantic resulted in increased thermo-tectonic subsidence rates on the northwest African continental margin. Since the Turonian, the thermo-tectonic subsidence development of the Agadir Basin directly reflected changes in relative plate motions between Africa and Eurasia. Plate-tectonic reconfigurations in adjacent domains, e.g. the southern Atlantic or the western Tethys did not significantly influence the eastern Central Atlantic continental shelf.

Two different long-term, large-scale stress fields and plate-force mechanisms controlled the Pliensbachian to Recent development of the Agadir Basin. In the Early Pliensbachian/Middle Toarcian (193.1/186.5 Myr) to Cenomanian (93.5, intra-C34) ridge-push intra-plate forces varied because of shifts in the sea-floor spreading axis and changes in sea-floor spreading halfrates in the Central Atlantic. They acted in NW–SE paleodirection or 20–30° relative to the Agadir continental shelf gradient. Variations in ridge-push intra-plate forces modulated the overall extensional stress fields and thermo-tectonic subsidence rates on the northwest African continental margin. In Turonian to Late Eocene and Recent times ridge-push forces were transmitted by strike-slip and thrusting along the convergent African–Eurasian plate boundary. Intra-plate compression was directed N–S to NNE–SSW or 90–110° relative to the Agadir continental shelf gradient.

Sequence stratigraphic methodology, eustatic sea-level changes—The results of numerical reverse basin modeling in the Agadir Basin show, that two basic requirements for the analysis of eustatic sea-level-changes and their amplitudes at passive continental margins cannot be applied to the northwest African continental margin: (1) variations in sediment flux were too high to assume, that indicative stratal patterns in seismic lines reflect exclusively changes in accommodation space; (2) thermo-tectonic and total subsidence/uplift rates varied for one dimension (+13.1 to −1.3 cm/kyr), even during the early and mature drift basin stages. Therefore the generally held assumption, that thermo-tectonic and total subsidence rates at passive continental margins were largely constant or followed a simple, steady trend dominated by thermal relaxation cannot be sustained (at least not for the northwest African continental margin). Improved approximations of the timing and amplitudes of eustatic sea-level changes in Meso- and Early Cenozoic times require the quantitative analysis (reverse basin, forward stratigraphic modeling) of passive continental margins of different oceanic basins.

Acknowledgements

Constructive and helpful reviews by Albert Bally and John Warme are gratefully acknowledged. The Department of the Interior of Morocco, the Gendarmerie Royale at Imouzzer-des-Ida-Outanane and the Dean of the Faculty of Science, University Chouaib Doukkali in El Jadida, kindly gave permissions for geological field-work in the WHA. We are greatly indebted to Abdallah and Hassan from the village of Tamarout near Imouzzer for their hospitality and logistical support. This project was funded by the Centre de Recherche National (CNR) of Morocco, the German Research Fund (DFG, Be 641/28 and Le 540/18), the German Academic Exchange Foundation (DAAD) and the University of Heidelberg.

References

Adams, A., Ager, D. V., & Harding, A. G. (1980). Géologie de la région d'Imouzzer des Ida-ou-Tanane (Haut Atlas occidental). *Notes du Sérvice Géologique du Maroc*, *41*(285), 59–80.

Aït Brahim, L., Chotin, P., Hinaj, S., Abdelouafi, A., El Adraoui, A., Nakcha, C., Dhont, D., Charroud, M., Sossey Alaoui, F., Amrhar, M., Bouaza, A., Tabyaoui, H., & Chaouni, A. (2002). Paleostress evolution in the Moroccan African margin from Triassic to present. *Tectonophysics*, *357*(1–4), 187–205.

Aït Chayeb, E. H., Youbi, N., El-Boukhari, A., Bouabdelli, M., & Amrhar, M. (1998). Le volcanisme Permien et Mésozoique inferieur du Bassin d'Argana (Haut-Atlas occidental, Maroc); un magmatisme intraplaque associe a l'ouverture de l'Atlantique central. *Journal of African Earth Sciences*, *26*(4), 499–519.

Algouti, A (1991). *Turonien supérieur et Sénonien du versant nord du Haut Atlas de Marrakech: Caractérisation sédimentologique et stratigraphique*. Unpublished State Doctorate (Doctorat de 3ème Cycle), Univ. Cadi Ayyad, Marrakech/Morocco, p. 250

Algouti, A., Chbani, B., & Azzaoui, K. A. (1993). Turonien supérieur et Sénonien dans la région d'Im-n-Tanout (Haut Atlas, Maroc): Sédimentologie, diagenèse, analyze séquentielle. *Revue de la Faculté des Sciences Semlalia*, *7*, 183–196.

Allen, P. A., & Allen, J. R. (1990). *Basin analysis*, Oxford: Blackwell Science Publications, p. 451.

Ambroggi, R. (1963). Étude géologique du versant méridional du Haut Atlas occidental et de la plaine du Souss. *Notes et Memoires du Sérvice Géologique du Maroc*, *157*.

Amrhar, M (1995). *Téctonique et inversion géodynamiques post-rift dans le Haut Atlas occidental: Structures, instabilités tectoniques et magmatisme liés a l'ouverture de l'Atlantique central et la collision Afrique–Europe*. Unpublished State Doctorate (Doctorat de 3ème Cycle), Univ. Cadi Ayyad, Marrakech/Morocco, p. 253

Beauchamp, W., Allmendinger, R. W., Barazangi, M., Demnati, A., Alji, M., & Dahmani, M. (1999). Inversion tectonics and the evolution of the High Atlas Mountains, Morocco, based on a geological–geophysical transect. *Tectonics*, *18*(2), 163–184.

Behrens, M., Krumsiek, K., Meyer, D. E., Schäfer, A., Siehl, A., Stets, J., Thein, J., & Wurster, P. (1978). Sedimentationsabläufe im Atlas-Golf (Kreide Küstenbecken Marokko). *Geologische Rundschau*, *67*(2), 424–453.

Behrens, M., & Siehl, A. (1982). Sedimentation in the Atlas Gulf I, Lower Cretaceous clastics. In U. von Rad, K. Hinz, M. Sarnthein, & E. Seibold (Eds.), *Geology of the northwest African continental margin* (pp. 427–438). Heidelberg: Springer.

Bellingham, P., & White, N. (2000). A general inverse method for modelling extensional sedimentary basins. *Basin Research*, *12*(3/4), 219–226.

Berggren, W. A., Kent, D. V., Swisher, C. C., & Aubry, M.-P. (1995). A revised Cenozoic geochronology and chronostratigraphy. In W. A. Berggren, D. V. Kent, M.-P. Aubry, & J. Hardenbol (Eds.), *Geochronology, time scales and global stratigraphc correlations* (pp. 129–212). *Society for Sedimentary Geology (SEPM), Special Publications 54*.

Bernardin, C (1988). *Interprétation gravimétrique et structure profonde del Meseta marocaine et de sa marge atlantique*. Unpublished State Doctorate (Doctorat de 3ème Cycle), Univ. St. Jerôme, Marseille, p. 162.

Boillot, G., Mougenot, D., Girardeau, J., & Winterer, E. L. (1989). Rifting processes on west Galicia margin, Spain. In A. J. Tankard, & H. R. Balkwill (Eds.), *Extensional tectonics and stratigraphy of the North Atlantic Margins* (pp. 363–378). *American Association of Petroleum Geologists Memoir 46*.

Boldreel, L. O., & Andersen, M. S. (1998). Tertiary compressional structures on the Faroe-Rockall Plateau in relation to Northeast Atlantic ridge-push and Alpine foreland stresses. In S. A. P. L. Cloetingh, L. O. Boldreel, B. T. Larsen, M. Heinesen, & L. Mortensen (Eds.), *Tectonics of sedimentary basin formation: Models and constraints* (*Vol. 300*) (pp. 13–28). *Tectonophysics*, Amsterdam: Elsevier.

Bond, G. C., Kominz, M. A., & Sheridan, R. E. (1995). Continental terraces and rises. In C. Busby, & R. Ingersoll (Eds.), *Tectonics of sedimentary basins* (pp. 149–178). Oxford: Blackwell.

Bott, M. H. P. (1982). *The interior of the earth, its structure, constitution and evolution.*, London: Arnold.

Bouaouda, M. S (1987). *Biostratigraphie du Jurassique inferieur et moyen des bassins côtiers d'Essaouira et d'Agadir (Marge Atlantique, Maroc).* Unpublished State Doctorate (Doctorat de 3ème Cycle), Univ. de Toulouse, p. 213

Bouaouda, M. S. (2002). Micropaléontologie de la plate-forme du Bathonien–Oxfordien des régions d'Imi Im-n-Tanout et du Jbilet occidental (Maroc). Essai de biozonation. *Revue de Paléobiologie*, *21*(1).

Bowman, S. A., & Vail, P. R. (1999). Interpreting the stratigraphy of the Baltimore Canyon section offshore New Jersey with PHIL, a stratigraphic simulator. In J. W. Harbaugh, W. L. Watney, E. C. Rankey, R. Slingerland, R. H. Goldstein, & E. K. Franseen (Eds.), *Numerical experiments in stratigraphy: Recent advances in stratigraphic and sedimentologic computer simulations* (pp. 117–138). *Society for Sedimentary Geology (SEPM), Special Publication 62*.

Brede, R., Hauptmann, M., & Herbig, H. G. (1992). Plate tectonics and intracratonic mountain ranges in Morocco; the Mesozoic–Cenozoic development of the Central High Atlas and the Middle Atlas. In V. Jacobshagen, & M. Sarntheim (Eds.), *Contributions to Moroccan geology* (*Vol. 81*) (pp. 127–141). *Geologische Rundschau*.

Brown, R. H. (1980). Triassic rocks of the Argana Valley, southern Morocco, their regional structural implications. *Bulletin American Association of Petroleum Geologists*, *64*(7), 988–1003.

Brown, L. F., & Fisher, W. L. (1974). Seismic stratigraphic interpretation and petroleum exploration. *American Association of Petroleum Geologists, Continuing Education Course Note Series*, *16*, 181.

Bulot, L. G. (2000). Early to Middle Ypresian (55–51 Ma). In J. Dercourt, E. Gaetani, B. Vrielynck, E. Barrier, B. Biju-Duval, M. F. Brunet, J.-P. Cadet, S. Crasquin, & M. Sandulescu (Eds.), *Atlas Peri-Tethys* (pp. 111–118). Paris: Commission for the Geological Map of the World (CGMW).

Burov, E. B., & Diament, M. (1995). The effective elastic thickness (T_e) of continental lithosphere: What does it really mean. *Journal of Geophysical Research*, *100*(B3), 3905–3927.

Cande, S., & Kent, D. V. (1995). Revised calibration of the geomagnetic polarity timescale for the Late Cretaceous and Cenozoic. *Journal of Geophysical Research*, *100*(4), 6093–6095.

Canerot, J., Cugny, P., Peybernes, B., Rahhali, I., Rey, J., & Thieuloy, J. P. (1986). Comparative study of the Lower and Mid-Cretaceous sequence on different Maghrebian shelves and basins, their place in the evolution of the North African Atlantic and Neotethysian margins. *Palaeogeography, Palaeoclimatology, Palaeoecology*, *55*(2–4), 213–232.

Chellai, E. H., & Perriaux, J. (1996). Evolution géodynamique d'un bassin d'avant-pays du domain Atlasique (Maroc): exemple des dépôts neogènes et quaternaires du versant septentrional de l'Atlas de Marrakech. *Comptes Rendus de l'Académie des Sciences, Serie II, 322,* 724–734.

Choubert, G. (1957). Carte géologique du Maroc au 1/500000. *Notes et Memoirs du Sérvice Géologique du Maroc*, *70*.

Christie-Blick, N., Mountain, G. S., & Miller, K. G. (1990). Seismic stratigraphy: Record of sea-level change. In R. Revelle (Ed.), *Sea-level change* (pp. 116–140). *National Research Council. Studies in Geophysics*, Washington: National Academy Press.

Cloetingh, S. (1988). Intra-plate stresses: A new element in basin analysis. In K. Kleinspehn, & Paola (Eds.), *New perspectives in basin analysis* (pp. 205–230). Heidelberg: Springer.

Deckart, K., Feraud, G., & Bertrand, H. (1997). Age of Jurassic continental tholeiites of French Guyana, Surinam and Guinea: Implications for the initial opening of the Central Atlantic Ocean. *Earth and Planetary Science Letters*, *150*, 205–220.

Defrentin, S., & Fauvelet, J. (1951). Presence de phyllopods triasiques dans la région d'Argana-Bigoudine Haut-Atlas occidental. *Notes et Memoires du Sérvice Géologique du Maroc*, *85*, 129–137.

Dercourt, J., Gaetani, E., Vrielynck, B., Barrier, E., Biju-Duval, B., Brunet, M. F., Cadet, J.-P., Crasquin, S., & Sandulescu, M. (2000). *Atlas Peri-Tethys*, Paris: Commission for the Geological Map of the World (CGMW), p. 268.

Dewey, J. F., Helman, M. L., Turco, E., Hutton, D. H. W., & Knot, S. D. (1989). Kinematics of the western Mediterranean. In M. P. Coward, D. Dietrich, & R. G. Park (Eds.), *Alpine Tectonics* (pp. 265–283). *Geological Society, London, Special Publications 45*.

Dewey, J. F., & Pitman, W. C. (1998). Sea-level changes: Mechanisms, magnitudes and rates. In J. L. Pindell, & C. Drake (Eds.), *Eustasy and the tectonostratigraphic evolution of northern South America*. *Society for Sedimentary Geology (SEPM), Special Publication 58*.

Dickinson, W. R., Armin, R. A., Beckvar, T. C., Goodlin, S. U., Janecke, R. A., Mark, R. D., Norris, G., Radel, G., & Wortman, A. A. (1987). Geohistory analysis of rates of sediment accumulation and subsidence for selected California Basins. In V. R. Ingersoll, & W. G. Ernst (Eds.), (*Vol. 6*) (pp. 1–23). *Cenozoic basin development of coastal California*.

Dore, A. G., Lundin, E. R., Jensen, L. N., Birkeland, O., Eliassen, P. E., & Fichler, C. (1999). Principal tectonic events in the evolution of the northwest European Atlantic margin. In A. J. Fleet, & S. A. R. Boldy (Eds.), *Petroleum Geology of northwest Europe* (pp. 41–61). *Fifth Conference, London, October 26–29*.

Du Dresnay, R. (1988). Répartition des dépôts carbonatés du Lias inférieur et moyen le long de la côte atlantique du Maroc: Conséquences sur la paléogéographie de l'Atlantique naissant. *Journal of African Earth Sciences*, *7*, 385–396.

Duffaud, F. (1960). Contribution a l'étude stratigraphique du bassin secondaire du Haut-Atlas Occidental, Maroc. *Bulletin de la Société Géologique de France*, *7*(2), 728–734.

Duffaud, F. (1981). Carte géologique du Maroc au 1/100000, Feuille Im-n-Tanout. *Notes et Memoirs du Sérvice Géologique du Maroc*, *204*.

Duffaud, F., Brun, L., & Plauchut, B. (1966). Le bassin Sud-Ouest Marocain. In D. Reyre (Ed.), *Bassins sédimentaires du littoral Africain* (pp. 5–26). *Publications d'Association du Service Géologique Africaine 1*.

Dutuit, J. M. (1966). Apport des découvertes des vertebrés à la stratigraphie du Trias continental du Couloir d'Argana (Haut-Atlas occidental, Maroc). *Notes et Memoirs du Sérvice Géologique du Maroc*, *26*(188), 29–31.

Dutuit, J. M., & Heyler, D. (1983). Taphonomie des gisements des vertebrés triasiques marocains (Couloir d'Argana) et paléogéographie. *Bulletin de la Société Géologique de France*, *25*(4), 623–633.

Duval, B., Cramez, C., & Vail, P. R. (1992). Types and hierarchy of stratigraphic cycles. In Centre National de la Recherche Scientifique (CNRS), & Institut Francais du Pétrole (IFP) (Eds.), *Sequence stratigraphy of European basins, Dijon 1992, Abstract Volume* (pp. 44–45).

Einsele, G. (2000). *Sedimentary basins; evolution, facies, and sediment budget*, Heidelberg: Springer, p. 792.

El Harfi, A., Lang, J., & Salomon, J. (1996). Le remplissage continental cénozoique du bassin d'avant-pays de Ouarzazate; implications sur l'évolution geodynamique du Haut-Atlas central (Maroc). *Comptes Rendus de l'Academie des Sciences, Serie II*, *323*(7), 623–630.

Emery, D., & Myrers, K. (1996). *Sequence stratigraphy*, Oxford: Blackwell, p. 297.

Ernst, W. G., & Dal Piaz, G. V. (1978). Mineral parageneses of eclogitic rocks and related mafic schists of the Piemonte ophiolite nappe, Breuil-St. Jacques area, Italian western Alps. *American Mineralogist*, *63*(7/8), 621–640.

Ettachfini, E. M. (1992). *Biostratigraphie et stratigraphie séquentielle: Leurs contributions réciproques pour le calage stratigraphique des dépôts Cénomano-Turoniens dans le Bassin d'Essaouira (Maroc). In 14ième Réunion des Sciences de la Terre*, p. 59.

Ettachfini, E. M. (1993). Le Vraconien, Cénomanien et Turonien du Bassin d'Essaouira (Haut-Atlas occidental, Maroc). *Strata, Serie II*, *18*, 247.

Ettachfini, E. M., El Kamali, N., & Bilotte, M. (1989). Essai de caractérisation bio-et lithostratigraphique des séquences sédimentaires dans le Crétacé de la région d'Im-n-Tanout (Haut-Atlas occidental, Maroc). In J. P. Gelard, & J. Beauchamp (Eds.), *Colloque Franco-Marocain de Géologie* (pp. 71–81). *Sciences Géologiques, Memoire 84*.

Fiechtner, L., Friedrichsen, H., & Hammerschmidt, K. (1992). Geochemistry and geochronology of Early Mesozoic tholeiites from Central Morocco. *Geologische Rundschau*, *81*(1), 45–62.

Fraissinet, C., Zouine, E. M., Morel, J.-L., Poisson, A., Andrieux, J., & Faure-Muret, A. (1988). Structural evolution of the southern and northern Central High Atlas in Paleogene and Mio-Pliocene times. In V. Jacobshagen (Ed.), *The Atlas system of Morocco; studies on its geodynamic evolution* (pp. 273–291). *Lecture Notes in Earth Sciences 15*, Heidelberg: Springer.

Froitzheim, N., Stets, J., & Wurster, P. (1988). Aspects of western High Atlas tectonics. In V. Jacobshagen (Ed.), *The Atlas system of Morocco; studies on its geodynamic evolution* (pp. 219–244). *Lecture Notes in Earth Sciences 15*, Heidelberg: Springer.

Giese, P., & Jacobshagen, V. (1992). Inversion tectonics of intracontinental ranges; High and Middle Atlas, Morocco. In V. Jacobshagen, & M. Sarntheim (Eds.), *Contributions to Moroccan geology* (pp. 249–259). *Geologische Rundschau 81*, Heidelberg: Springer.

Göerler, K., Helmdach, F.-F., Gaemers, P., Heissig, K., Hinsch, W., Maedler, K., Schwarzhans, W., & Zucht, M. (1988). The uplift of the Central High Atlas as deduced from Neogene continental sediments of the Ouarzazate Province, Morocco. In V. H. Jacobshagen (Ed.), *The Atlas system of Morocco; studies on its geodynamic evolution* (pp. 361–404). *Lecture Notes in Earth Sciences 15*, Heidelberg: Springer.

Gomez, F., Beauchamp, W., & Barazangi, M. (2000). Role of the Atlas Mountains (northwest Africa) within the African–Eurasian plate-boundary zone. *Geology*, *28*(9), 775–778.

de Graciansky, P.-C., Hardenbol, J., Jacquin, T., & Vail, P. R. (1998). Mesozoic and Cenozoic sequence stratigraphy of European basins. *Society for Sedimentary Geology (SEPM), Special Publication 60*, 786.

Gradstein, F. M., Agterberg, F. P., Ogg, J. G., Hardenbol, J., Van Veen, P., Thierry, J., & Huang, Z. (1994). A Mesozoic time scale. *Journal of Geophysical Research*, *99*(12), 24051–24074.

Gradstein, F. M., Agterberg, F. P., Ogg, J. G., Hardenbol, J., Van Veen, P., Thierry, J., & Huang, Z. (1995). A Triassic and Jurassic time scale. In W. A. Berggren, A. William, D. V. Kent, V. Dennis, M.-P. Aubry, & J. Hardenbol (Eds.), *Geochronology, time scales and global stratigraphic correlation* (pp. 95–126). *Society for Sedimentary Geology (SEPM), Special Publications 54*.

Gradstein, F. M., Jansa, L. F., Srivastava, S. P., Williamson, M. A., Bonham Carter, G., & Stam, B. (1990). Aspects of North Atlantic paleo-oceanography. In M. J. Keen, & G. L. Williams (Eds.), *Geology of the continental margin of Eastern Canada* (pp. 351–389). *Geological Survey of Canada, Geology of Canada 2*.

Guiraud, R., & Bosworth, W. (1997). Senonian basin inversion and rejuvenation of rifting in Africa and Arabia; synthesis and implications to plate-scale tectonics. In S. Cloetingh, M. Fernandez, J. A. Munoz, W. Sassi, & F. Horvath (Eds.), *Structural controls on sedimentary basin formation* (*Vol. 282*) (pp. 39–82). *Tectonophysics*, Amsterdam: Elsevier.

Hafid, M (1999). *Incidences de l'évolution du Haut Atlas Occidental et de son avant-pays septentrional sur la dynamique Meso-Cenozoïque de la marge atlantique (entre Safi et Agadir).* Unpublished State Doctorate (Doctorat de 3ème Cycle), Univ. Ibn Tofail, Kenitra/ Morocco, p. 283.

Hafid, M. (2000). Triassic–Early Liassic extensional systems and their Tertiary inversion, Essaouira Basin (Morocco). *Marine and Petroleum Geology*, *17*, 409–429.

Hafid, M., Salem, A. A., & Bally, A. W. (2000). The western termination of the Jebilet–High Atlas system (Offshore Essaouira Basin, Morocco). *Marine and Petroleum Geology*, *17*, 431–443.

Haq, B. U., Hardenbol, J., & Vail, P. R. (1987). Chronology of fluctuating sea-levels since the Triassic. *Nature*, *235*, 1156–1167.

Hardenbol, J., Thierry, J., Farley, M. B., Jacquin, T., de Graciansky, P.-C., & Vail, P. R. (1998). Mesozoic and Cenozoic sequence chronostratigraphic framework of European basins. In P.-C. de Graciansky, J. Hardenbol, T. Jacquin, & P. R. Vail (Eds.), *Mesozoic and Cenozoic sequence stratigraphy of European basins* (pp. 3–15). *Society for Sedimentary Geology (SEPM), Special Publications 60*.

Harrison, C. G. A. (1990). Long-term eustasy and epeirogeny in continents. In R. Revelle (Ed.), *Sea-level change* (pp. 141–158). *National Research Council, Studies in Geophysics*, Washington: National Academy Press.

Hartley, R., Watts, A. B., & Fairhead, J. D. (1996). Isostasy of Africa. *Earth and Planetary Science Letters*, *137*, 1–18.

Haworth, R. T., Keen, C. E., & Williams, H. (1994). Transects of the ancient and modern continental margins of Eastern Canada. In R. C. Speed (Ed.), *Phanerozoic evolution of North American continent-ocean transitions, Decade of North American Geology, Accompanying Volume* (pp. 87–127). Boulder: Geological Society of America.

Heyman, M. A. W. (1989). Tectonic and depositional history of the Moroccan continental margin. *American Association of Petroleum Geologists, Memoir 46*, 323–340.

Jabour, H., Morabet, A. M., & Bouchta, R. (2000). Hydrocarbon systems of Morocco. In S. Crasquin-Soleau, & E. Barrier (Eds.), *Peri-Tethys Memoir 5; New data on peri-Tethyan sedimentary basins* (pp. 143–157). *Memoires du Muséum National d'Histoire Naturelle 182*.

Jacobshagen, V. (1992). Major fracture zones of Morocco; the South Atlas and the Transalboran fault systems. In V. Jacobshagen, & M. Sarntheim (Eds.), *Contributions to Moroccan geology* (pp. 185–197). *Geologische Rundschau 81*.

Jacobshagen, V. H., Brede, R., Hauptmann, M., Heinitz, W., & Zylka, R. (1988). Structure and post-Palaeozoic evolution of the Central High Atlas. In V. H. Jacobshagen (Ed.), *The Atlas system of Morocco; studies on its geodynamic evolution* (pp. 245–271). *Lecture Notes in Earth Sciences 15*, Heidelberg: Springer.

Jaïdi, S. E. M., Bencheqroun, M. A., & Diouri, M. M. (1970a). *Carte géologique du Maroc au 1/100.000, Feuille NH-29-XXI-2, El Khemis de Meskala. Éditions du Service Géologique du Maroc, Notes et Memoires 202*.

Jaïdi, S. E. M., Bencheqroun, M. A., & Diouri, M. M. (1970b). *Carte géologique du Maroc au 1/100.000, Feuille NH-29-XXI-1, Tamanar. Éditions du Service Géologique du Maroc, Notes et Memoires 201*.

Jacquin, T., & de Graciansky, P.-C. (1998), Major transgressive/regressive cycles: the stratigraphic signature of European basin development. In P.-C. de Graciansky, J. Hardenbol, T. Jacquin, & P. R. Vail (Eds.), *Mesozoic and Cenozoic Sequence Stratigraphy of European Basins* (pp. 15–30). *Society for Sedimentary Geology (SEPM), Special Publications 60*.

Jalil, N. E. (1999). Continental Permian and Triassic vertebrate localities from Algeria and Morocco and their stratigraphical correlations. In B. C. Storey, B. S. Rubridge, D. I. Cole, & M. J. De Wit (Eds.), *Gondwana-10; event stratigraphy of Gondwana* (*Vol. 29*) (pp. 219–226). *Journal of African Earth Sciences*, London, New York: Pergamon.

Jalil, N.-E., & Dutuit, J.-M. (1996). Permian captorhinid reptiles from the Argana Formation, Morocco. *Palaeontology*, *39*(4), 907–918.

Jansa, L. F., Bujak, J. P., & Williams, G. L. (1980). Upper Triassic salt deposits of the western North Atlantic. *Canadian Journal of Earth Sciences*, *17*(5), 547–559.

Jansa, L. F., & Wade, J. A. (1975). Geology of continental margin of Nova Scotia and Newfoundland. In W. J. M. Van der Linden, & J. A. Wade (Eds.), *Geological Survey of Canada, Paper 74-30* (pp. 51–106).

Jimenez-Munt, I., & Negredo, A. M. (2003). Neotectonic modelling of the western part of the Africa–Eurasia plate boundary; from the Mid-Atlantic Ridge to Algeria. *Earth and Planetary Science Letters*, *205*(3/4), 257–271.

Keen, C. E., Loncarevic, B. D., Reid, I., Woodside, J., Haworth, R. T., & Williams, H. (1990). Tectonic and geophysical overview. In M. J. Keen, & G. L. Williams (Eds.), *Geology of the continental margin of Eastern Canada, Geology of Canada 2* (pp. 31–85).

Kent, D. V., & Gradstein, F. M. (1986). A Jurassic to Recent chronology. In P. R. Vogt, & B. E. Tucholke (Eds.), (*Vol. M*) (pp. 45–50). *The Geology of North America, the western North Atlantic Region.*

Kingston, D. R., Dishroon, C. P., & Williams, P. A. (1983). Global basin classification. *Bulletin American Association of Petroleum Geologists*, *67*(12), 2175–2193.

Klitgord, K. D., Hutchinson, D. R., & Schouten, H. (1988). US Atlantic continental margin; structural and tectonic framework. In R. E. Sheridan, & J. A. Grow (Eds.), (*Vol. I-2*) (pp. 19–56). *The Geology of North America, the Atlantic continental margin: US*.

Klitgord, K. G., & Schouten, H. (1986). Plate kinematics of the Central Atlantic. In P. R. Vogt, & B. E. Tucholke (Eds.), (*Vol. M*) (pp. 351–378). *The Geology of North America, the western North Atlantic Region*.

Labbassi, K. (1997). Étude de la subsidence Trias supérieur-Eocene du Bassin d'Essaouria (Maroc occidental): Essai de quantification. *Gaia*, *14*, 77–89.

Labbassi, K., Medina, F., Rimi, A., Mustaphi, H., & Bouatmani, R. (2000). Subsidence history of the Essaouira Basin (Morocco). In S. Crasquin-Soleau, & E. Barrier (Eds.), *Peri-Tethys Memoir 5; New data on peri-Tethyan sedimentary basins* (pp. 129–141). *Memoires du Muséum National d'Histoire Naturelle 182*.

Leeder, M. R. (1992). Upper Palaeozoic basins of the British Isles—Caledonide inheritance versus Hercynian plate margin processes. *Journal of the Geological Society of London*, *139*, 479–491.

Leeder, M. R. (1995). Continental rifts and proto-oceanic rift throughs. In C. J. Busby, & R. V. Ingersoll (Eds.), *Tectonics of sedimentary basins* (pp. 119–148). Oxford: Blackwell.

Leeder, M. R. (1999). Sedimentology and sedimentary basins, from turbulence to tectonics. Oxford: Blackwell, p. 592.

Leinfelder, R., Schmid, D. U., Nose, M., & Werner, W. (2002). Jurassic reef patterns, the expression of a changing globe. In W. Kiessling, E. Flügel, & J. Golonka (Eds.), *Phanerozoic reef patterns* (pp. 465–520). *Society for Sedimentary Geology (SEPM), Special Publication 72*.

Le Roy, P (1997). *Les bassins Ouest-marocains; leur formation et leur évolution dans le cadre de l'ouverture et du développement de l'Atlantique central (marge africaine)*. Unpublished Doctoral Thesis, Université de Bretagne Occidental, Brest, p. 328.

Le Roy, P., Guillocheau, F., Piqué, A., & Morabet, A. M. (1998). Subsidence of the Atlantic Morrocan margin during the Mesozoic. *Canadian Journal of Science*, *35*(4), 476–493.

Le Roy, P., & Piqué, A. (2001). Triassic–Liassic western Moroccan syn-rift basins in relation to the Central Atlantic opening. *Marine Geology*, *172*, 359–381.

Makris, J., Demnati, A., & Klussman, J. (1985). Deep seismic soundings in Morocco and a crust and upper mantle model deduced from seismic and gravity data. *Annales Geophysicae*, *3*, 369–380.

Masse, J.-P. (2000). Early Aptian (112–114 Ma). In J. Dercourt, E. Gaetani, B. Vrielynck, E. Barrier, B. Biju-Duval, M. F. Brunet, J.-P. Cadet, S. Crasquin, & M. Sandulescu (Eds.), *Atlas Peri-Tethys* (pp. 119–127). Paris: Commission for the Geological Map of the World (CGMW).

Mauffret, A., Mougenot, D., Miles, P. R., & Malod, J. A. (1989). Results of multichannel reflection profiling of the Tagus abyssal plain (Portugal)—Comparison with the Canadian margin. In A. J. Tankard, & H. R. Balkwill (Eds.), *Extensional tectonics and stratigraphy of the North Atlantic margins* (pp. 379–393). *American Association of Petroleum Geologists, Bulletin 46*.

Medina, F. (1989). Landsat imagery interpretation of Essaouira Basin (Morocco). Camparison with geophysical data and structural implications. *Journal of African Earth Sciences*, *9*(1), 69–75.

Medina, F. (1994). *Evolution structurale du Haut-Atlas Occidental et des régions voisines du Trias a l'actuel. Dans le cadre de l'ouverture de l'Atlantique central et la collision Afrique–Europe*. Unpublished State Doctorate (Doctorat de 3ème Cycle), Univ. Mohammed V, Rabat/ Morocco, p. 271.

Medina, F. (1995). Syn- and post-rift evolution of the El Jadida–Agadir Basin (Morocco): Constraints for the rifting models of the Central Atlantic. *Canadian Journal of Science*, *32*, 1273–1291.

Medina, F., & Errami, A. (1996). L'invertion tectonique dans le bassin trasique de Tine Melil (Haut atlas occidental, Maroc). Implications sur le fonctionnement de la faille de Tizi n'Test. *Gaia*, *12*, 9–18.

Meulenkamp, J. E., Sissingh, W., Calvo, J. P., Daams, R., Studencka, B., Londeix, L., Cahuzac, B., Kovac, M., Nagymarosy, A., Meulenkamp, J. E., Sissingh, W., Calvo, J. P., Daams, R., Studencka, B., Londeix, L., Cahuzac, B., Kovac, M., Nagymarosy, A., Rousu, A., Badescu, D., Beniamovskii, V. N., Scherba, I. G., Roger, J., Platel, J.-P., Hirsch, F., Sadek, A., Abdel-Gawad, G. I., Ben-Ismail-Lattrache, K., Zaghbib-Turki, D., Bouaziz, S., Karoui-Yaakoub, N., & Yaich, C. (2000a). Late Lutetian (44–41 Ma). In J. Dercourt, E. Gaetani, B. Vrielynck, E. Barrier, B. Biju-Duval, M. F. Brunet, J.-P. Cadet, S. Crasquin, & M. Sandulescu (Eds.), *Atlas Peri-Tethys* (pp. 163–170). Paris: Commission for the Geological Map of the World (CGMW).

Meulenkamp, J. E., Sissingh, W., Calvo, J. P., Daams, R., Studencka, B., Londeix, L., Cahuzac, B., Kovac, M., Nagymarosy, A., Meulenkamp, J. E., Sissingh, W., Calvo, J. P., Daams, R., Studencka, B., Londeix, L., Cahuzac, B., Kovac, M., Nagymarosy, A., Rousu, A., Badescu, D., Beniamovskii, V. N., Scherba, I. G., Roger, J., Platel, J.-P., Hirsch, F., Sadek, A., Abdel-Gawad, G. I., Ben-Ismail-Lattrache, K., Zaghbib-Turki, D., Bouaziz, S., Karoui-Yaakoub, N., & Yaich, C. (2000b). Early to Middle Ypresian (55–51 Ma). In J. Dercourt, E. Gaetani, B. Vrielynck, E. Barrier, B. Biju-Duval, M. F. Brunet, J.-P. Cadet, S. Crasquin, & M. Sandulescu (Eds.), *Atlas Peri-Tethys* (pp. 155–162). Paris: Commission for the Geological Map of the World (CGMW).

Michard, A. (1976). Elément de géologie marocaine. *Notes et Mémoires du Sérvice Géologique du Maroc,* 252.

Minshull, T. A., & Charvis, P. (2001). Ocean island densities and models of lithospheric flexure. *Geophysical Journal International*, *145*(3), 731–739.

Morabet, A. M., Bouchta, R., & Jabour, H. (1998). An overview of the petroleum systems of Morocco. In D. S. MacGregor, R. T. J. Moody, & D. D. Clarke-Lowes (Eds.), *Petroleum geology of North Africa* (pp. 283–296). *Geological Society, Special Publication 132*.

Morel, J.-L., Zouine, E.-M., Andrieux, J., & Faure-Muret, A. (2000). Déformations néogenes et quaternaires de la bordure nord haut atlasique (Maroc); role du sôcle et conséquences structurales. *Journal of African Earth Sciences*, *30*(1), 119–131.

Mueller, B., Reinecker, J., Heidbach, O., & Fuchs, K. (2000). The 2000 release of the world stress map.

Mustaphi, H., Medina, F., Jabour, H., & Hoepffner, C. (1997). Le Bassin du Souss (zone de faille du Tizi n'Test, Haut Atlas occidental, Maroc); résultat d'une inversion tectonique controlée par une faille de détachement profonde. *Journal of African Earth Sciences*, *24*(1/2), 153–168.

NACSN (North American Commission on Stratigraphic Nomenclature). (1983). North American stratigraphic code. *Bulletin American Association of Petroleum Geologists, 67,* 841–875.

Olivet, J.-L. (1996). La cinématique de la plaque Iberique. *Bulletin des Centres de Rechérches Éxploration–Production Elf Aquitaine*, *20*(1), 131–195.

Olsen, P. E. (1997). Stratigraphic record of the Early Mesozoic breakup of Pangea in the Laurasia†Gondwana rift system. *Annual Review of Earth and Planetary Sciences*, *25*, 337–401.

Ouzzani, M. T., Eyssautier, M. L., Marçais, M. J., Choubert, M. G., & Fallot, M. P. (1956). *Empire Chérifien, 500.000^e Feuille Marrakesh*, Rabat: Ministère de la Production Industrielle et des Mines.

Philip, J., & Floquet, M. (2000a). Late Maastrichtian (69.5–65 Myr). In J. Dercourt, E. Gaetani, B. Vrielynck, E. Barrier, B. Biju-Duval, M. F. Brunet, J.-P. Cadet, S. Crasquin, & M. Sandulescu (Eds.), *Atlas Peri-Tethys* (pp. 145–152). Paris: Commission for the Geological Map of the World (CGMW).

Philip, J., & Floquet, M. (2000b). Early Campanian (83–80.5 Myr). In J. Dercourt, E. Gaetani, B. Vrielynck, E. Barrier, B. Biju-Duval, M. F. Brunet, J.-P. Cadet, S. Crasquin, & M. Sandulescu (Eds.), *Atlas Peri-Tethys* (pp. 137–144). Paris: Commission for the Geological Map of the World (CGMW).

Piqué, A., & Laville, A. (1995). L'ouverture initiale de l'Atlantique central. *Bulletin de la Société Géologique de France*, *166*, 725–738.

Pitman, W. C., & Talwani, M. (1972). Sea-floor spreading in the North Atlantic. *Geological Society of America Bulletin*, *83*(3), 619–646.

Posamentier, H. W., Jervey, M. T., & Vail, P. R. (1989). Eustatic controls on clastic deposition—conceptual framework. In C. K. Wilgus, B. S.

Hastings, C. G. S. C. Kendall, H. W. Posamentier, C. A. Ross, & J. C. van Wagoner (Eds.), *Sea-level changes: An integrated approach. Society for Sedimentary Geology (SEPM), Special Publications 42*.

Prosser, S. (1993). Rift-related linked depositional systems and their seimic expression. In G. D. Williams, & A. Dobb (Eds.), *Tectonics and seismic sequence stratigraphy* (pp. 35–66). *Geological Society Special Publication 71*.

von Rad, U., Hinz, K., Sarnthein, M., & Seibold, E. (1982). *Geology of the northwest African Continental Margin*, Heidelberg: Springer, p. 703.

Rey, J., Canerot, J., Peybernes, B., Taj-Eddine, K., & Thieuloy, J. P. (1988). Lithostratigraphy, biostratigraphy and sedimentary dynamics of the Lower Cretaceous deposits on the northern side of the western High Atlas (Morocco). *Cretaceous Research*, *9*(2), 141–158.

Roeser, H. A. (1982). Magnetic anomalies in the magnetic quiet zone off Morocco. In U. von Rad, K. Hinz, M. Sarnthein, & E. Seibold (Eds.), *Geology of the northwest African continental margin* (pp. 61–68). Heidelberg: Springer.

Roest, W. R., Danobeitia, J., Verhoef, J., & Collette, B. J. (1992). Magnetic anomalies in the Canary Basin and the Mesozoic evolution of the Central North Atlantic. *Marine Geophysical Research*, *14*, 1–24.

Roest, W. R., & Srivastava, S. P. (1989). Sea-floor spreading in the Labrador Sea: A new reconstruction. *Geology*, *17*, 1000–1004.

Rüffer, T., & Zühlke, R. (1995). Sequence stratigraphy and sea-level changes in the Early to Middle Triassic of the Alps: A global comparison. In B. U. Haq (Ed.), *Sequence stratigraphy and depositional response to eustatic, tectonic and climatic forcing* (pp. 161–207). Amsterdam: Kluwer.

Saadi, M. (1982). Schema structural du Maroc. *Notes et Mémoires du Service Géologique du Maroc*, *278B*.

Savostin, L. A., Sibuet, J.-C., Zonenshain, L. P., le Pichon, X., & Roulet, M.-J. (1986). Kinematic evolution of the Tethys Belt from the Atlantic Ocean to the Pamirs since the Triassic. *Tectonophysics*, *123*, 1–35.

Schaer, J.-P. (1987). Evolution and structure of the High Atlas of Morocco. In J.-P. Schaer, & J. Rodgers (Eds.), *The anatomy of mountain ranges* (pp. 107–128). Princeton: University Press.

Schlager, W. (1993). Accomodation and supply—a dual control on stratigraphic sequences. *Sedimentary Geology*, *86*, 111–136.

Schlee, J. S., & Klitgord, K. D. (1988). Georges Bank basin; a regional synthesis. In R. E. Sheridan, & J. A. Grow (Eds.), (*Vol. I-2*) (pp. 243–268). *The Atlantic continental margin: US, The Geology of North America*, Boulder: Geological Society of America.

Speed, R. C. (1994). North American continent-ocean transitions over Phanerozoic time. In R. C. Speed (Ed.), *Phanerozoic evolution of North American continent-ocean transitions, The Decade of North American Geology (DNAG), Continent-Ocean Transect Volume* (pp. 1–86).

Srivastava, S. P., Roest, W. R., Kovacs, L. C., Oakey, G., Levesque, S., Verhoef, J., & Macnab, R. (1990). Motion of Iberia since the Late Jurassic; results from detailed aeromagnetic measurements in the Newfoundland Basin. In G. Boillot, & J.-M. Fontbote (Eds.), *Alpine evolution of Iberia and its continental margins* (*Vol. 184*) (pp. 229–260). *Tectonophysics*, Amsterdam: Elsevier.

Srivastava, S. P., Sibuet, J.-C., Cande, S., Roest, W. R., & Reid, I. D. (2000). Magnetic evidence for slow sea floor spreading during the formation of the Newfoundland and Iberian margin. *Earth and Planetary Science Letters*, *182*, 61–76.

Srivastava, S. P., & Tapscott, C. R. (1986). Plate kinematics of the North Atlantic. In P. R. Vogt, & B. E. Tucholke (Eds.), (*Vol. M*) (pp. 379–404). *The western North Atlantic region, The Geology of North America*, Boulder: Geological Society of America.

Srivastava, S. P., & Verhoef, J. (1992). Evolution of Mesozoic sedimentary basins around the North Central Atlantic: A preliminary plate kinematic solution. In J. Parnell (Ed.), *Basins on the Atlantic Seaboard: Petroleum geology, sedimentology and basin evolution* (pp. 397–420). *Geological Society, Special Publication 62*.

Srivastava, S. P., Verhoef, J., & Macnab, R. (1988). Results from a detailed aeromagnetic survey across the northeast Newfoundland margin, Part II: Early opening of the North Atlantic between the British Isles and Newfoundland. *Marine and Petroleum Geology*, *5*, 324–337.

Stamm, R., & Thein, J. (1982). Sedimentation in the Atlas Gulf III: Turonian Carbonates. In U. von Rad, K. Hinz, M. Sarnthein, & E. Seibold (Eds.), *Geology of the northwest African continental margin* (pp. 459–474). Heidelberg: Springer.

Stampfli, G. M. (1993). Le Brianconnais, terrain exotique dans les Alpes? *Eclogae Geologicae Helvetiae*, *86*(1), 1–45.

Steiner, C., Hobson, A., Favre, P., Stampfli, G. M., & Hernandez, J. (1998). Mesozoic sequence of Fuerteventura (Canary Islands): Witness of Early Jurassic sea-floor spreading in the Central Atlantic. *Geological Society of America, Bulletin*, *110*(10), 1304–1317.

Sutter, J. F. (1988). Innovative approaches to the dating of igneous events in the Early Mesozoic basins of the eastern United States. *Bulletin US Geological Survey, B, 1776,* 194–200.

Tadili, B., Ramdani, M., Ben Sari, D., Chapochnikov, K., & Bellot, A. (1986). Structure de la crôute dans le Nord du Maroc. *Annales Geophysicae*, *B4*, 99–104.

Taj-Eddine, K (1991). *Le Jurassique terminal et le Crétacé basal dans l'Atlas atlantique (Maroc): Biostratigraphie, sédimentologie, stratigraphie séquentielle et géodynamique*. Unpublished State Doctorate (Doctorat de 3ème Cycle), Univ. Cadi Ayyad, Marrakech/Morocco, p. 285.

Thierry, J. (2000a). Middle Toarcian (180–178 Ma). In J. Dercourt, E. Gaetani, B. Vrielynck, E. Barrier, B. Biju-Duval, M. F. Brunet, J.-P. Cadet, S. Crasquin, & M. Sandulescu (Eds.), *Atlas Peri-Tethys* (pp. 61–70). Paris: Commission for the Geological Map of the World (CGMW).

Thierry, J. (2000b). Middle Callovian (157–155 Ma). In J. Dercourt, E. Gaetani, B. Vrielynck, E. Barrier, B. Biju-Duval, M. F. Brunet, J.-P. Cadet, S. Crasquin, & M. Sandulescu (Eds.), *Atlas Peri-Tethys* (pp. 71–83). Paris: Commission for the Geological Map of the World (CGMW).

Thierry, J. (2000c). Early Kimmeridgian (146–144 Myr). In J. Dercourt, E. Gaetani, B. Vrielynck, E. Barrier, B. Biju-Duval, M. F. Brunet, J.-P. Cadet, S. Crasquin, & M. Sandulescu (Eds.), *Atlas Peri-Tethys* (pp. 85–97). Paris: Commission for the Geological Map of the World (CGMW).

Thierry, J. (2000d). Early Tithonian (141–139 Myr). In J. Dercourt, E. Gaetani, B. Vrielynck, E. Barrier, B. Biju-Duval, M. F. Brunet, J.-P. Cadet, S. Crasquin, & M. Sandulescu (Eds.), *Atlas Peri-Tethys* (pp. 99–110). Paris: Commission for the Geological Map of the World (CGMW).

Thorne, J. A., & Swift, D. J. P. (1991). Sedimentation on continental margins, VI: A regime model for depositional sequences, their component systems tracts, and bounding surfaces. In D. J. P. Swift, G. F. Oertel, R. W. Tillman, & J. A. Thorne (Eds.), *Shelf sand and sandstone bodies* (pp. 189–255). *Special Publication, International Association of Sedimentologists 14*.

Tixeront, M. (1973). Lithostratigraphie et minéralisation cuprifère et uranifère stratiforme syngénétique et familière des formations détritiques des formations permo-triassique du Couloir d'Argana, Haut Atlas Occidental (Maroc). *Notes et Memoires du Sérvice Géologique du Maroc*, *33*(249), 147–177.

Tixeront, M. (1974). Carte géologique et minéralisations de couloir d'Argana. *Notes et Memoires du Sérvice Géologique du Maroc*, *205*.

Todd, R. G., & Mithcum, R. M., Jr. (1977). Seismic stratigraphy and global cahnges of sea-level, part 8: Identification of Upper triassic, Jurassic and Lower Cretaceous seismic sequences in Golf of Mexico and offshore West Africa. In C. E. Payton (Ed.), *Seismic stratigraphy—application to hydrocarbon exploration* (pp. 145–163). *American Association of Petroleum Geologists, Memoir 26*.

Tourani, A., Lund, J. J., Benaouiss, N., & Gaupp, R. (2000). Stratigraphy of Triassic syn-rift deposition in western Morocco. In G. H. Bachmann, & I. Lerche (Eds.), (*9/10*) (pp. 1193–1215). *Epicontinental Triassic, Zentralblatt für Geologie und Paläontologie*.

Trappe, J. (1992). Microfazies zonation and spatial evolution of a carbonate ramp: Marginal Moroccan phosphate sea during Paleogene. *Geologische Rundschau*, *81*(1), 105–126.

Tucholke, B. E., & McCay, F. W. (1986). Paleogeographic and paleobathymetric evolution of the North Atlantic Ocean. In P. B. Vogt, & B. E. Tucholke (Eds.), *(Vol. M)* (pp. 589–602). *The Western North Atlantic region, The Geology of North America,* Boulder: Geological Society of America

Turcotte, D. L., & Schubert, G. (1982). *Geodynamics—applications of continuum physics to geological problems*, New York: Wiley, p. 450.

Turcotte, D. L., & Schubert, G. (2002). *Geodynamics*, Cambridge: University Press, p. 456.

Vågnes, E., Gabrielsen, R. H., & Haremo, P. (1998). Late Cretaceous-Cenozoic intra-plate contractional deformation at the Norwegian continental shelf; timing, magnitude and regional implications. In S. A. P. L. Cloetingh, L. O. Boldreel, B. T. Larsen, M. Heinesen, & L. Mortensen (Eds.), *Tectonics of sedimentary basin formation: Models and constraints* (*Vol. 300*) (pp. 29–46). *Tectonophysics*, Amsterdam: Elsevier.

Vail, P. R., Mitchum, R. M., Jr., & Thompson, S. (1977). Seismic stratigraphy and global changes of sea-level, part 4: Global cycles of relative sea level. In C. E. Payton (Ed.), *Seismic stratigraphy—application to hydrocarbon exploration* (pp. 83–97). *American Association of Petroleum Geologists, Memoir 26*.

Vogt, P. R. (1973). Early events in the opening of the North Atlantic. In D. H. Tarling, & S. K. Runcorn (Eds.), *Implications of continental drift to the earth sciences* (pp. 693–712). London: Academic Press.

Vogt, P. R., & Tucholke, B. E. (1986) (*Vol. M*). *The geology of North America, the western North Atlantic Region*, Geological Society of America, p. 696.

Wade, J. A., & MacLean, B. C. (1990). The geology of the southeastern margin of Canada. In M. J. Keen, & G. L. Williams (Eds.), *Geology of the continental margin of Eastern Canada* (pp. 167–238). *Geology of Canada 2*.

Walker, R. G., & James, N. P. (1992). *Facies models—response to sea-level change*, St Johns/Newfoundland: Geological Association of Canada, p. 409.

Weijemars, A. (1987). revision of the Eurasian–African plate boundary in the western Mediterranean. *Geologische Rundschau*, *76*, 667–676.

Welte, D. H., Horsfield, B., & Baker, D. R. (1997). *Petroleum and basin evolution*, Heidelberg: Springer, p. 535.

Wiedmann, J., Butt, A., & Einsele, G. (1978). Vergleich von marokkanischen Kreide-Küstenaufschlüssen und Tiefseebohrungen (DSDP): Stratigraphie, Paläoenvironment und Subsidenz an einem passiven Kontinentalrand. *Geologische Rundschau*, *67*(2), 454–508.

Wiedmann, J., Butt, A., & Einsele, G. (1982). Cretaceous stratigraphy, environment, and subsidence history at the Moroccan continental margin. In U. von Rad, K. Hinz, M. Sarnthein, & E. Seibold (Eds.), *Geology of the northwest African continental margin* (pp. 366–395). Heidelberg: Spriner.

Wurster, P., & Stets, J. (1982). Sedimentation in the Atlas Gulf II: Mid-Cretaceous events. In U. von Rad, K. Hinz, M. Sarnthein, & E. Seibold (Eds.), *Geology of the northwest African continental margin* (pp. 439–458).

Ziegler, P. A., Cloetingh, S., Guiraud, R., & Stampfli, G. M. (2001). Peri-Tethyan platforms: Constraints on dynamics of rifting and basin inversion. In P. A. Ziegler, W. Cavazza, A. H. F. R. Robertson, & Crasquin-Soleau (Eds.), *Peri-Tethys Memoir 6; Peri-Tethyan rift/wrench basins and passive margins* (pp. 9–49). *Mémoires du Muséum National d'Histoire Naturelle 186*.

Zoback, M. L. (1992). The World Stress Map Project. *Journal of Geophysical Research*, *97*(8), 11,703–12,013.

Zouine, E. M (1993). *Geodynamique recent du Haut Atlas. Evolution de sa bordure septentrionale et du Moyen Atlas sud-occidental au cours de Cenozoïque*. Unpublished State Doctorate (Doctorat de 3ème Cycle) Univ. Mohamed V, Rabat/Morocco, p. 300.

Rainer Zühlke is senior lecturer at the Institute of Geology and Paleontology in Heidelberg. After his study at the University of Freiburg and professional experience in seismic stratigraphy, he received his doctoral degree in 1996 from the University of Heidelberg (Germany). His research interests include sedimentology, basin analysis and basin process modeling. Recent work has focused on high-resolution sequence stratigraphy, integrated cyclostratigraphy and the modeling of carbonate platforms and basins in different plate-tectonic settings.

Mohammed-Said Bouaouda is lecturer-scientist at the Faculty of Science in El Jadida. He received his doctoral degree in 1987 from the University of Toulouse (France). Research activities focus on the stratigraphy, biostratigraphy (benthic foraminifera, dasycladacean algae), paleogeography and geodynamic evolution of the Atlantic Basins of Morocco, especially during the Jurassic. The scientific collaboration within the project presented here includes stratigraphic modeling.

Brahim Ouajhain is assistant professor at the Faculty of Science in El Jadida. He received his doctoral degree in 1989 from the Caddi Ayyad University of Marrakesh (Morocco). His research interests include the sedimentology of Jurassic carbonates and their diagenesis in the Essaouira and Agadir Basins, dolomitization evolution and modeling, sequential microstratigraphy of cements by cathodoluminescence, reef diagenesis and its associated porosity.

Thilo Bechstädt is full professor of Sedimentary Geology at the University of Heidelberg. He obtained his doctoral degree in 1972 from the University of Innsbruck, Austria. He worked at the universities of Innsbruck, Freiburg, Munich and Heidelberg as well as with different oil and mining companies in Austria, Germany, Greece, Vietnam and Libya. His research interests deal with different aspects of basin analysis (including paleogeographic reconstructions, structural analysis of complex basins, diagenetic evolution, and basin modeling).

Reinhold Leinfelder is full professor of Paleontology and Historical Geology at the Ludwig Maximilian University of Munich and director of the Bavarian States Collections of Paleontology and Geology, including the Paleontological Museum of Munich. He received his doctoral degree in 1985 from the University of Mainz, Germany. He has worked at the Universities of Mainz, Stuttgart and Munich. Research interests include control and evolution of reef growth, sequence stratigraphy of mixed systems, paleogeographic and paleoecologic reconstructions, basin analysis, and microbial and algal carbonates.